Evaluating the Wind Repowering Potential in Europe

Angelos Chatziangelou

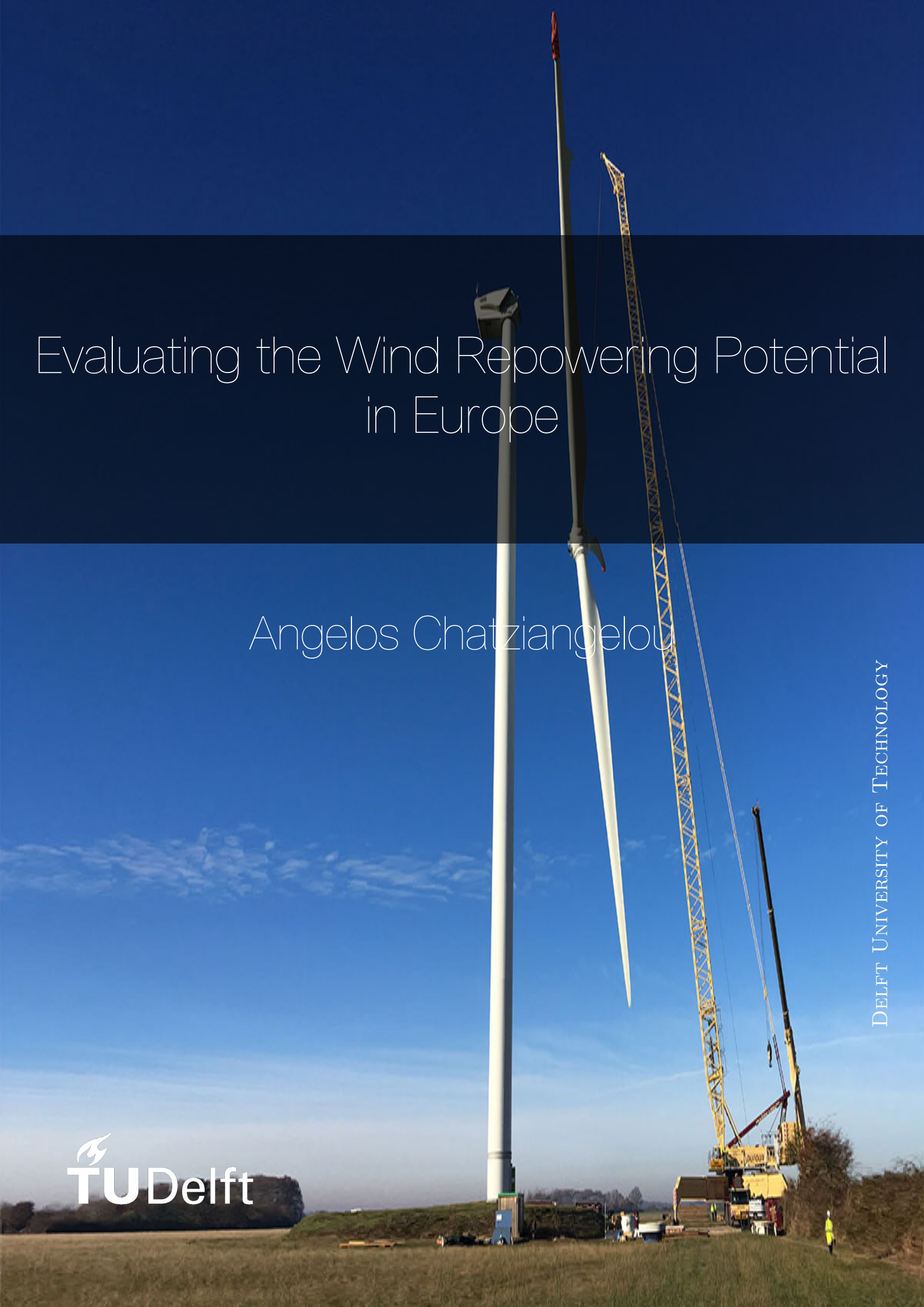

Delft University of Technology

TU Delft

Evaluating the Wind Repowering Potential In Europe

Comparing repowering against baseline scenarios
across capacity, energy, cost, and land-use metrics

by

Angelos Chatziangelou

Master Thesis

for the purpose of obtaining the degree of Master of Science
in Sustainable Energy Technologies
at the Delft University of Technology

to be defended publicly on June 30, 2025

Student number: 6055885

Chair: Dr. S.J. (Stefan) Pfenninger-Lee

Daily supervisor: A.C. (Jann) Launer

Committee member: Dr. N. (Nihit) Goyal.

Picture by Wind Europe [1]

TU Delft Delft University of Technology

JUST WiND 4 ALL

Abstract

Achieving Europe's carbon neutrality by 2050 demands the expansion of all of the renewable energy sources, and especially onshore wind. Constraints such as aging wind turbines reaching their operational lifetime, limited land availability, and mounting social and environmental pressures constrain the escalation of new sites. The strategy of wind repowering—replacing turbines reaching their end-of-life with larger, higher-performance models on existing footprints— promises to increase the installed capacity, leverage the existing grid and site infrastructure, and reduce generation costs.

This thesis delivers the first continental-scale, quantitative evaluation of the onshore wind repowering strategy in Europe by collecting a European wind-park database, overlaying site classifications from the Global Wind Atlas and EuroDEM elevation topography, and applying a lifecycle capacity model to project decommissioning and repowering trajectories through 2050. Complementary modules estimate repowered rotor dimensions, select candidate turbines, and compute energy yields using ERA5 reanalysis, while a cost model integrates decommissioning expenses, projected CAPEX/OPEX, and financial metrics (LCOE, NPV, IRR). A spatial-footprint submodel then quantifies land requirements under competing repowering and greenfield-replacement scenarios.

Multiple repowering approaches were applied with fluctuating spatial constraints, resulting in an additional 60–82 GW of nameplate capacity by 2050—equivalent to a 33–45 % increase over a straight decommissioning-and-replacement baseline—and can generate up to 425.34 TWh annually, covering approximately 14.8 % of Europe's 2022 electricity demand versus 11.9 % or 342.87 TWh under the baseline. From a financial standpoint, assuming a wholesale electricity price of €80/MWh and a moderate (14 %) learning-rate scenario, repowering marginally lowers the mean LCOE from €68.0/MWh (replacement) to €67.4/MWh; over 46.6 % of sites achieve a higher NPV under repowering; By reusing foundations, roads, and grid connections, repowering cuts additional land requirements by 37–41 % relative to a straight replacement baseline. These results demonstrate that under moderate technological progress, repowering can cost-effectively expand Europe's wind energy production, maximize site efficiency, and minimize environmental footprint.

Contents

1 Introduction **14**

2 Background **15**

2.1 Evolution of Wind Turbine Repowering Concepts 15

2.1.1 Replacement vs. Repowering Paradigms 15

2.1.2 Spatial and Technical Constraints in Prior Work 17

2.1.3 Cost Modelling and Financial Metrics in Wind Projects 19

2.1.4 Land-Use Efficiency Metrics and Spatial Optimization 20

2.2 Knowledge Gaps 20

2.3 Research Question 21

3 Methods **22**

3.1 Capacity Model 22

3.1.1 Data Acquisition & Pre-Processing 23

3.1.2 Rotor-Diameter Estimation 31

3.1.3 Estimation of Wind Park Land-use 34

3.1.4 Terrain Complexity: Ruggedness & Slope 36

3.1.5 Future of Wind Turbine Specifications 37

3.1.6 Representative Repowered Wind Turbines 38

3.1.7 Repowering Strategy Approaches 39

3.1.8 Key Assumptions 44

3.2 Energy Yield Model 44

3.2.1 Key Assumptions 46

3.3 Costs Model 47

3.3.1 Decommissioning vs. Repowering Cost Components 47

3.3.2 Capital Expenditure (CAPEX) 48

3.3.3 Operational Expenditure (OPEX) 50

3.3.4 Costs Overview 51

3.3.5 Financial Metrics-LCOE, NPV & IRR Calculations . . . 52
3.3.6 Key Assumptions . . . 54
3.4 Land-use Model . . . 55
3.4.1 Turbine Spacing Rules & Footprint Metrics . . . 55
3.4.2 Power-Density & Land-Sparing . . . 56
3.4.3 Energy Density . . . 56
3.4.4 Key Assumptions . . . 57

4 Results **58**
4.1 Capacity Potential of Wind Repowering . . . 58
4.1.1 Current State of Wind Farms in Europe . . . 58
4.1.2 Projected Decommissioning Trajectory . . . 61
4.1.3 Estimation of Repowered Capacity . . . 62
4.2 Energy Yield Potential of Wind Repowering . . . 65
4.2.1 Capacity Factor: The True Driver of Energy Yield . . . 65
4.2.2 Yield per Country and Strategy . . . 66
4.2.3 Energy Yield GIS Comparison & Demand Coverage . . . 68
4.3 Cost Comparison . . . 70
4.3.1 Repowering vs. Replacement Financial Metrics . . . 70
4.3.2 Levelized Cost of Electricity Comparison . . . 71
4.3.3 IRR-NPV and Electricity Price Sensitivity Analysis . . . 73
4.3.4 Example Wind Park Case Study . . . 75
4.4 Land Use Comparison . . . 77
4.4.1 Power Density Comparison . . . 77
4.4.2 Energy Density Comparison . . . 79
4.4.3 Land Savings Assessment . . . 79

5 Conclusion and Discussion **81**
5.1 Conclusion . . . 81
5.2 Future Research Directions . . . 82

5.3 Discussion . . . 83
5.3.1 Methodological Reflections and Limitations . . . 83
5.3.2 Park Size & Configuration . . . 83
5.3.3 Energy and Economic Performance . . . 83
5.3.4 Regional Heterogeneity . . . 84
5.3.5 Site-Specific Constraints on Repowering Potential . . . 84
5.3.6 Outlook . . . 85

A Appendix **95**

A.1 Methods . . . 95
A.1.1 Capacity Model . . . 95
A.1.2 Energy Yield Model . . . 96
A.1.3 Costs Model . . . 102
A.2 Results . . . 104
A.2.1 Capacity Model . . . 104
A.2.2 Energy Yield Comparison . . . 108
A.2.3 Cost Comparison . . . 109
A.2.4 Land-Use Comparison . . . 110

List of Figures

1 Progress towards renewable energy source targets for EU-27 [2] . . . 15

2 Installed wind power in Europe reaching the end of its useful lifetime annually and with two different assumptions of operational life expectancy of 20 (red) and 25 (yellow)[3]. 16

3 Frequency distribution of currently installed wind turbines in Germany according to the commissioning Year (yc) [4]. . . . 16

4 Projection of power and rotor diameters of onshore wind turbines from 2000 to 2025 (with 2020- 2025 being projections) [5] . . . 17

5 Typical wind turbine power curve [6] . . . 18

6 Overall model flowchart - Capacity- Costs- Land-Use . . . 22

7 Capacity sub-model workflow . . . 23

8 The Wind Power - Wind energy database incompleteness percentages by country [7] . 25

9 Installed onshore wind turbine capacity per country in the region of Europe with different colors for differ wind park sizes [7] . . . 26

10 IEC wind classification map of Europe based on global Wind Atlas v.3 [8] . . . 28

11 Elevation map of Europe (EuroDem) [9] . . . 29

12 Wind turbine lifespan probability model (blue line) and function (function range between medium and high wind speed shown in Grey with USA average represented as a black line) over time (for a single wind turbine installed in 2016)[10]. . . . 30

13 Operational life distribution of onshore wind turbines acquired from the The Wind Power Database [7] . . . 30

14 Comparison of regression lines from Gonzalez and Arantegui (left) and NYSERDA (right). 32

15 Comparison of regression fits in Log-Log and Linear scales. . . . 33

16 Side-by-side comparison of regression plots. . . . 33

17 Wind farm array losses [11] . . . 35

18 Wind turbine size trends 2000-2030 . . . 37

19 Average (Left) and maximum (Right) wind turbine size annually (1975-2022) . . . 37

20 Detailed analysis of each repowering approach capacity calculation flow chart . . . 40

21 Difference in Rated Capacity Between Installed Onshore Turbines and Assigned Reference Models Across the EU . . . 45

22 Costs sub-model . . . 47

23 Decommissioning costs and recycling profits based on ADAME [12],Nordex estimation 48

24 Cost of grid interconnection for solar and wind parks from 2000-2023 [13] 49

25 Wind turbine price indices and price trends, 1997-2023 [14] 50

26 Full-service (initial and renewal) O&M pricing indexes and weighted average O&M costs in different Countries 51

27 Environmental sub-model 55

28 Wind power capacity by country in Europe originate from The Wind Power - Wind energy database [7] 58

29 Onshore (left) and offshore (right) capacity distribution of wind turbines in Europe . . 59

30 Distribution of onshore wind turbine sizes in Europe categorized into three categories: Small, Medium, and Large 59

31 Distribution of offshore wind turbine sizes in Europe categorized into three categories: Small, Medium, and Large 60

32 Total number of wind parks per country with single wind turbine parks percentages . 60

33 Total onshore wind capacity in Europe without new installations 61

34 Annual decommissioning rate of wind parks in Europe per year and by country (Assuming 20 years of life-span) 61

35 Repowering capacity effectiveness by country and approach against decommissioning and replacement (baseline) scenario 62

36 Total cumulative operating capacity - Repowering vs. Replacement strategy in Europe with modeling starting from 2022 (2000-2050) 63

37 Installed repowered and non-repowered onshore wind turbine capacity per country in the region of Europe for two approaches with different degrees of flexibility 65

38 Total installed wind turbine capacity (MW) vs energy yield (TWh) per Country for capacity maximization repowering approach (approach 2) 66

39 Energy production per country Old vs. repowering approaches in the EU 67

40 Energy production per country old vs. repowering approaches in the EU 67

41 (a) No-Loss Hybrid (Yield-Based) approach locations and capacity difference. 68

42 Yield-based and Capacity-Based Demand Coverage of Repowered Wind Turbines (NLH Approach) 69

43 Box-and-whisker plot comparing CAPEX for the repowering versus decommissioning + replacement scenarios. Boxes span the interquartile range (25th–75th percentiles), the bold line marks the median CAPEX, and whiskers extend to the minimum and maximum observed values. 70

44 Box-and-whisker plot of average EU LCOE for onshore wind under three learning-rate scenarios (10 %, 14 %, 20 %). Boxes span the interquartile range (25th–75th percentiles), the bold line indicates the median LCOE, and whiskers extend to the minimum and maximum observed values. 71

45 Repowering (Approach 2 and 6) vs. Decommissioning and Replacement LCOE comparison per country 72

46 Relative repowering (Approach 2 and 6) vs. Decommissioning and Replacement LCOE comparison per country 72

47 Box-and-whisker comparison of Net Present Value (NPV) and Internal Rate of Return (IRR) between the repowering (Approach 2: Capacity Maximization, no spatial expansion) and decommissioning scenarios for the 6,850 active European onshore wind parks (12 210 park–scenario pairs). Boxes span the interquartile range (25th–75th percentiles), the orange line marks the median, and whiskers extend to the minimum and maximum observed values. 73

48 Comparison of key financial metrics vs. electricity price for repowering and decommissioning scenarios. 74

49 Decommissioning and replacement, and repowering NPV comparison map of Europe ($\mathrm{NPV}_{rep} = the NPV of repowered turbines and NPV_{dec}$ = the NPV of the decommissioning and replaceme

50 ensitivity analysis of financial metrics (NPV, IRR, payback period) and LCOE to wholesale electricity price for a representative UK onshore wind park under two scenarios—repowering (Approach 2: Capacity Maximization, no spatial expansion) versus decommissioning + replacement. Each box spans the interquartile range (25th–75th percentiles) of metric values across the price sweep, the bold line marks the median, and whiskers extend to the minimum and maximum observed values. 76

51 Land-use of wind parks in EU countries 77

52 Power density ($\mathrm{MW/km^2}$)*percountryandapproach* 78

53 Energy density (TWh/km^2) per country and approach 79

54 Minimum and maximum land saved from the implementation of repowering against the baseline (Decommissioning and replacement) scenario, considering all approaches . . . 80

55 Linear regression of turbine's capacity vs. rotor diameter 95

56 Weibull distribution curves 102

57 Electricity wholesale prices per country in Europe and average prices in Europe (2005-2025)[15] 103

58 Decommissioned capacity by country total 104

59 Decommissioned capacity by country Onshore 104

60 Top 20 wind turbine models used in Europe by percentage of installations 105

61 Top 20 wind turbine types in Europe evaluated by installed capacity 106

62 Capacity factor difference between baseline and repowering (Capacity Maximization approach 2) scenarios 108

63 Comparison of annual energy production before and after repowering. 108

64 Total electricity consumption in EU (1990-2022) 110

65 Required land area to reach repowered capacity comparison Baseline vs. Repowered for all approaches 110

List of Tables

1 Repowering / Decommissioning & Replacement Strategies . . . 22

2 Comparison of completeness percentages for each category in the European and Onshore Europe datasets. Red-highlighted data represents information that was not used in the study. . . . 24

3 Basic parameters for wind turbine classes (2019) [16] . . . 27

4 Percentage distribution of IEC Classes in Europe. . . . 28

5 Regression Error Parameters for Different Turbine Classes. . . . 34

6 Comparison of Extracted and Real Rotor Diameters with Updated percentage error. . . . 34

7 Comparison of TRI and Slope threshold values for terrain classification . . . 37

8 Wind turbine models sorted by IEC class [17, 18] . . . 39

9 Comparison of approaches for wind turbine selection . . . 43

10 Key Assumptions – Capacity Model . . . 44

11 Data Sources and Their Descriptions . . . 45

12 Key Assumptions – Energy Yield Model . . . 46

13 Cost breakdown by component (EUR/kW) . . . 49

14 Cost comparison between decommissioning + new build and repowering strategies (€/kW) . . . 52

15 Projected onshore wind turbine CAPEX in 2050 under alternative learning-rate scenarios, with decommissioning & replacement strategy[19] . . . 52

16 Key cost model assumptions for repowering and decommissioning strategies. . . . 54

17 Key land-use assumptions in the methodology chapter. . . . 57

18 Wind energy repowering projection and analytics for 2050 . . . 63

19 Total annual energy production and relative gains by repowering approach . . . 69

20 Global land-use summary by approach number. . . . 78

21 Land area saved and power-density improvements under each repowering approach. . . . 80

22 Summary of Ramp-up Region Modeling Approaches Using Only Rated, Cut-in, and Cut-out Speeds. . . . 98

23 Error metrics for the uphill slope (Cut-in to Rated Speed) . . . 99

24 Wind Shear by Terrain Features, Surface Roughness, and Obstacles (IEA Expert Group Report on Recommended Practices [20] . . . 101

25 Representative turbine model for each unique capacity 102

26 Offshore top 10 manufacturers and turbines with their percentage of installations . . . 107

27 Onshore top 10 manufacturers and turbines with their percentage of installations . . . 107

28 Wind park statistics by country 109

29 Wind park data by country (in km^2) 111

1 Introduction

The urgency of climate change mitigation requires quick actions, such as transforming energy systems and focusing on expanding renewable energy production. Wind power is one of the leading renewable technologies in Europe in terms of energy production, thus playing a crucial role in reducing greenhouse gas emissions and supporting Europe's goals for energy transition. Europe aims to significantly increase its wind generation capacity to meet ambitious climate targets [21]. However, the current projections for wind energy expansion face substantial hurdles, including long permitting times, limited production and deployment capacities, and concerns about new wind farms' social and environmental impact [22]. These challenges require innovative solutions to wind energy development that address these constraints while optimizing financial efficiency.

Europe's high population density makes it challenging to find suitable locations for wind farms near populated areas [23]. This often leads to conflicts with other land use interests, resulting in strong opposition from local communities and citizen groups. At the same time, many existing wind turbines are nearing the end of their operational lifetime [24], highlighting the urgent need to increase wind energy capacity. An option to consider is offshore wind, which has a higher capacity factor than onshore wind farms. However, due to technical, geographical, and other limitations, offshore wind power cannot yet completely replace onshore wind, such as in nations with shallow water depths [25]. As a result, Europe's energy transition faces significant barriers due to limited land availability, social acceptance challenges, and the constraints of offshore wind.

One promising solution to address the energy transition challenges is wind repowering. Repowering involves replacing wind turbines with newer and more advanced models once their operational life cycle comes to an end [3]. This process not only enhances the energy yield but also allows for the reuse of existing infrastructure, such as grid connections and road access [26]. Moreover, implementing a repowering strategy can have a positive impact by strengthening the effectiveness of Europe's energy transition, helping to achieve its renewable energy goals.

This thesis aims to evaluate the potential of wind repowering in Europe as an alternative to new installations, assessing its impact on costs, production capacity, and land-use effects. Through a scenario-based analysis, the research provides a clearer understanding of repowering's role in the energy transition, offering insights into the European research initiative JustWind4All [27]. The outcomes of this study are expected to contribute as data inputs in the JustWind4All research group model.

Link to MSc Sustainable Energy Technology

This project's goals align with the Sustainable Energy Technologies Master's program by addressing Technical, Financial, and Environmental effects in the field of renewable technologies, namely wind power. Positioned within the Economics and Society track, this research focuses on upgrading existing aging wind turbines to increase their energy production and cost-effectiveness without requiring additional land. This study supports SET's mission to develop innovative, sustainable energy solutions that facilitate a socially accepted, accelerated energy transition by quantifying repowering's benefits and considering its broader impacts.

2 Background

2.1 Evolution of Wind Turbine Repowering Concepts

2.1.1 Replacement vs. Repowering Paradigms

Europe is at the forefront of the global energy transition, with a commitment to achieving carbon neutrality by 2050. To meet this goal, the European Union has established ambitious targets, including reducing greenhouse gas emissions by at least 55% by 2030 compared to 1990 levels [28] and significantly increasing the share of renewable energy to at least 42.5% [29] of total consumption. In 2023, renewable energy accounted for 24.1% [2] of Europe's total energy consumption, as shown in Figure 1, highlighting the progress made thus far toward these goals. Wind energy stood out as the largest contributor to renewable energy sources, providing 17% [2] of Europe's green energy production. This underscores its indispensable role in achieving the continent's ambitious climate and energy targets.

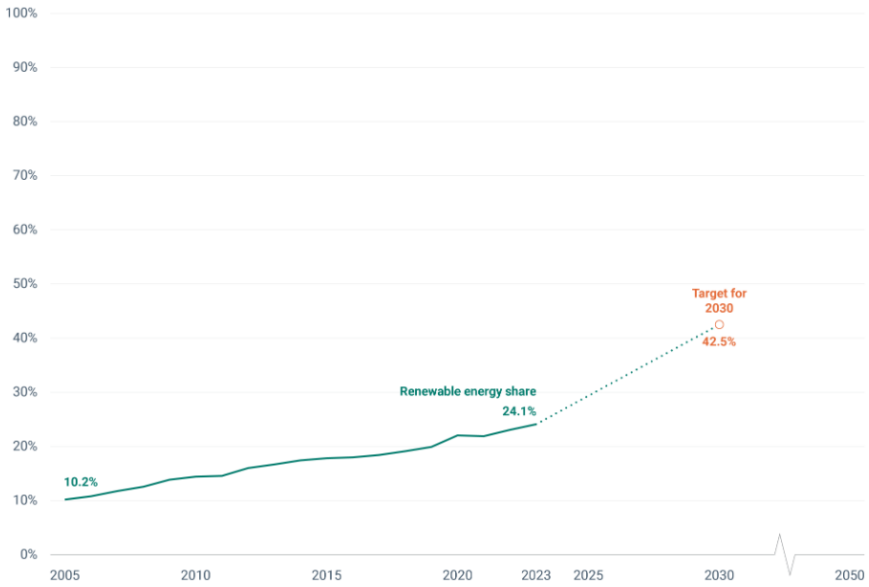

Figure 1: Progress towards renewable energy source targets for EU-27 [2]

However, the limited lifespan of wind turbines is a significant challenge in achieving Europe's energy targets. Most wind turbines have a useful operational lifetime of 20 years, which can be extended to 25 years with specific retrofitting measures offered by manufacturers [3]. In the coming years, a capacity of 35 GW to over 80 GW by 2030 will reach the end of their operational lifespan across Europe, as shown in Figure 2. This reality presents both a challenge and an opportunity. On one hand, older turbines often occupy prime locations with advantageous wind conditions but are relatively outdated and under-performing. On the other hand, their decommissioning opens pathways for upgrading these sites with more advanced and efficient technology.

When wind farms reach the end of their lifespan, operators have several options to consider [30]. These include full decommissioning in line with national regulations, extending turbine life through inspections and retrofitting [31], overhauling equipment by replacing specific components, or adopting a repowering strategy. Repowering, which involves upgrading wind farm equipment with advanced technologies, offers the greatest potential for boosting energy production and leveraging existing infrastructure [32]. This makes it a particularly attractive strategy for addressing Europe's renewable energy needs while minimizing additional land use.

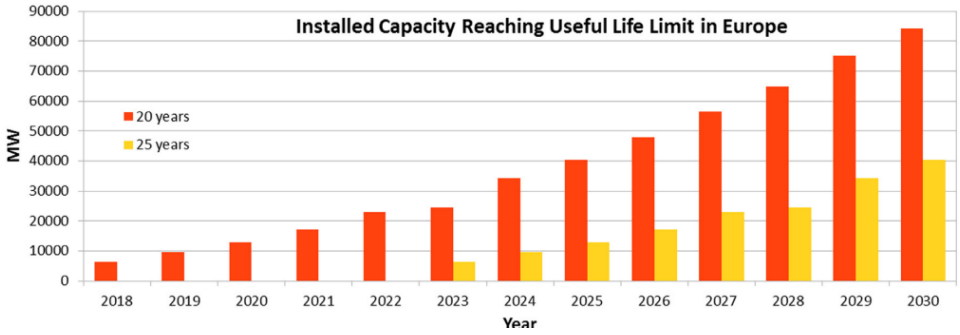

Figure 2: Installed wind power in Europe reaching the end of its useful lifetime annually and with two different assumptions of operational life expectancy of 20 (red) and 25 (yellow)[3].

Efforts to expand wind capacity through conventional means, such as extending turbine lifespans or constructing new installations, face significant barriers. For example, in Germany, achieving carbon neutrality requires phasing out coal-based electricity by 2038 [4]. This demands a substantial increase in renewable energy production to offset the loss of conventional sources. Yet, as depicted in Figure 3, a large number of existing turbines are nearing the end of their operational life, and refurbishment alone is unlikely to provide the necessary capacity expansion [4]. Similarly, in Italy, studies indicate that extending the lifespan of current installations falls short of achieving the significant energy production increases required to meet targets [33].

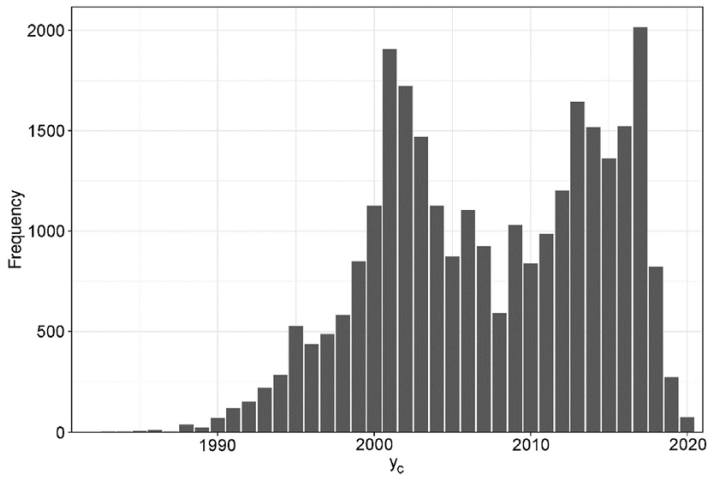

Figure 3: Frequency distribution of currently installed wind turbines in Germany according to the commissioning Year (yc) [4].

Geographical and technical challenges further constrain the potential for offshore wind development in many regions, such as Germany and Spain, making onshore development essential [25, 34]. Conventional approaches, like decommissioning or refurbishment, are further limited by economic and policy challenges. For instance, in Brazil, financial factors such as energy tariffs and operational costs heavily influence the viability of wind projects [35]. In Italy, the need for streamlined policies and incentives has been emphasized to support the expansion of wind infrastructure [33].

These challenges underscore the need for innovative strategies that go beyond conventional methods. Repowering emerges as a promising solution that can help overcome these barriers while maximizing the efficiency of existing wind farm locations. By upgrading aging turbines with modern, high-capacity

models, repowering not only addresses the urgent need for capacity expansion but also aligns with Europe's ambitious renewable energy targets. Moreover, it leverages prime locations already assessed for wind conditions, offering a cost-effective and sustainable approach to meet the growing demand for renewable energy [4, 3].

2.1.2 Spatial and Technical Constraints in Prior Work

Many studies in the scientific literature analyze the potential and challenges of wind farm repowering, focusing on its ability to improve energy efficiency and capacity in different regional contexts. Repowering requires the installation of new and more efficient wind turbines to achieve increased energy yields. Technological advancements in turbine design—such as innovations in rotor blade aerodynamics, larger rotor diameters, and taller towers—have significantly enhanced efficiency and output, as illustrated in Figure 4. These advancements have resulted in an increase in capacity factors and energy yields for modern turbines compared to older technologies [36, 6]. For instance, rotor diameters expanded from 76 meters in 2001 to 155 meters by 2021, while rated power increased from 2 MW to 5.5 MW. This development has enabled greater wind-swept areas and significantly higher energy generation [36]. Wind repowering, therefore, not only replaces aging turbines with newer, larger, and more efficient models but also often reduces the number of turbines while tripling energy output. For example, in Malpica, Spain, a repowering project replaced 69 older turbines with just seven modern units, doubling the wind farm's energy production [6].

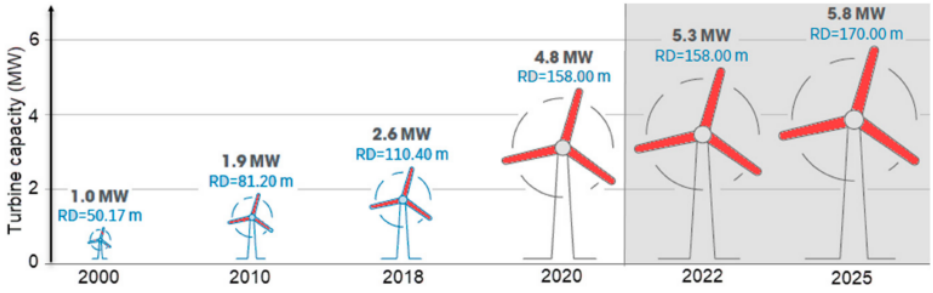

Figure 4: Projection of power and rotor diameters of onshore wind turbines from 2000 to 2025 (with 2020- 2025 being projections) [5]

In India, several studies have demonstrated the significant potential of repowering aging wind farms. Prabu and Kottayil [37] examined both partial and total repowering options. Partial repowering involves upgrading specific components, such as blades, gearboxes, or nacelle components, while retaining existing towers and foundations [38]. In contrast, total repowering entails replacing entire turbines with newer models. Their study highlighted that achieving India's ambitious renewable energy targets, such as 60 GW of wind capacity by 2022, would likely require total repowering at high-potential sites. This approach could increase generation capacity by up to 50%, replacing outdated, lower-capacity turbines with modern, high-efficiency models to maximize energy production [39]. Similarly, Verma and Ahmed [40] used the Wind Atlas Analysis and Application Program (WAsP) to demonstrate that repowering could enhance energy output by up to 70% within the same footprint, significantly improving energy efficiency. However, challenges like removing old turbines, land ownership disputes, and feed-in tariff ambiguities present obstacles. Despite these issues, the potential for repowering in India remains substantial, especially for turbines with capacities below 500 kW.

In Germany, repowering has yielded mixed outcomes largely influenced by regulatory frameworks. Stetter et al. [41] emphasized that policy changes are essential to unlocking repowering's full potential in areas constrained by strict distance regulations. Their spatial analysis indicated that optimizing

turbine placement at the same height as older models could add up to 10.57 GW of capacity to the German energy grid. Conversely, Jan Frederick et al. [42] found that new regulatory restrictions might reduce the number of turbines and total capacity by approximately 40%, due to stricter distance and urban planning requirements.

The United Kingdom demonstrates a contrasting scenario, where strategic repowering has resulted in significant capacity increases despite reductions in turbine numbers. Windemer [43] observed that repowered sites achieved an average capacity increase of 155%, even with a 39% reduction in turbine numbers. Taller turbines, with an average height increase of 90.4%, accessed stronger and more consistent wind speeds, leading to higher energy yields. These findings underscore the importance of leveraging modern technology, although site-specific challenges remain a limiting factor.

Globally, Ahmed et al. [44] found that replacing old turbines with advanced models could enhance energy production by up to 74%. Leveraging existing infrastructure helps minimize project delays and costs, making repowering a cost-effective and efficient option. Nevertheless, their research highlights the need to account for site-specific conditions and ensure community acceptance for successful implementation.

Despite its promise, repowering also faces challenges. Installing larger turbines often necessitates upgrades to foundations, access roads, and grid connections, and taller turbines may increase environmental risks, such as collisions with birds and bats [34]. Social acceptance can also be a barrier, as larger turbines may provoke resistance due to their visual impact [34, 44]. Additionally, decommissioning older turbines introduces complexities, particularly in recycling materials like blades [44]. Some previously suitable sites may no longer be viable for repowering due to environmental changes, urban development, or stricter land-use regulations [34].

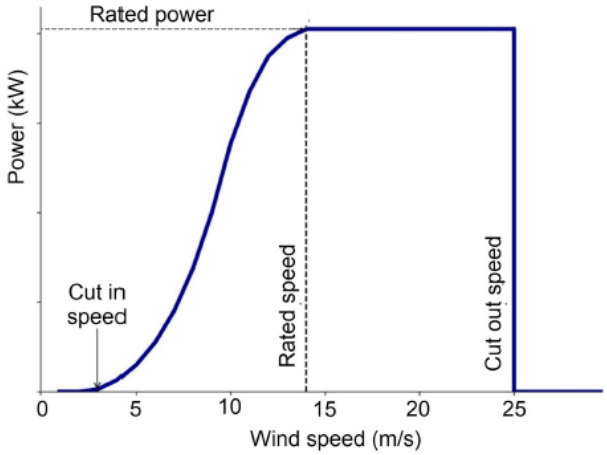

Figure 5: Typical wind turbine power curve [6]

Wind repowering offers a compelling strategy for improving energy output and capacity. Technological advancements, including larger rotor diameters and taller towers, have enabled significant energy gains while reducing turbine numbers. Regional case studies from India, Germany, and the UK illustrate diverse opportunities and challenges, underscoring the importance of tailored approaches. Strategic site selection, supportive policies, and community engagement are critical to fully realizing the potential of repowering in achieving renewable energy goals.

2.1.3 Cost Modelling and Financial Metrics in Wind Projects

Repowering wind farms presents the opportunity to achieve cost savings while extending the operational life of existing wind infrastructure. By upgrading outdated turbines or replacing them with modern, higher-capacity models, repowering can reduce overall costs, making it an economically viable alternative to constructing new installations [45, 33, 46]. This subsection explores the financial benefits of repowering as evidenced by recent studies, categorized into regional examples, offshore strategies, and overarching challenges.

There are several costs associated with repowering, including decommissioning costs, installation of new wind turbines, grid enhancement, etc. Cooperman et al. [38] studied the costs associated with different end-of-life (EOL) options for wind turbines to estimate various decommissioning expenses. Decommissioning wind turbines involves several EOL options, each with distinct processes and cost implications. Landfilling, the most common disposal method, poses challenges due to the bulkiness and durability of composite materials in turbine blades. Tip fees for landfills vary, averaging $ 60.63 per metric ton for shredded material or $ 19 per cubic meter for large segments. Alternatives to land-filling include mechanical recycling, where blades are ground into smaller fragments for reuse in lower-value products, and cement co-processing, which incorporates ground blade materials into clinker production. While these recycling options can reduce environmental impacts, they often incur higher costs due to pre-processing and transport. Emerging techniques such as high-voltage fragmentation and pyrolysis provide opportunities for recovering valuable materials but are limited by high energy demands and low technology readiness levels. Repowering strategies requiring the removal and replacement of turbines must factor in these decommissioning costs alongside adopting sustainable EOL practices, emphasizing the need for integrated planning.

In Spain, Colmenar-Santos and Campíñez-Romero [45] assessed whether repowering can remain a viable option in Spain's energy mix, particularly under market-driven conditions. Their analysis highlights that repowering can reduce the Levelized Cost of Electricity (LCOE) by up to 20% compared to constructing new wind farms. This is especially true when supported by favorable feed-in tariffs and regulatory frameworks, showcasing its economic competitiveness for older installations in high-resource areas nearing the end of their operational life.

Similarly, in Italy, Laura Serri et al. [33] analyzed three repowering scenarios: maintaining the original capacity with fewer, larger turbines (H1), increasing capacity by 1.5 times (H2), and doubling the capacity (H3). While practical constraints limited the feasibility of doubling capacity, scenarios H1 and H2 showed internal rates of return (IRR) between 5% and 9%. However, these figures represent a decline from earlier installations (1%-19%) due to reduced economic incentives stemming from declining government subsidies and financial support. Payback periods for repowered projects were extended to 8.5–13.5 years, compared to just 4.5 years for the original plants. These findings underline the importance of moderate government incentives to ensure the financial viability of repowering projects, thereby maximizing the potential of prime wind sites.

Hou et al. [46] explored cost-optimization strategies for offshore wind farm repowering, demonstrating that upgrading older turbines with modern configurations can reduce the LCOE by 15–25% compared to replacing turbines with identical models. Implementing advancements in turbine technology led to an 80% increase in annual energy production, significantly improving the economic feasibility of repowering projects. These strategies are especially crucial for offshore wind farms nearing the end of their operational life, offering a robust alternative to conventional refurbishment practices. In a related finding, Prabu and Kottayil [37] suggested that partial repowering—upgrading specific components rather than replacing entire turbines—can offer cost savings of up to 30% compared to full turbine replacement. This approach is particularly advantageous when financial constraints or local conditions limit the feasibility of complete overhauls.

Despite the demonstrated benefits, financial uncertainty remains a significant barrier to repowering projects. Himpler and Madlener [47] highlighted the impact of fluctuating electricity prices on project feasibility. Their study revealed that revenue forecasts often capture only a fraction of the projected income, discouraging investment. Historical government tariffs ranged from €33 to €52/MWh, with additional subsidies of €13 to €23/MWh. However, variability in financial support over time has created uncertainty for developers. To address this, the study recommends implementing stable government-guaranteed incentives to ensure consistent returns and enhance the attractiveness of repowering projects for investors.

Repowering offers significant financial benefits, from reducing LCOE to enhancing cost-efficiency through targeted strategies like partial repowering. However, its feasibility depends heavily on supportive regulatory and financial frameworks. While advancements in turbine technology and site optimization bolster its potential, challenges such as economic uncertainty and fluctuating electricity prices underscore the need for consistent policies and incentives to unlock repowering's full viability.

2.1.4 Land-Use Efficiency Metrics and Spatial Optimization

Hoen et. al [48] state that wind repowering offers a significant opportunity to optimize land use by replacing older, less efficient turbines with fewer, larger, and more powerful ones. Advances in turbine technology, such as increased rotor diameters and hub heights, allow for higher energy yields within the same land area, despite the need for greater spacing due to setbacks and noise considerations. This can lead to a reduction in the overall number of turbines installed while increasing total capacity and energy output. Additionally, fewer turbines result in less direct land disturbance for infrastructure like roads and pads, minimizing environmental impacts on ecosystems and wildlife. However, these benefits must be balanced with community concerns, such as visual impacts and equitable distribution of economic benefits, as landowner payments may become more concentrated.

The article "Life Cycle Assessment of a Wind Farm Repowering Process" by Martínez et al. [3] examines the environmental impacts associated with repowering wind farms through a life cycle assessment (LCA). Their results highlight that repowering can lead to a 30% reduction in greenhouse gas emissions over the entire life cycle of a wind farm. By increasing resource efficiency and lowering the ecological footprint compared to initial installations, repowering has been shown to be a more sustainable option.

2.2 Knowledge Gaps

This thesis addresses critical gaps in understanding the potential of wind repowering in Europe. One key gap in current literature is quantifying the additional wind capacity that can be achieved through repowering, compared to decommissioning and replacement in Europe. Existing studies assess the potential benefits of repowering but lack detailed analyses incorporating turbine power curves and site-specific wind characteristics. Additionally, there is limited exploration of how the repowering of potential sites can alter the power density regionally. This thesis addresses this gap by modeling repowering scenarios, estimating capacity and energy projections of 2050 at both regional and European scales, and providing a clearer comparison to baseline repowering strategies.

Moreover, another significant gap is the incomplete economic assessment of repowering. Many studies emphasize the effects of repowering on the levelized cost of electricity (LCOE) but do not fully account for decommissioning costs, repowering costs, and infrastructure reuse. This thesis fills this gap by incorporating a detailed cost model that evaluates repowering and decommissioning costs, offering a detailed comparison of financial outcomes while also providing financial metrics for both scenarios.

Lastly, the environmental benefits of wind repowering, particularly in terms of land use, remain underexplored at a continental scale. While repowering can significantly reduce land requirements by reusing existing sites and infrastructure, few studies provide scenario-based analyses quantifying these impacts. This thesis addresses this gap by assessing land-use efficiency under repowering and no-repowering scenarios, focusing on metrics like land area savings and power density. This analysis highlights repowering's role in minimizing environmental footprints while supporting sustainable wind energy expansion.

2.3 Research Question

This study addresses the Research Question: **"What are the differences in wind generation capacity, costs, and land use between implementing a repowering strategy and not repowering in Europe by 2050?"**

This study evaluates the potential of wind repowering in Europe by comparing multiple scenarios and approaches for future wind capacity development. It analyzes the achievable capacity expansions, economic trade-offs, and land-use implications of each scenario and compares them to the baseline scenario of decommissioning and replacement. The core emphasis lies in quantifying the long-term capacity gains and financial advantages of repowering, which are essential for understanding its viability as a sustainable energy strategy.

To address the main research question, the following sub-questions have been identified:

1. What is the total power capacity potential of wind turbines reaching the end of their operational lifetime in Europe, categorized by region, year, and how big is the maximum capacity and energy yield achievable through wind repowering?
2. What are the estimated costs of decommissioning versus repowering aging wind turbines, and how do these compare in terms of economic feasibility?
3. What are the avoided environmental impacts, particularly regarding land use, by choosing repowering over constructing new wind farms?

The results can directly be applied to energy system models developed within the research group, and contribute to the European research project JustWind4All [27]. Ultimately, evidence-based recommendations can be provided to policymakers and stakeholders aiming to accelerate Europe's energy transition.

3 Methods

I use a model that contains three sub-models the capacity, costs, and land-use model presented with flowcharts that detail the inputs, outputs, and internal processes. Figure 6 maps the processes of each sub-model of the Methods section,

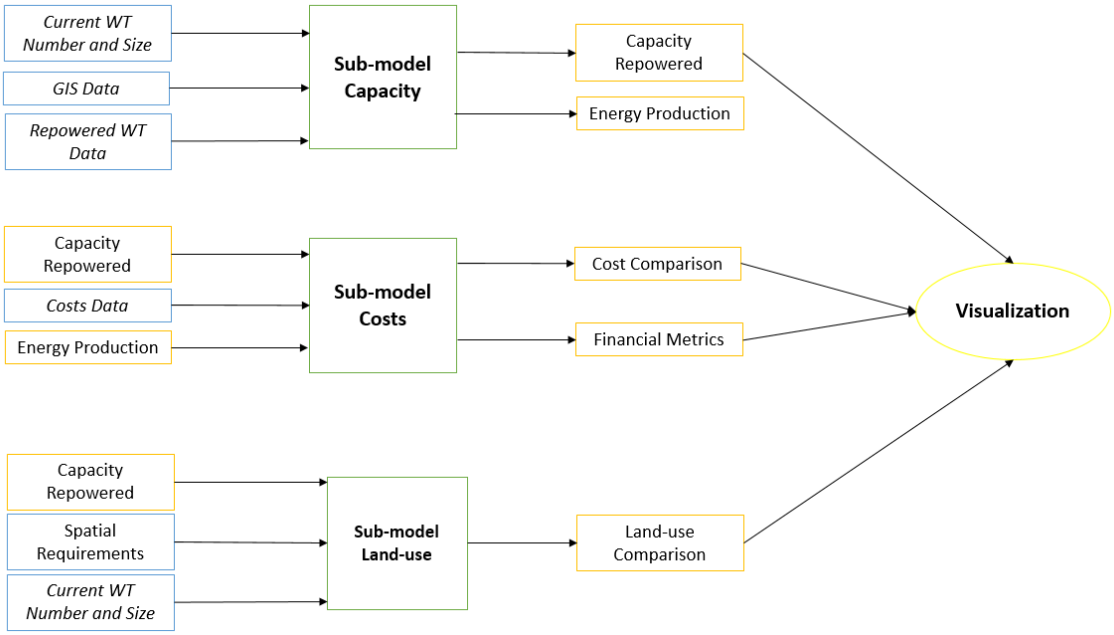

Figure 6: Overall model flowchart - Capacity- Costs- Land-Use

As wind parks reach the end of their design life, two main strategies were investigated, based on site-specific technical, land-use, and economic factors. Table 1 summarizes each approach and briefly discusses the key considerations of each scenario.

Table 1: Repowering / Decommissioning & Replacement Strategies

Scenario	**Description**
Repowering	Dismantle the existing turbine and install modern, higher-capacity turbines on existing foundations when a wind turbine reaches its operational lifetime. The reuse of the existing infrastructure (grid, substations, roads, etc.) lowers the capital expenses.
Decommissioning & Replacement	Completely dismantle turbines and infrastructure, clear the site, build new foundations, and install the same turbine model at an alternate location.

3.1 Capacity Model

The Capacity Model calculated the potential capacity expansion of the repowering strategy when applied to the European continent. The results acquired show for each wind park in Europe if repowering is feasible, and if so what's the capacity expansion potential.

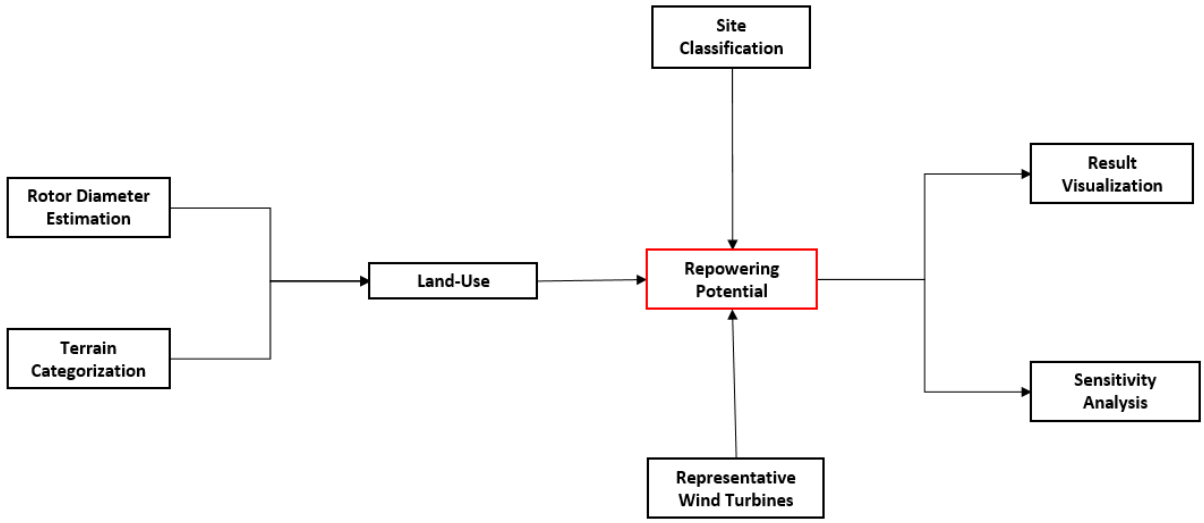

Figure 7: Capacity sub-model workflow

Depicted in Figure 7 is the capacity sub-model used to estimate repowering potential across Europe. The process begins by clustering all required input data, then derives each turbine's rotor diameter and categorizes its terrain type (flat vs. complex). Next, the model applies each turbine's design life to predict its decommissioning year and filter out non-operating units. It then incorporates site classification and land-use constraints, and finally references a candidate list of new turbines to determine how much capacity can be replaced or upgraded. The final output includes the decommissioning year of outdated turbines, the new turbines that will replace them, and the resulting capacity difference while ensuring the spatial occupation of the turbines remains unchanged. Finally, a sensitivity analysis follows, altering the land restrictions reflecting on capacity gains for different levels of land flexibility.

3.1.1 Data Acquisition & Pre-Processing

Different wind park data and GIS maps were necessary for the modeling process, such as a global wind farms database, site specifications (Wind speeds, elevation, IEC class), and data for the existing and new wind turbines. These data inputs were essential for completing the data accumulation phases. The accuracy of the data had to be high because a detailed data analysis and visualization process was conducted. This step not only provided a clearer understanding of the data but also highlighted potential patterns and insights critical for the study, thus making the accuracy of the data a crucial parameter.

For the data on global capacity, a database with the globally installed wind turbines was necessary. The main database that was used was provided by The Wind Power - Wind energy databases [7], which presents a significant amount of the installed wind turbines globally, 38444 entries to be exact, with many of their characteristics. Namely, the variables of interest are the capacity, location, hub height, commissioning, and decommissioning dates as well as whether the wind park is onshore or offshore. Moreover, the model of the wind turbine and the manufacturer are necessary information for the model presented in the following chapter.

The incompleteness percentage for a column is calculated using the formula:

$$\text{Incompleteness Percentage} = \left(\frac{\text{Number of invalid cells}}{\text{Total Number of Entries}} \right) \times 100\% \quad (1)$$

The number of invalid cells represents the total count of entries considered invalid, which may include **null** values or specific placeholders indicating missing data, such as **#ND**. Additionally, the total number of entries refers to the complete count of rows within the column.

Table 2: Comparison of completeness percentages for each category in the European and Onshore Europe datasets. Red-highlighted data represents information that was not used in the study.

Category	**Onshore Europe Completeness (%)**	**European Completeness (%)**
Area	99.85	99.86
Total power	99.47	99.38
Longitude	97.62	97.68
Latitude	97.62	97.68
Number of turbines	97.30	95.39
City	94.02	91.34
Manufacturer	93.37	91.43
Commissioning date	95.73	93.66
Turbine	86.93	85.14
Hub height	76.53	74.92
Developer	42.05	42.24
Owner	28.15	29.87
Operator	33.25	32.89
2nd name	14.36	14.49
State code	2.83	2.75
Altitude/Depth	6.93	7.41
Decommissioning date	6.38	6.28

Table 2 was created to evaluate the completeness of the database. The percentage of the non-defined and blank objects was calculated for each database column. Fields such as State code, Altitude/Depth, and Decommissioning date consistently show high error percentages, exceeding 90%, indicating widespread incompleteness due to future projection operational uncertainties. Operational data, including Owner, Operator, and Developer, remain problematic, with error rates above 57%, but they are not necessary for this research. Conversely, technical parameters such as Hub height and Turbine exhibit moderate error percentages, with onshore Europe demonstrating slightly better documentation. Locational data, including Latitude and Longitude, is consistently well-documented, with error percentages below 3%, reflecting strong locational data coverage.

Parameters marked in bold indicate parameters of interest for the capacity model. Categories with completeness levels below 75%, highlighted in red, are considered unreliable for use in the model due to their high incompleteness, and for that reason, they are not used as input for the model.

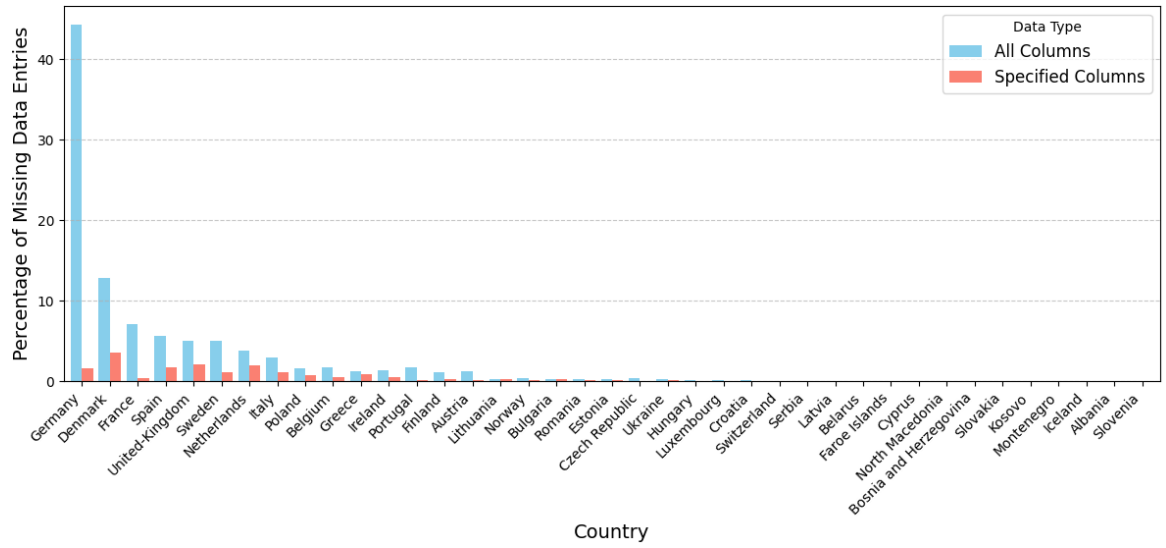

Figure 8: The Wind Power - Wind energy database incompleteness percentages by country [7]

Not all countries share the same percentage of missing values. Based on that fact, Figure 8 was created to identify the countries that cause the incompleteness in the dataset. The calculation was made by filtering out all the wind parks that had one or more blank or non-defined entries in their description. The specified columns are the variables of interest previously mentioned. It is clear that in terms of specified data, the database is accurate enough to be trusted as an input in the model. With Denmark with the highest error percentage of 3.6% followed by the United Kingdom with 2.3% and the Netherlands with 1.9 %, these countries also have the highest amount of entries in the database due to their high wind capacity (See Figure 28).

GIS-Based Wind Resource & Topography

A map was designed to evaluate the total onshore installed capacities of each country in Europe, with data from The Wind Power database [7]. Even if some countries are not in the European Union, they were evaluated for being part of the European region. This map visualizes the distribution of onshore wind turbine parks in Europe, highlighting regional disparities and areas of concentrated development. Each dot represents a wind park, with different colors depending on the total capacity of each wind park, offering insights into the wind energy adoption per country across the continent.

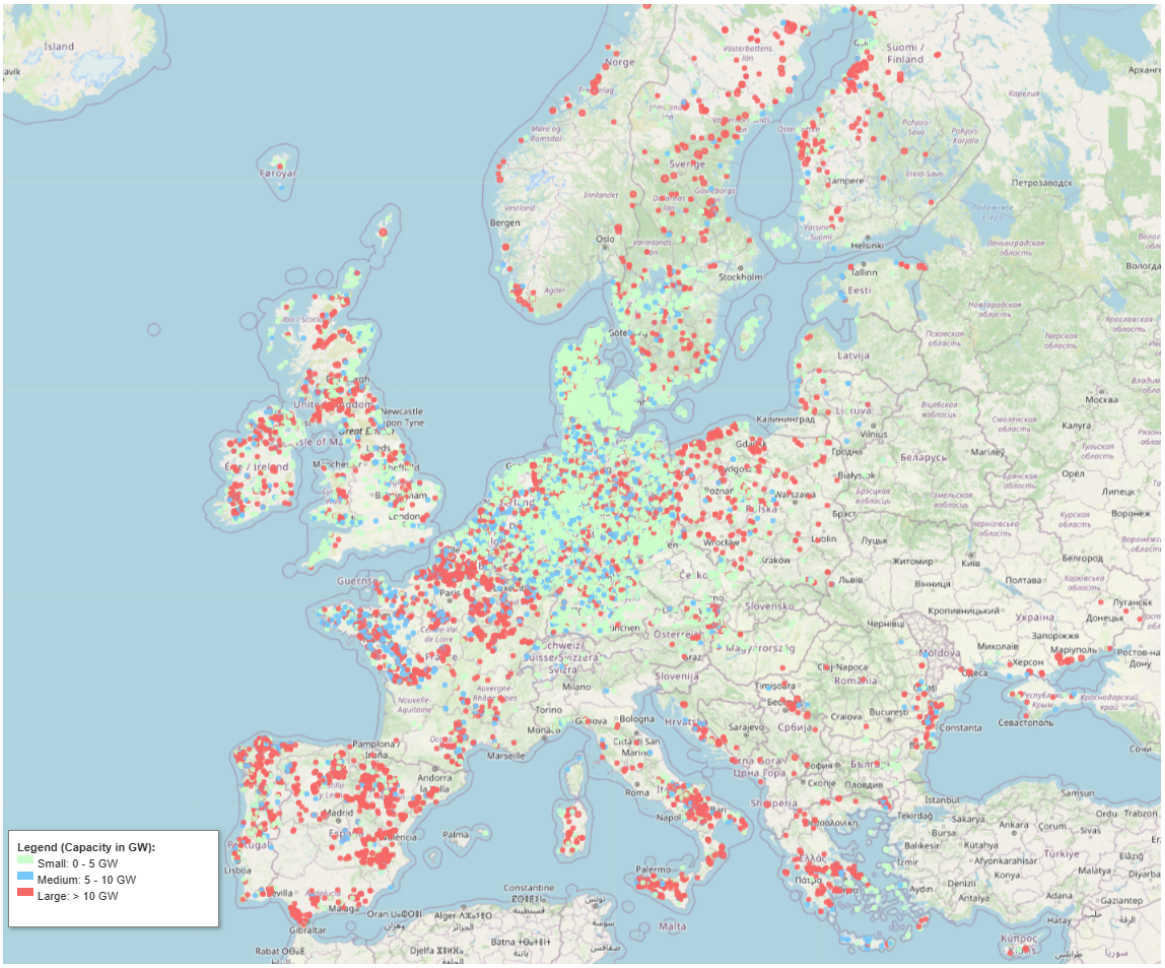

Figure 9: Installed onshore wind turbine capacity per country in the region of Europe with different colors for differ wind park sizes [7]

Regions with the highest density of wind turbines include Germany, Denmark, the United Kingdom, and the Iberian Peninsula. Germany stands out with particularly dense clusters in its northern and central regions, driven by favorable wind conditions and robust policy support. Denmark also exhibits a high concentration of installations, reflecting its leadership in renewable energy and strong reliance on wind power to meet its energy needs. Similarly, the UK and Ireland show significant turbine density along coastal regions, leveraging their wind-rich environments.

Southern Europe, particularly Spain and Portugal, features notable installations, demonstrating the successful integration of wind energy despite a climate traditionally dominated by solar energy [49]. Scandinavia, including Sweden and Norway, also shows significant deployment, complementing their energy mix. In contrast, Eastern Europe and Southeastern Europe reveal sparse coverage, with limited installations in Poland, the Baltic states, and parts of Italy.

GIS-Based IEC Wind Class Assignment

The first step in calculating repowering potential was to identify the classification of the onshore wind turbines currently installed in Europe. Based on the IEC 61400-1 [16] regulations published in 2019, wind turbines into classified depending on the wind speed and turbulence conditions of the selected site.

The parameter values apply at hub height and:

Table 3: Basic parameters for wind turbine classes (2019) [16]

Wind turbine class	**I**	**II**	**III**	**S**
V_{ave} (m/s)	10	8.5	7.5	
V_{ref} (m/s)	50	42.5	37.5	Values specified by the designer
$V_{\text{ref,T}}$ (m/s) (tropical)	57	57	57	
A+ I_{ref}	0.18	0.18	0.18	
A I_{ref}	0.16	0.16	0.16	
B I_{ref}	0.14	0.14	0.14	
C I_{ref}	0.12	0.12	0.12	

- V_{ave} is the annual average wind speed.
- V_{ref} is the reference wind speed average over 10 minutes.
- $V_{ref,T}$ is the reference wind speed average over 10 minutes applicable for areas subject to tropical cyclones.
- A+, A, B, C designate categories for turbulence intensity:
  - **A+**: Very high turbulence characteristics.
  - **A**: Higher turbulence characteristics.
  - **B**: Medium turbulence characteristics.
  - **C**: Lower turbulence characteristics.
- I_{ref} is a reference value of turbulence intensity.

For example, the Vestas V66/2000 (66m rotor diameter, 2000 kW generator) is a Class I turbine, suitable for sites with annual average wind speeds above 10 m/s. It has a specific power of 1.7 m^2/kW and would yield a capacity factor of 22.3% in central Scotland. In comparison, the larger-bladed V80/2000 (Class II, 2.5 m^2/kW 398 Wm^-2) would yield 31.4%, and the V110/ 2000(Class III, 4.8 m^2/kW 210 W/m^-2)would yield 47.9% in the same location. All are 2 MW turbines, but one produces twice as much energy as the other. This simplified comparison overlooks the constraints on turbine spacing but shows how the energy yield differs for different turbines at the same location [50].

The dataset lacked detailed information on site-specific conditions for the installed and operational wind turbines. To address this gap, data from the Global Wind Atlas v.3 [8] was incorporated. This dataset provides a GIS file that identifies the classification of each location based on its longitude and latitude across all continents. Using this information, wind classifications were systematically assigned to each existing onshore wind park in Europe. This approach ensures that capacity upgrades for repowered wind parks are more accurate, as the model incorporates wind conditions as constraints. The model aligns with site-specific wind characteristics by restricting replacements to wind turbines within the same classification, thereby maintaining compatibility with the existing environmental conditions.

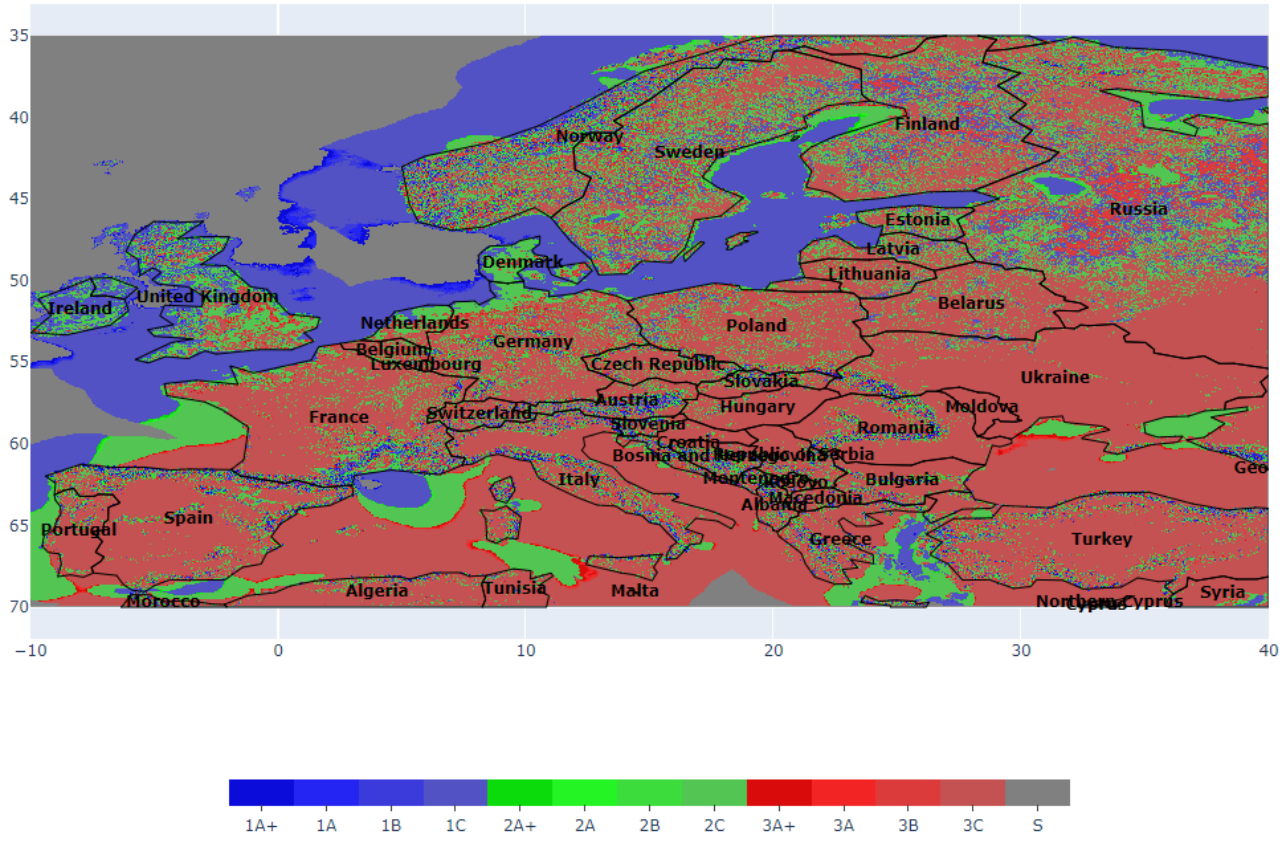

Figure 10: IEC wind classification map of Europe based on global Wind Atlas v.3 [8]

Finally, Figure 10 illustrates the classification map that was used in this study to identify site-specific qualifications and constraints. These 13 different classes are presented in the bottom label with different colors, and it can be seen that most European countries have a type of low wind speed sites on the onshore, mostly occupied by classes 2 and 3. The majority of the wind turbine locations of the Wind Power - database [7] belong to classes 2C and 3A+, as shown in Table 4.

IEC_Class	Percentage (%)
2C	42.13
3A+	31.62
2B	16.12
3A	5.59
2A	2.46
3B	1.30
2A+	0.44
3C	0.18
1C	0.06
S	0.04
1B	0.00

Table 4: Percentage distribution of IEC Classes in Europe.

GIS-based Elevation Map of Europe

The database completeness on Altitude/Depth is 6.93%, so an external GIS file was used as an input

for the elevation data of Europe. Figure 11 shows the elevation map of Europe. This elevation data was necessary to determine the complexity of the terrain in which the wind turbines were installed.

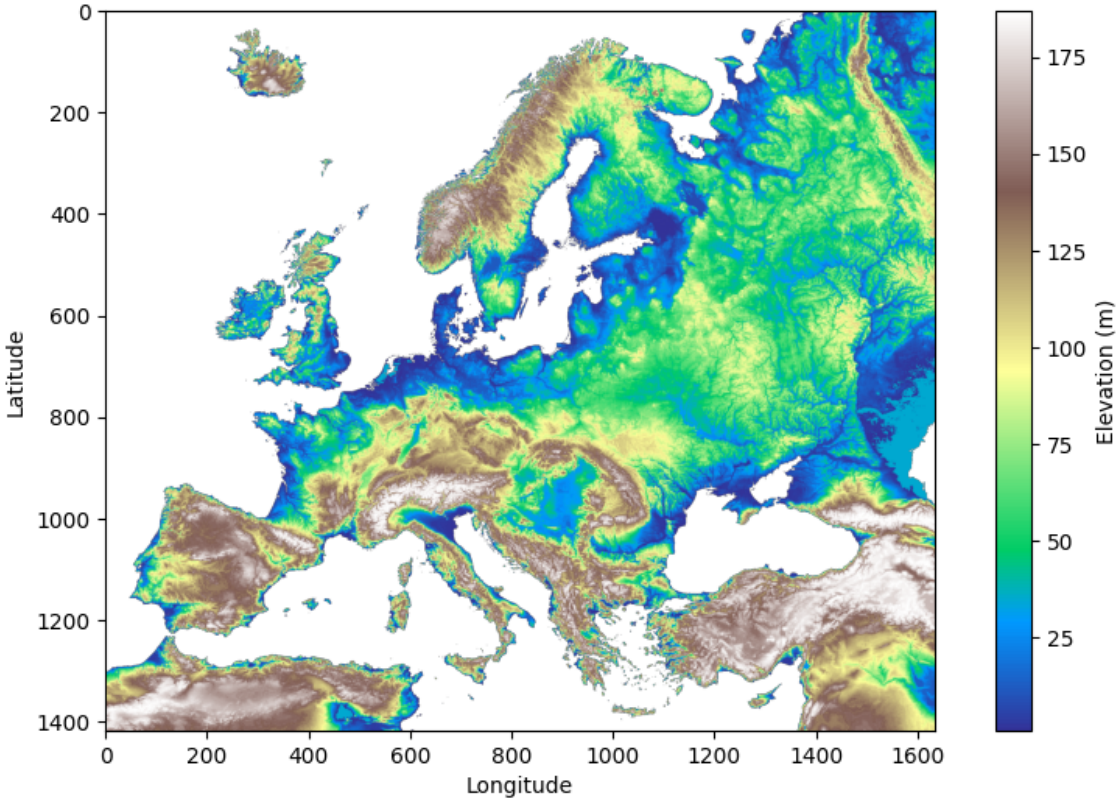

Figure 11: Elevation map of Europe (EuroDem) [9]

Terrain complexity affects air quality and, consequently, the capacity factor of a wind turbine. Therefore, different layouts are selected for complex versus flat terrains. EuroDEM [9] provides the elevation above sea level for every location in Europe and was used to evaluate the complexity of wind farm terrain based on the altitude differences in nearby areas.

Operating Life Expectancy of the Turbines

It was found in the literature that the life span of a typical wind turbine is approximately 20 years. The lifetime expectancy of wind turbines is influenced by various factors, including structural loads, fatigue damage, maintenance strategies, and environmental conditions. Wind turbines are typically designed for a lifespan of 20 to 30 years. However, the variability in wind speeds, dynamic loading, and operational stresses often leads to earlier degradation of components, such as rotor blades and drivetrain systems, especially in offshore environments [51]. Another source indicates that wind turbines are typically designed to operate for 20 to 25 years, though this lifespan can be extended with proper maintenance and favorable environmental conditions [52]. In some cases, turbines have been found to age prematurely, with actual lifespans of just 7 to 10 years before requiring significant replacements [53].

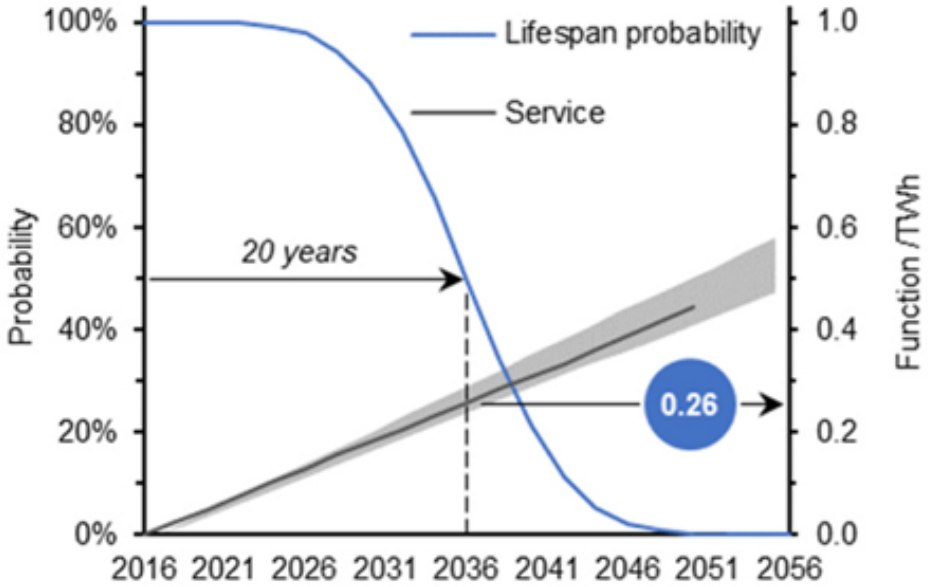

Figure 12: Wind turbine lifespan probability model (blue line) and function (function range between medium and high wind speed shown in Grey with USA average represented as a black line) over time (for a single wind turbine installed in 2016)[10].

Begona et. al. [54] in the "Life Cycle Assessment of two different 2MW class wind turbines" and publications from National Renewable Energy Laboratory such as the Cost of Energy Review [55] also assume 20 years of operational lifetime for wind turbines. Additionally, Figure 12 illustrates the lifespan probability and the production of a wind turbine installed in 2016 in the United States over 40 years. After 20 years, the energy production of wind turbines drops significantly below 50% and the service costs increase linearly (Grey line), making the turbine non-profitable [10]. Lastly, the distribution of the operational lifetime of wind turbines with data from The Wind Power-Wind energy databases [7] is depicted in Figure 13. The number of onshore entries is 1615, while the mean and median years for onshore operational life are 19.47 and 20, respectively.

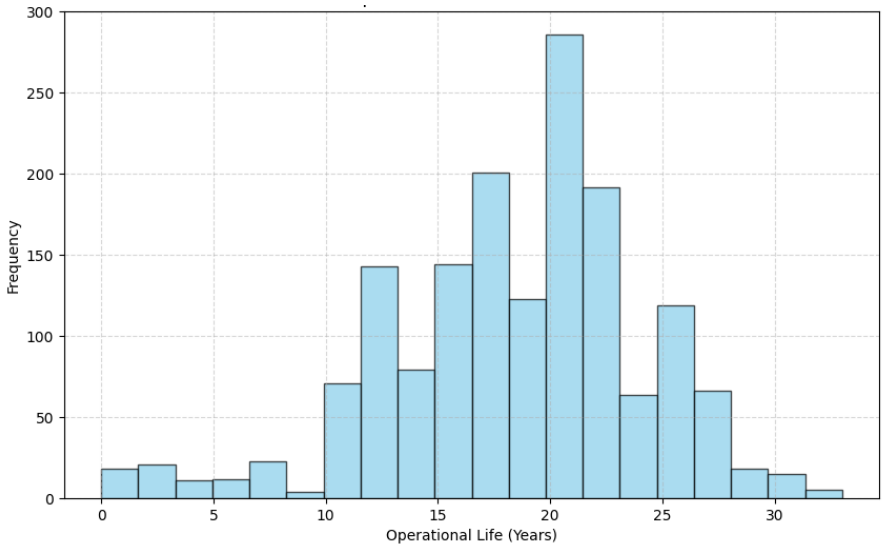

Figure 13: Operational life distribution of onshore wind turbines acquired from the The Wind Power Database [7]

As a wind turbine ages, its energy production gradually declines due to wear and efficiency losses, while operation and maintenance costs continue to rise. Eventually, the increasing expenses outweigh the revenue generated, rendering the turbine unprofitable. As a result of both the studies and the database operational life distribution, a 20-year operational lifespan is assumed for the modeling process.

3.1.2 Rotor-Diameter Estimation

Additionally, an estimation of rotor diameters was necessary due to the lack of specific data for all wind turbines. Rules of thumb in the literature use the rated power and rated wind speed, assuming a constant air density. According to C. Bak. et. al. [56], the rotor diameter for a wind turbine is given by

$$D = \sqrt{\frac{4P_{\text{rated}}}{\pi\,\rho\,v_{\text{rated}}^3\,C_p}}. \tag{2}$$

The Wind Power Database [7] that was used lacked data such as the rated wind speed of the installed wind turbines, so another method was selected to estimate the rotor diameters of the turbines. Even though there was no data in the technical specifications of the turbines apart from Capacity and Hub Height, the turbine's name column was complete by almost 87%. A pattern in the naming of the wind turbines was observed, which was followed by most of the manufacturers. Wind turbine models are often coded using manufacturer-specific conventions, making direct extraction of rotor diameter non-trivial.

To extract the rotor diameters function uses pattern matching (via regular expressions) tailored to different manufacturers:

- **Gamesa, Nordex, Vestas, Enercon**: Format "G90/2000" ,Rotor = 90m.
- **Siemens, Siemens-Gamesa**: Format "SG 8.0-167 DD", Rotor = 167m.
- **GE Energy**: Format : "3.2-130", Rotor Diameter = 130m.
- **Senvion**: Format "MM92/2050" , "6M126" Rotor = 92m, 126m.

According to the different patterns for every manufacturer, the rotor diameters of the wind turbines were extracted at a rate of 67%, equal to 16,195 turbines. For the remaining 33% of the entries, this technique could not be used due to the high variance in manufacturers and naming methods. Therefore, for the rest of the models, regression was applied to estimate the rotor diameters.

Regression

Due to the inaccuracies of the linear regression that was implemented (See Appendix A.1.1), other regression techniques were considered. Several studies have explored the relationship between wind turbine rotor diameter and generator capacity using regression analysis. For instance, NYSERDA, in their report "Analysis of Turbine Layouts and Spacing Between Wind Farms" [57], utilized a non-linear extrapolation method to predict rotor diameters for specific capacities. Similarly, Gonzalez and Arantegui [58], in their study on the technological evolution of onshore wind turbines, applied a comparable non-linear regression technique for the same purpose. Figure 14 presents the regression lines from these two studies.

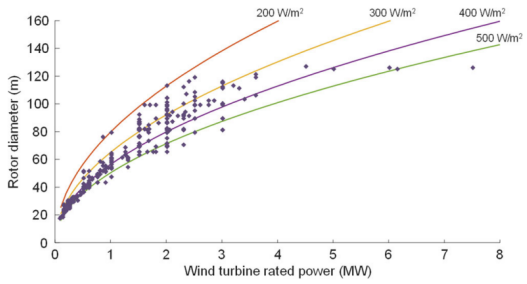

(a) Regression analysis from Gonzalez and Arantegui [58].

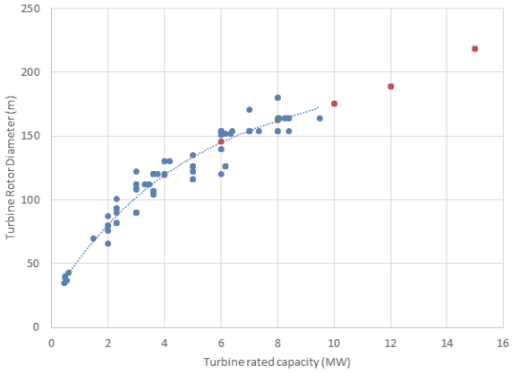

(b) Non-linear extrapolation from NYSERDA [57].

Figure 14: Comparison of regression lines from Gonzalez and Arantegui (left) and NYSERDA (right).

Traditional linear regression may fail to capture the multiplicative nature of this relationship. Instead, a power-law model is assumed, which can be linearized via logarithmic transformation. This log-log regression approach is well suited for such power-law relationships because it transforms a nonlinear multiplicative model into a linear one, facilitating parameter estimation and interpretation. This methodology has been successfully applied in previous studies [59, 58, 57] and is adopted in this work to robustly model the relationship between rotor diameter and turbine capacity.

Log-Log Regression

We assume that the relationship between the rotor diameter, y, and the single wind turbine capacity, x, follows a power-law model:

$$y = c\,x^b,$$

where c is a constant and b is the scaling exponent. Taking the base-10 logarithm of both sides, we obtain:

$$\log_{10}(y) = \log_{10}(c) + b\,\log_{10}(x).$$

By defining $a = \log_{10}(c)$, the model becomes:

$$\log_{10}(y) = a + b\,\log_{10}(x).$$

This equation is linear in the transformed variables and can be estimated using ordinary least squares regression [59]. Once the parameters a and b are estimated, the original relationship is recovered as:

$$y = 10^a\,x^b.$$

The following graphs are the results of the regression algorithm. Figure (a) illustrates the non-linear relationship between rotor diameter and capacity of the turbines, and Figure (b) plots both axes to a logarithmic scale to depict the log-log relationship.

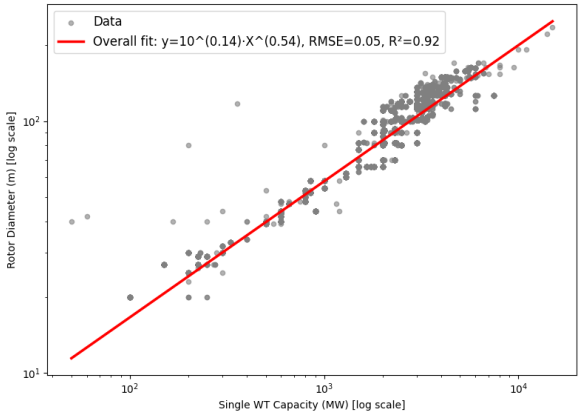

(a) Log-Log regression: Rotor diameter vs. Single WT capacity

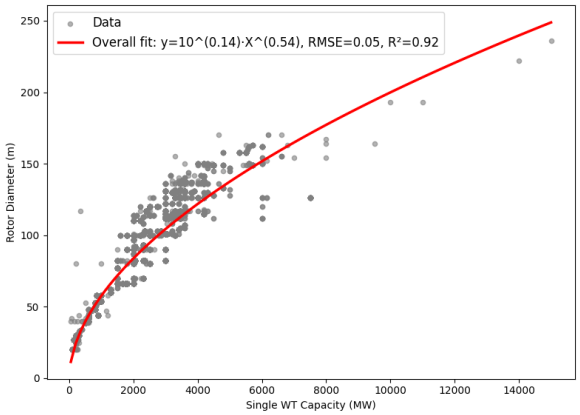

(b) Linear scale of rotor diameter vs. Single WT capacity

Figure 15: Comparison of regression fits in Log-Log and Linear scales.

To improve the accuracy of rotor diameter approximations, we enhanced our log–log regression model by clustering the turbines into distinct classes. Instead of using a single regression fit for all data, separate fits were computed for each class, thereby capturing class-specific scaling behaviors. For the turbine division into classes, only the number of the class was considered instead of using both the number and the letter (Turbulence indicator), for simplification purposes. This targeted approach significantly reduced prediction errors by tailoring the model to the unique characteristics of each cluster.

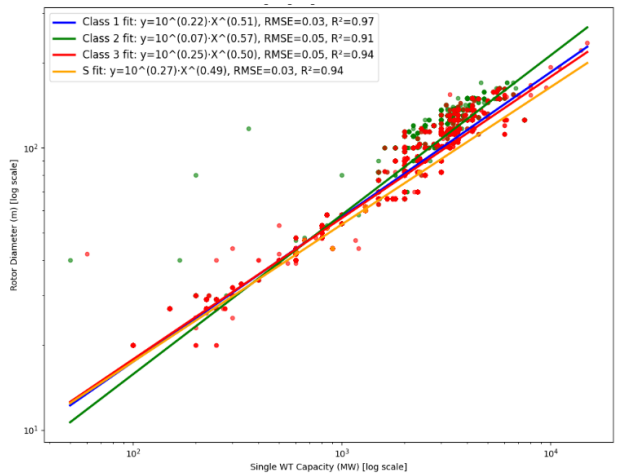

(a) Log-Log Regression: Rotor Diameter vs. Single WT Capacity with Classification Division

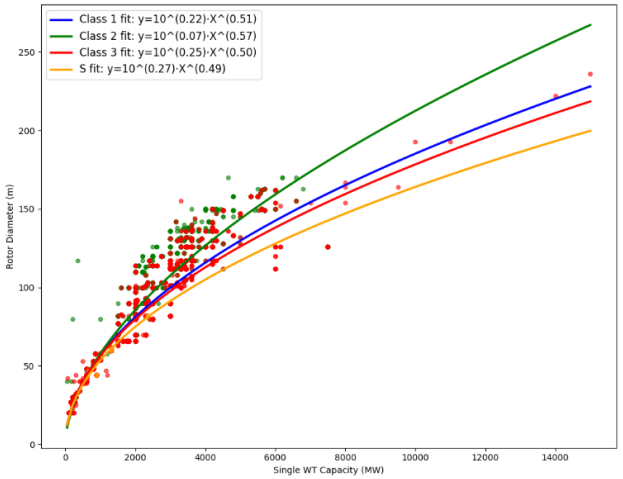

(b) Linear Scale of Rotor Diameter vs. Single WT Capacity with Classification Division

Figure 16: Side-by-side comparison of regression plots.

Figure 16 illustrates four regression curves on a linear scale, each corresponding to a different turbine-class grouping. The curves are derived from log–log regressions, which capture the power and rotor diameter relationship. By plotting these best-fit curves on a linear scale, the class-specific differences become visible: each class shows a slightly different intercept and slope, indicating variations in how rotor diameter scales with capacity. Notably, the data points cluster reasonably well around their respective fits, suggesting that class-based modeling is effective at reducing prediction errors.

Regression Group	RMSE	R^2
Class 1	0.03	0.97
Class 2	0.05	0.91
Class 3	0.05	0.94
S	0.03	0.94

Table 5: Regression Error Parameters for Different Turbine Classes.

The regression models for the various turbine classes show strong predictive accuracy. Notably, the Class 1 regression demonstrates exceptional performance with an R^2 value of 0.97, accompanied by a minimal RMSE of 0.03, indicating a nearly perfect fit. Similarly, the S regression shows a high level of accuracy, with an RMSE of 0.03 and an R^2 of 0.94. Although the Class 2 and Class 3 regressions have slightly higher RMSE values and marginally lower R^2 values, due to their larger sample size, they still capture the underlying relationships effectively.

The table below presents some results of the log-log regression algorithm, validating its results:

Turbine Model	Extracted RD (m)	Real RD (m)	Error (%)
Tornado 250/26	28.1	26	8.08
B37/450	37.7	37	1.89
NM48/750	48.7	48	1.46
NM60/1000	56.4	60	-6.00
NM52/900	53.51	52	2.90
B62/1300	64.2	62	3.55
NM72c/1500	72.7	72	0.97
1.5s	72.7	70.5	3.12
2.5xl	97	100	-3.00
AW-3000/116	107.6	116	-7.24
B82/2300	85.4	82	4.15
SL 3000/113	107.6	113	-4.78
A3000	107.6	116	-7.24
126 4.0 MW	126.6	126	0.48

Table 6: Comparison of Extracted and Real Rotor Diameters with Updated percentage error.

It is evident from the data presented in Table 6 that the algorithm's error is minimal, although it tends to increase for larger wind turbines. Consequently, Figure **??** was created to identify the distribution of predicted rotor diameter values, revealing a high density of predictions in the 10 m to 100 m range.

3.1.3 Estimation of Wind Park Land-use

To evaluate the repowering potential of currently installed wind parks, estimating their total spatial occupancy is essential. A crucial factor in this assessment is the selection of turbine spacing, which directly affects energy output and land use efficiency. Research indicates that reducing turbine spacing increases wake effects, leading to diminished energy production and higher fatigue loads on downstream turbines [60]. For instance, array losses can exceed 20% when the crosswind spacing is below 4D, whereas these losses decrease significantly when spacings exceed 5D, as illustrated in Figure 17.

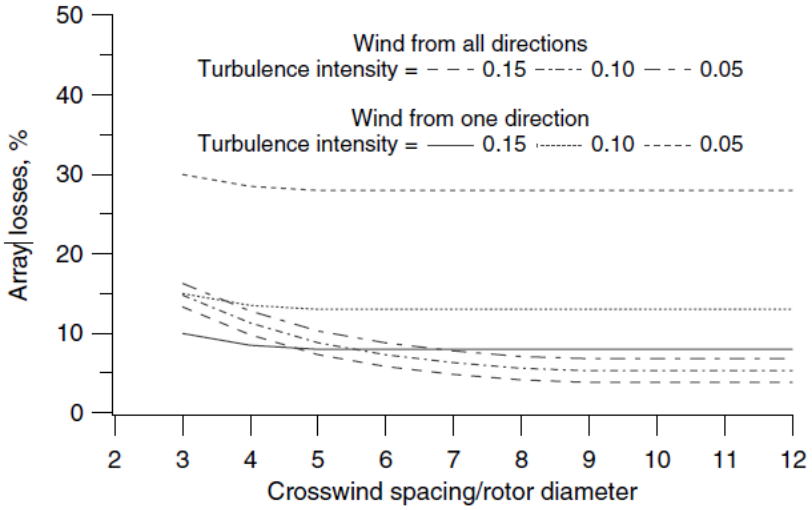

Figure 17: Wind farm array losses [11]

While closer turbine spacing increases the number of turbines per unit area, it negatively impacts the average energy yield per turbine due to increased turbulence and wake interactions [11]. The widely accepted 7D × 4D configuration minimizes wake losses to below 10% while remaining compatible with real-world wind farm layouts and industry best practices [60]. For wind farms situated in flat terrains, an optimal turbine spacing of 7D × 4D was selected, aligning with research that suggests spacing in homogeneous, flat landscapes should range between 5D and 7D in the prevailing wind direction [61]. This configuration minimizes wake interactions while ensuring efficient land use and high energy production [62]. Additionally, earlier studies by Crespo et al. (2003) have recommended spacing between 5D to 9D in the prevailing wind direction and 3D to 5D perpendicular to the wind flow to reduce wake losses and optimize land utilization [63]. The 7D × 4D spacing represents an averaged value within these ranges, balancing energy efficiency and land constraints.

For wind farms located in complex terrains, a different spacing layout is necessary due to wind speed acceleration over hills, increased turbulence, and topography-induced flow separation [64]. To mitigate these effects, a wider spacing of 10D in the prevailing wind direction and 6D perpendicular is advised. Studies by Whiteman et al. (2016) [65] suggest that this spacing reduces turbulence-induced fatigue loads and enhances energy yield in hilly or mountainous regions. Similarly, Crespo et al. (2003) recommended spacing between 7D to 12D in the prevailing wind direction and 5D to 7D perpendicular to account for terrain-induced turbulence and variations in wind speed [63, 66]. Given these findings, a slightly narrower 9D × 6D configuration was chosen as a representative value for complex terrain scenarios.

The selected spacing values for this thesis project—7D × 4D for flat terrains and 9D × 6D for complex terrains—were determined as a balanced representation of multiple studies. These values were chosen to reflect the most common recommendations while ensuring optimal energy capture, reduced wake effects, and practical land use efficiency. The averaging approach ensures that the model incorporates a realistic and widely accepted spacing strategy, accommodating both energy production goals and physical site constraints.

The total area occupied by wind farms operating in Europe was calculated based on the information given. The calculation was performed using the following formula:

$$\text{Total Area (km}^2\text{)} = D \cdot S \cdot N$$

Where:

- D: Estimated Rotor Diameter (km)
- S: Spatial Requirements per Single Wind Turbine (km^2)
- N: Number of Operating Wind Turbines

3.1.4 Terrain Complexity: Ruggedness & Slope

As mentioned in the previous section, different layouts need to be selected for different terrains. Europe is not flat, and the landscape is different for every country as depicted in figure 11. For that reason, an algorithm was developed to assign a classification based on the terrain of all the wind farm locations in Europe based on the Global Wind Database [7].

The algorithm classifies each turbine site as being in flat or complex terrain by analyzing a localized window of DEM data using two complementary metrics: the Terrain Ruggedness Index (TRI) and slope analysis. In a 5×5 pixel window centered at each site, the TRI is computed as the average absolute difference in elevation between the central pixel and its neighbors, following the methodology introduced by Riley et al. [67].

Simultaneously, the local slope is estimated using a finite-difference gradient method that calculates the derivatives in both the x and y directions, and then converts the gradient magnitude into degrees. Based on calibration and a review of the literature—including studies by Barthelmie et al. (2009) [68] and McKenna et al. (2022) [50]—the chosen threshold values are 3.0 m for TRI and 5.0° for slope. Sites where either metric exceeds its threshold are classified as complex, while those that do not are assigned as flat. Table 7 summarizes the range of TRI and slope thresholds reported in the literature along with the values adopted in this study, which represent a balanced compromise between sensitivity to topographic variability and robustness in automated terrain classification.

The Terrain Ruggedness Index (TRI) is computed as follows:

$$\text{TRI} = \frac{1}{N} \sum_{i=1}^{N} |E_i - E_c| \tag{3}$$

where E_c is the center pixel elevation, E_i represents the surrounding pixel elevations, and N is the number of pixels in the window.

The local slope is calculated using the finite-difference gradient method:

$$\text{Slope} = \arctan\left(\sqrt{\left(\frac{\partial z}{\partial x}\right)^2 + \left(\frac{\partial z}{\partial y}\right)^2}\right) \tag{4}$$

The selected thresholds—3.0 m for TRI (see Equation (3)) and 5.0° for slope (see Equation (4))—were chosen after comparing multiple studies and calibrating against regional datasets, ensuring that the classification accurately distinguishes between flat and complex terrain for large-scale wind resource assessments.

Table 7: Comparison of TRI and Slope threshold values for terrain classification

Metric	Literature Range	Selected Value	References
TRI (m)	2.5–3.5 m	3.0 m	Riley et al. (1999) [67]; Barthelmie et al. (2009) [68]
Slope (°)	4.5°–6.0°	5.0°	Barthelmie et al. (2009) [68]; McKenna et al. (2022) [50]

3.1.5 Future of Wind Turbine Specifications

Furthermore, based on the GWEC Global Wind Report [69], the primary reason for increasing rotor diameters, even in low-power wind turbines, is to enhance energy capture. Larger rotors sweep a greater area, allowing turbines to harness more wind energy. For example, in 2000 an average 2 MW wind turbine had a diameter of 76m [69], the new models, for example, Vestas V110-2.0 MW [70] and GE's 2 MW [71] Platform have a rotor diameter of 110 and 116 meters respectively.

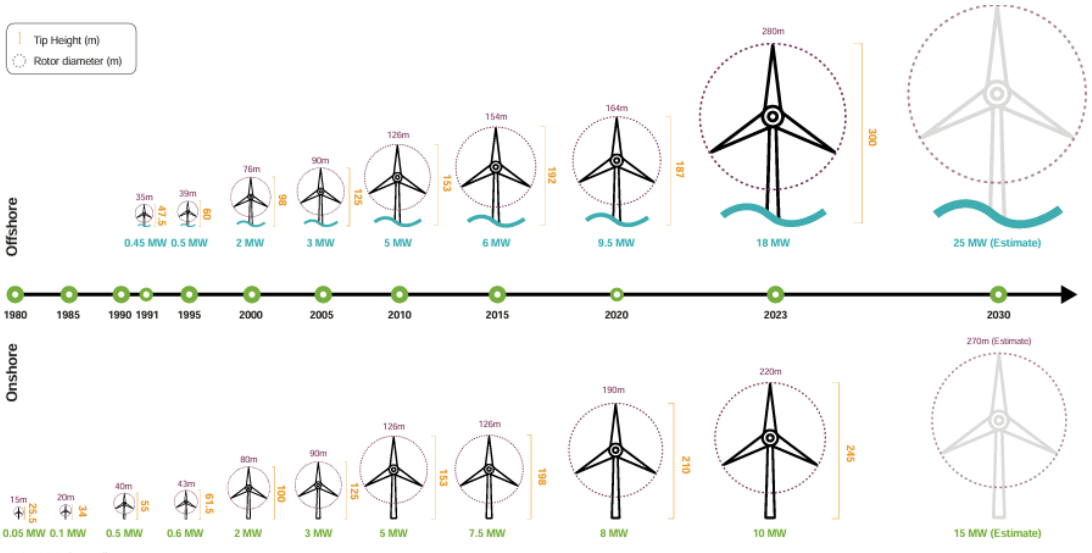

Figure 18: Wind turbine size trends 2000-2030

In Figure 19, the plots of the average wind turbine size and the maximum wind turbine size over the period from 1975 to 2022 are shown. The first graph displays a steep upward trend in the average wind turbine size, starting from less than 500 kW and reaching a cap of 4.3 MW, indicating exponential growth. The second graph presents the maximum wind turbine capacity for each year within the same period, starting from under 500 kW and reaching a maximum of 15 GW in 2021.

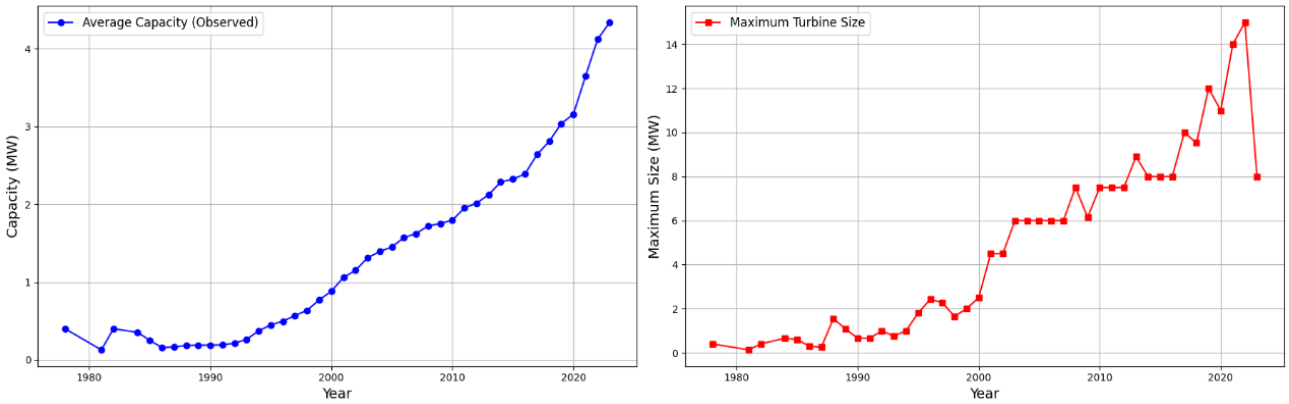

Figure 19: Average (Left) and maximum (Right) wind turbine size annually (1975-2022)

The growth in both average and maximum wind turbine sizes, as reflected in Figure 19, demonstrates a clear trajectory of innovation necessary to enhance energy production and simultaneously reduce costs. Over the past 35 years, technological advancements have enabled a doubling of tower heights and rotor diameters, accompanied by an eightfold increase in nameplate capacities [72].. This aligns with findings from McKenna et al [73], which indicate that overcoming challenges in materials, such as adopting carbon-fiber composites for longer rotor blades and improving transport and installation techniques, is pivotal for achieving higher capacities. Moreover, Simon Watson on Quantifying the Variability of Wind Energy [74] emphasizes the importance of precise wind resource assessment and forecasting for siting larger turbines, which can maximize energy yield while accounting for increased variability at greater hub heights. This upward trend in turbine size is expected to persist, driven by the combined benefits of larger turbines—higher energy output and economies of scale—though diminishing returns and increasing material and structural challenges that may eventually impose practical limits.

This trend is evident in both onshore and offshore wind turbines. In 2023, offshore wind turbines had an average rotor diameter of approximately 280 meters, up from 35 meters in 1991. It is expected that in 2030, new designs will make it possible to reach an average rotor diameter of over 350 meters [75]. Additionally, larger rotors allow turbines to capture more wind energy by sweeping a greater area, which is particularly beneficial in areas with lower wind speeds. This increase in energy capture leads to higher electricity production and improved efficiency [76].

The database's last entry was in 2022, the current largest wind turbine models that have been installed and producing energy for offshore and onshore are at 26 and 15 MW, respectively. As of January 2025, the largest onshore wind turbine is the Sany Renewable Energy SI-270150, a 15-megawatt (MW) prototype installed in Jilin Province, China [77]. This turbine features 131-meter-long blades, resulting in a swept area of approximately 57,256 square meters, equivalent to nearly 11 American football fields. In the offshore sector, China's Dongfang Electric Corporation has completed a 26 MW offshore wind turbine, which is currently the world's largest. This turbine has a hub height of 185 meters and a rotor diameter exceeding 310 meters, with a swept area surpassing 10 standard football fields [78].

3.1.6 Representative Repowered Wind Turbines

Moreover, representative wind turbines for Repowering need to be included in the model. Larger and newer models are necessary because the projection to 2050 requires the installation of newer wind turbines rather than replacing the old wind turbines to keep the same capacity. For that reason, a few wind turbines were selected to represent the future technologies presented in the following table 8.

Table 8: Wind turbine models sorted by IEC class [17, 18]

Model	Capacity (MW)	Rotor Diameter (m)
IEC Class I		
Siemens SWT 3-101	3.0	101
Siemens SWT 4.3-120	4.3	120
Siemens SWT 3.6-107	3.6	107
Siemens Gamesa SG 6-154	6.0	154
Siemens Gamesa SG 8.5-167	8.5	167
Nordex 100-3300	3.3	100
IEC Class II		
E82 3000	3.0	82
Vestas V90-3.0	3.0	90
Vestas V136-4.0	4.0	136
Siemens Gamesa SG 4.5-145	4.5	145
IEC Class III		
Enercon E-115-3.000	3.0	115
Siemens SWT 6.6-170	6.6	170
Nordex N131-3000	3.0	131
IEC Class S		
Enercon E126-4000	4.0	126
Enercon E175-6000	5.0	175
Vestas V150-6.0	6.0	150
Vestas V164-9500	9.5	164
Nordex 149-4500	4.5	149

Recent trends in wind energy development show a shift towards larger capacity onshore wind turbines, with manufacturers prioritizing turbines of 5MW and above. Although 2MW wind turbines were common in onshore installations, advancements in turbine efficiency and cost-effectiveness have driven an industry-wide preference for larger models. These developments align with global market trends favoring higher-capacity turbines due to their increased energy yield, reduced levelized cost of electricity (LCOE), and improved performance in varying wind conditions. Additionally, modern wind farms are being designed with fewer but more powerful turbines to optimize land use and minimize wake effects, further reinforcing the transition away from sub-2 MW turbines [69]. Considering all of the above, it is expected that the new onshore wind turbine installations will mostly feature capacities of 2MW and above, with a growing emphasis on multi-MW models exceeding 4MW, which were incorporated in Table 8.

3.1.7 Repowering Strategy Approaches

To assess repowering potential under varying degrees of spatial flexibility, we implemented several distinct algorithms. Each methodology computes Europe's overall capacity gain by substituting existing turbines with models drawn from Table 8. Although the replacement rules differ between approaches, they all share the same objective: maximizing the achievable capacity within each site's available area.

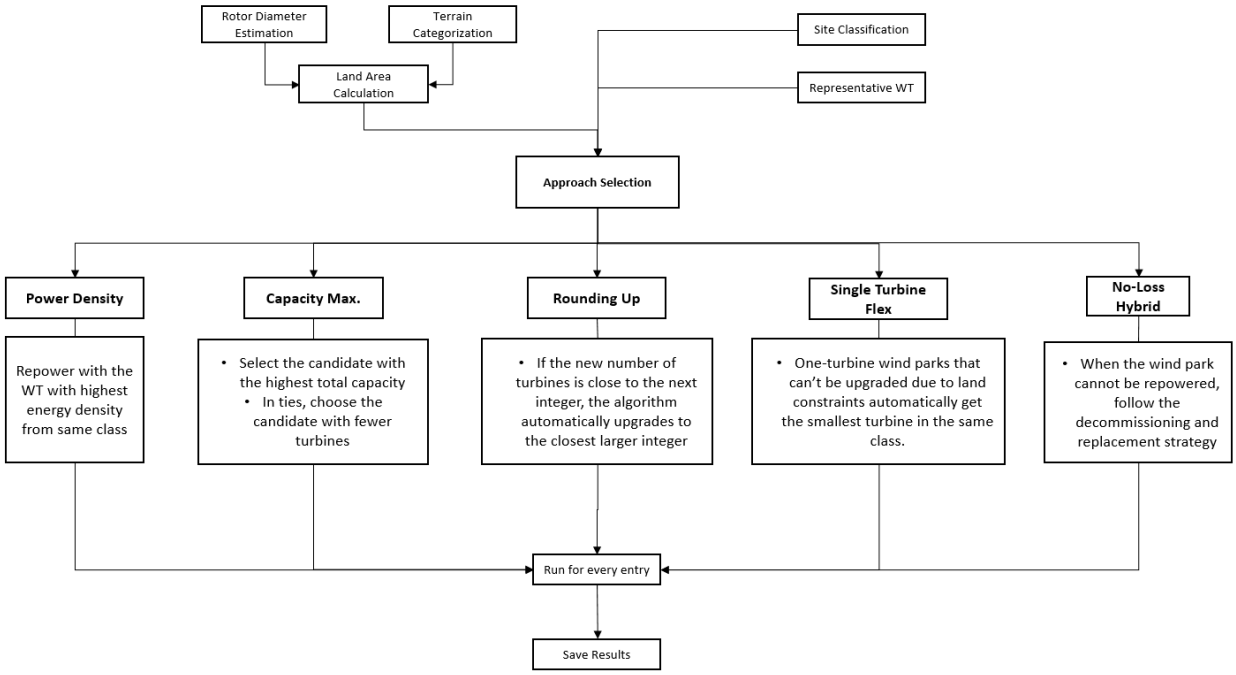

Figure 20: Detailed analysis of each repowering approach capacity calculation flow chart

The methodology which is depicted in Figure 20 integrates site-specific parameters—namely, the IEC wind class and terrain type, with turbine performance characteristics to yield an optimal configuration for each wind farm. The process begins with the extraction and pre-processing of wind farm data from the main database [7], where sites are filtered based on their decommissioning date, on the 20-year operational life assumption, and assigned an IEC classification that reflects local wind conditions. The land occupied by the previously installed wind turbines is considered available land area for the new repowered turbines, which layout is selected based on terrain slope and ruggedness index. A predefined turbine database, structured with model identifiers, rated capacities, rotor diameters, and corresponding IEC classes, serves as the candidate pool for selection.

Approach 1: Power Density (PD)

The turbine selection function filters the candidate list by IEC class. For each turbine in this subset, the performance ratio is computed as:

$$PowerDensity = \frac{Capacity(MW)}{LandAreaRequired(m^2)} \tag{5}$$

The turbine with the highest capacity density is selected as optimal, as it offers the highest output per unit of land area, which is a critical consideration in maximizing site efficiency.

Following selection, the script estimates the number of turbines that can be installed within the existing wind farm area by dividing the total available area by the area required per turbine. Multiplying this count by the turbine's capacity yields the total new potential capacity, enabling a direct comparison with current configurations.

Approach 2: Capacity Maximization (CM)

Capacity Maximization Approach 2 follows the same strategy as approach 1 but with three additional

modifications:

- It evaluates each candidate by calculating its total capacity (number of turbines × individual turbine capacity) based on the available area.
- It also aims to maximize the overall installed capacity on the site, potentially favoring a turbine that allows more capacity even if its energy density is lower than another option.
- Lastly, if multiple candidates yield the same total capacity, the selection favors the candidate requiring fewer turbines, and if all options allow only one turbine, it defaults to the turbine with the smallest rotor diameter.

The exact steps that are followed throughout this approach are the following:

1. Area Determination and Turbine Fit:
   For each turbine candidate in the specified IEC class, the required land area per turbine is calculated as:
   $$\text{Area} = \begin{cases} 28 \times (\text{Rotor Diameter})^2, & \text{for flat terrain} \\ 54 \times (\text{Rotor Diameter})^2, & \text{for complex terrain} \end{cases}$$
   The theoretical number of turbines that can fit in the available area is then:
   $$n_{\text{turbines}} = \frac{\text{Available Area}}{\text{Turbine Area}}$$
2. Candidate Selection Based on Total Capacity and Tie-Breaking:
   For each turbine candidate, the total capacity is computed as:
   $$\text{Total Capacity} = \text{Turbine Count} \times \text{Individual Turbine Capacity}$$
   The candidate with the maximum total capacity is selected. In the event of a tie, the candidate requiring fewer turbines is favored.

Approach 3: Rounding up (RU)

An additional function is now added to Approach 2, loosening the spatial constraints of the repowering strategy. If the new number of turbines is close to the next integer, the algorithm automatically upgrades to the closest larger integer.

- Rounding Rule for Turbine Count:
  If $n_{\text{float}} \geq 1$, the script calculates the integer part $\lfloor n_{\text{float}} \rfloor$ and the fractional part $n_{\text{float}} - \lfloor n_{\text{float}} \rfloor$. The turbine count is determined by:
  $$\text{Turbine Count} = \begin{cases} \lceil n_{\text{float}} \rceil, & \text{if } (n_{\text{float}} - \lfloor n_{\text{float}} \rfloor) \geq 0.8 \\ \lfloor n_{\text{float}} \rfloor, & \text{otherwise} \end{cases}$$
  If $n_{\text{float}} < 1$, the turbine count defaults to 1.

Approach 4: Single Turbine Flex (STF)

We follow the same methodology as in Approach 3, with one key modification:

- For wind parks with a single turbine, spatial constraints do not apply. Instead, these parks can upgrade to the smallest rotor turbine available within the same classification, maintaining the number of turbines at 1.

Approach 5: No-Loss Hybrid (NLH)

This approach ensures no wind farm suffers a loss of capacity during repowering, treating each site's original capacity as a minimum performance threshold:

- **Preserve or Improve Capacity:** No degradation of existing capacity is permitted; each park's post-repowering output must match or exceed its current power.
- **Decommission & Full Replacement Fallback:** If, after the implementation of Approach 2, there is no class-consistent upgrade, a complete rebuild is then carried out, installing the same turbine models reaching the original capacity.

The fallback step not only maintains baseline generation but also captures any opportunity for additional gains offered by modern, higher-performing turbines. A hybrid scenario considering both repowering (Approach 2 logic) and decommissioning and replacement in specific cases.

Approach 6: No-Loss Hybrid (NLH–Yield Based)

This approach builds on Approach 2's fixed-area repowering by adding an annual energy-yield comparison against a full decommissioning & replacement:

- **Repowered Scenario:** Compute repowered capacity per Approach 2 (no spatial flexibility) and estimate its annual energy yield using the site's wind data and each turbine's power curve.
- **Replacement Scenario:** Calculate the annual energy yield for a complete decommissioning and rebuild scenario.
- **Selection:** Compare the two yields and choose the scenario (repowered vs. replacement) that delivers the higher annual energy output.

Note: Approach 6 is only possible once reliable energy-yield estimates exist for both repowering and replacement scenarios.

Table 9 was created to summarize all the differences in the wind turbine selection method and additional functionalities between approaches.

Table 9: Comparison of approaches for wind turbine selection

	WT Selection Method	**Evaluation Metric**	**Rounding / Upgrade**	**Special Handling**
1. PD	Short WT based on power density	Selects the highest density within a class	Floor division	Only considers candidates with $n_{\text{float}} \geq 1$
2. CM	WT with the highest total capacity	Computes Total Capacity = Turbine Count × Capacity; selects maximum (ties by fewer turbines)	Floor division	Excludes any model if the area cannot fit at least one turbine
3. RU	Same as Approach 2	Same as Approach 2	Rounds up if fractional part $\geq$ 0.8; otherwise floor	Only considers candidates with $n_{\text{float}} \geq 0.8$
4. STF	Same as Approach 2, with enhanced selection, with forced installation	Same as Approach 2	Rounds as in Approach 3; forced installs default to count = 1	Single-turbine parks that can't fit normally: selects the smallest rotor in the same class
5. NLH-Capacity Based	Same as Approach 2, except when upgrades fail, decommissioning & replacement is applied	Ensures repowered capacity meets or exceeds original capacity	Floor division for same-class; fallback installs minimum turbines to match the original	Decommissions all legacy turbines and rebuilds using the full model pool to guarantee no capacity loss
6. NLH-Yield Based	Same as Approach 2, except selection is based on annual energy yield; if repowering yields less, retains original	Maximizes annual energy production by choosing the higher of original vs. repowered yield	Floor division for same-class; fallback installs minimum turbines to preserve or improve yield	Decommissions all legacy turbines and rebuilds using the full model pool to guarantee no yield loss

3.1.8 Key Assumptions

Table 10: Key Assumptions – Capacity Model

Assumption	Details
Operational lifetime	All turbines are assumed to have a 20-year operational life expectancy.
Wind Turbine Classification	To classify the turbines based on location, turbulence was ignored—each site is described solely by wind speeds.
Decommissioning schedule	Each turbine is replaced exactly in the year it reaches its 20-year lifetime; no early retirements or life extensions are modeled.
Construction lead time	A one-year build period is assumed, so repowered capacity only comes online one year after decommissioning.
IEC classification	Every site is assigned an IEC wind class via the Global Wind Atlas v3; repowered turbines must belong to the same class as the legacy machine.
Terrain classification	Terrain is classified solely based on topographic ruggedness index (TRI) and slope; no additional site-specific geotechnical constraints are included.
Turbine spacing & land use	Layout rules are uniform: flat terrain uses 7 D × 4 D spacing; complex terrain uses 9 D × 6 D. Turbine layouts otherwise remain identical to legacy parks.
Candidate turbine database	A predefined pool of modern turbines (sorted by IEC class) is treated as exhaustive—no emerging or prototype machines beyond this pool are considered.
Land availability	Once a turbine is decommissioned, its entire footprint (foundation, roads, grid connection) is assumed fully available for repowering—no competing land uses.

3.2 Energy Yield Model

The energy production of both existing and repowered wind parks was quantified using meteorological data and wind turbine power curves for every wind park in Europe. All analyses were implemented in Python, employing the atlite [79] library for resource assessment. Atlite is an open-source Python library built on xarray that transforms weather data, such as wind speeds or solar radiation, into energy system-relevant datasets. It's optimized for efficient performance, which makes it particularly suitable for working with large-scale weather datasets. That was not the only method used to calculate the energy yield; another version can be found in chapter A.1.2, where an approximation of the power curves and a wind characterization via Weibull distribution was applied. Ultimately, for more accurate results and optimized time management, the first method was selected to be implemented for this thesis.

All the datasets used for the annual energy production calculation include:

Table 11: Data Sources and Their Descriptions

Data Source	Reference	Description
Existing wind park characteristics	[7]	Location, nameplate capacity, number of turbines, commissioning dates
Repowered wind park characteristics	-	Recommended turbine models, repower counts, new capacity and layouts
ERA5 reanalysis fields	[80]	Hourly gridded wind speed, temperature and pressure data at 100 m
Spatial boundaries (NUTS regions)	[81]	Administrative regions for aggregation of wind park metrics
Manufacturer power curves	[82]	Turbine-specific power output vs. wind speed performance curves

ERA5, produced by the Copernicus Climate Change Service at ECMWF, is the fifth-generation global climate reanalysis, extending from January 1940 to today. It delivers hourly estimates of a broad suite of atmospheric, oceanic, and land variables. In this study, we utilize the monthly 100 m wind-speed reanalysis data covering the period 2003–2022 [80].

Not all wind turbines of the old, existing turbine models were available, so a standardized power-curve method for each turbine was implemented. Specifically, each park's single-turbine capacity (kW) was matched to the closest model in a comprehensive manufacturer dictionary. A nearest-neighbor approach minimizes deviation between actual and representative capacities.

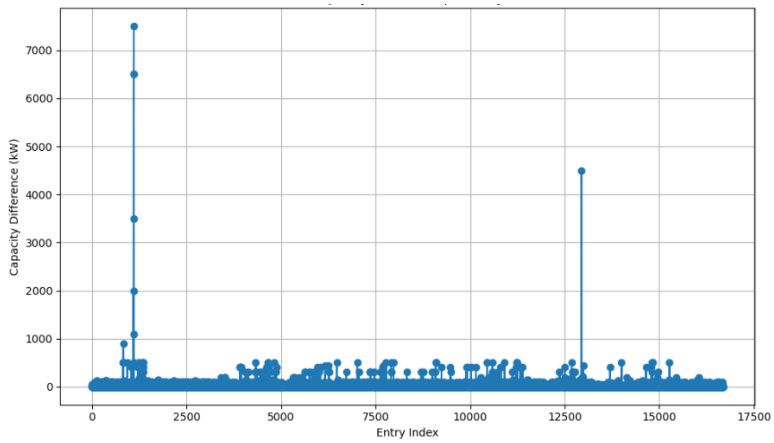

Figure 21: Difference in Rated Capacity Between Installed Onshore Turbines and Assigned Reference Models Across the EU

The new representative wind turbines are selected from a pool of many models acquired from the Renewable Ninja open-source scripts [7], and they are listed in Table 25, ranging from 100 KW to 7500 KW. The total deviation from the original wind turbines was 0.22 GW in total, which does not affect the results significantly. In Figure 21, each entry's difference from the representative is presented. The large spikes occur due to the 14 and 15 MW wind turbines installed in Denmark and

the Netherlands, creating a visually striking difference in capacity.

For each representative model, the layout points assigned to the entry are filtered, only retaining the total installed capacity per park. Then, a layout object is generated that maps point locations and capacities, and based on the powered curve, to compute hourly capacity factors within each NUTS polygon. Finally, the mean capacity factor per wind park is calculated by averaging over an 8,760-hour time series. Lastly, the annual energy production is calculated with the following formula:

$$E_{new} = C_{new}(MW) \cdot CF_{turbine} \cdot 8,760h \tag{6}$$

3.2.1 Key Assumptions

Table 12: Key Assumptions – Energy Yield Model

Assumption	Details
Meteorological data	Uses ERA5 hourly reanalysis at 100 m (2003–2022) to capture wind speeds; assumes this period and vertical resolution adequately represent long-term resource variability without further bias correction.
Resource-to-production conversion	Employs `atlite` to translate 100 m wind fields into hourly capacity factors for each park; assumes `atlite` interpolation and park-mapping algorithms yield accurate CF estimates.
Representative turbine matching	Existing turbines are paired with the nearest model from a predefined database; assumes any capacity mismatch (< 0.22 GW total deviation across all parks) is negligible.
Power curve fidelity	Applies manufacturer-provided power curves unchanged—no adjustments for degradation, low-temperature cut-out, or site-specific tuning; assumes these curves accurately reflect actual turbine performance at hub height.
Wake and availability losses	Ignores intra-park wake interactions and assumes 100 % availability (no downtime or grid curtailment); thus, each turbine operates at its theoretical capacity factor continuously.
Spatial aggregation	Assigns each wind park to its enclosing NUTS 3 polygon and averages CF over all grid cells within that region; assumes homogeneous wind conditions and turbine densities inside each NUTS 3.
Uniform hub height proxy	Treats ERA5 data at a uniform 100 m as a valid proxy for all actual hub heights (which may vary); assumes deviations in hub height do not materially affect estimated CF.
Time aggregation	Computes annual CF by averaging the 8,760 hourly values; assumes no significant inter-annual variability beyond the 2003–2022 window and that this average is representative for future-year yield estimates.
Curtailment and grid constraints	Excludes any losses due to local grid curtailment, transmission bottlenecks, or market dispatch rules; assumes all generated energy is deliverable and counted in total yield.
No future climate adjustment	Maintains the 2003–2022 ERA5 climatology for repowered turbines through 2050; does not model climate-change–induced shifts in wind patterns or extreme-event frequency.

3.3 Costs Model

For a complete evaluation of the strategies, a cost evaluation is required. Based on literature and similar studies, the costs of various sub-tasks were evaluated and cross-checked. The goal was to compare the costs between the two strategies and integrate these findings into the capacity model to provide key insights into the financial efficiency of repowering versus decommissioning in the EU. Additionally, metrics such as decommissioning and repowering costs per MW were assessed, and financial metrics such as LCOE, IRR, and payback periods were compared between the two modeled scenarios.

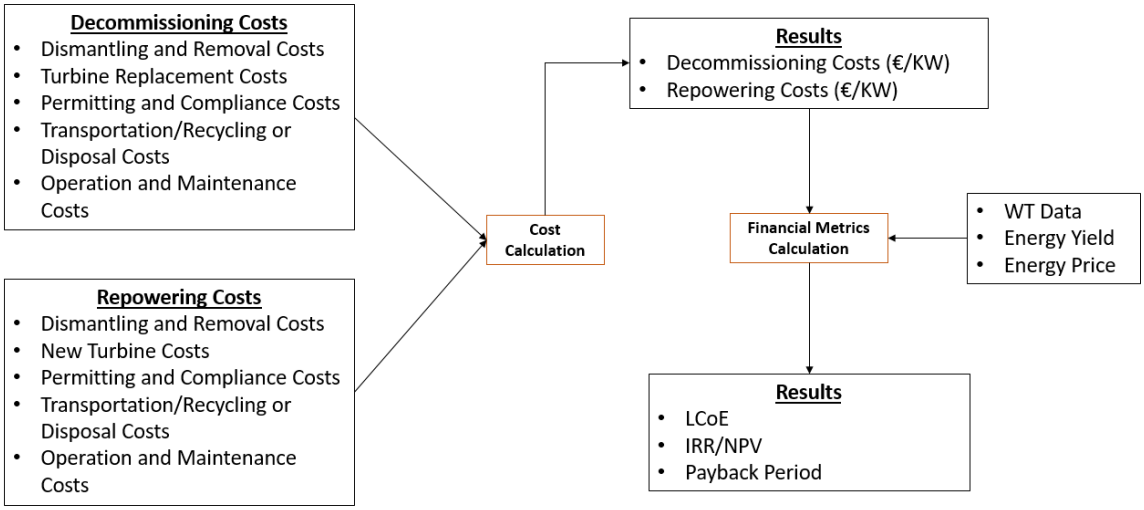

Figure 22: Costs sub-model

Figure 22 depicts the costs sub-model, which calculates the costs associated with decommissioning and repowering. Initially, the individual costs for each step of each strategy are used as an input into the model. Then, the costs per MW are calculated for both the decommissioning and repowering scenarios, considering the savings repowering can produce by reusing the existing infrastructure. Finally, based on the energy produced by the wind turbines and the results from the capacity model, financial metrics such as NPV, LCOE, payback period, and IRR are determined for each entry and each strategy.

3.3.1 Decommissioning vs. Repowering Cost Components

Turbine Dismantling and Material Recycling

Turbine dismantling involves the safe removal of the entire turbine, including blades, nacelle, and tower, using heavy machinery and specialized cranes. Various studies report a wide range of dismantling costs. For example, Colmenar et al. [83] acknowledge that pure dismantling and waste disposal costs are around €67.5/kW; when offset by a turnover from recycled materials of approximately €25.9/kW, the net dismantling cost comes to about €41.6/kW. Additionally, Cooperman [38] provides an estimate for tearing down a complete rotor at about $26/kW (approximately €26/kW at a hub height of 80 m), with an adjustment of about $0.40/kW for each meter of deviation from 80 m. Although these figures vary depending on turbine size, project location, and local labor/material costs, the key point is that even in repowering projects, where turbine removal is still required. The dismantling costs remain similar to those in full decommissioning, although salvage revenues from recycling metals (such as

steel, copper, and aluminum) help offset the overall expense. For example, Figure 23 illustrates some of these expenses of disposal and revenues of the recycling process of a Nordex wind turbine.

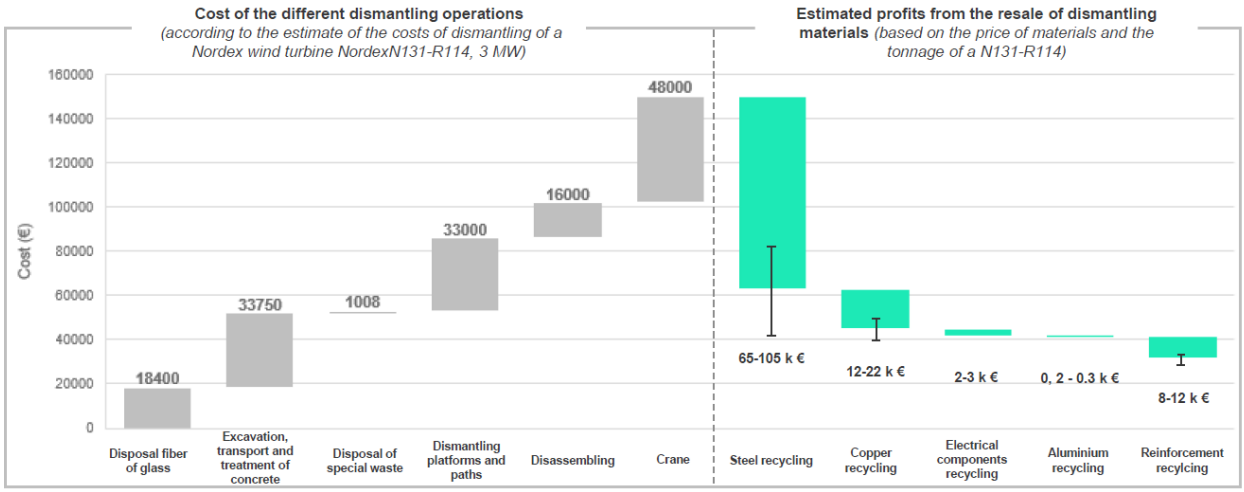

Figure 23: Decommissioning costs and recycling profits based on ADAME [12],Nordex estimation

Blade Disposal

Wind turbine blades are predominantly composed of composite materials, which present unique recycling challenges. Despite these challenges, the cost associated with blade disposal is relatively modest compared to other components of turbine decommissioning. Cooperman et al. [38] estimate that the cost for blade disposal is approximately €15/kW. This figure reflects the fact that blade processing—whether by mechanical recycling, grinding, or landfilling—accounts for only a small fraction of the overall lifecycle cost. Although there may be opportunities to recover some value through recycling or reuse of composite materials, the financial impact of blade disposal remains nearly identical in both decommissioning and repowering scenarios.

3.3.2 Capital Expenditure (CAPEX)

Civil Works

New foundation construction for onshore wind turbines typically represents a significant share of initial project capital costs. Studies indicate that foundations account for about 7–10% of the total installed cost of an onshore wind farm. In practice, this corresponds to roughly €50–150 per kW of installed capacity for new foundations, though the exact figure varies by project size and site conditions. For example, an NREL cost model estimated a foundation cost of about $59/kW (approximately €50–55/kW) for modern turbines [84]. On the other hand, when repowering existing wind farms, reusing the existing foundations can yield substantial cost savings per kW compared to building brand-new foundations. One industry report notes that a specialized foundation repowering solution can cut foundation-related costs by up to around 45% compared to new construction [85]. Often 0–€50 per kW in additional costs if reuse is viable. In ideal cases (same turbine rating), no new foundation expense is needed aside from inspections. If modifications are required, costs on the order of €10–30/kW may occur for reinforcement or adapters [86].

Grid Connection

One of the most significant benefits of repowering is the ability to reuse existing grid infrastructure. Typical grid interconnection costs can range around $100–300 per kW (approximately €90–270/kW) for new wind projects [13]. In greenfield developments, new grid connections must be established at considerable expense; however, repowering projects can bypass these costs by re-purposing existing substations, inter-array cables, and grid connections. Both the Sia Partners survey [87] and the NREL Report [84] illustrate that the pre-existing electrical infrastructure dramatically reduces capital outlay, enhancing the overall economic feasibility of repowering compared to new builds. In this study, the assumption is that new grid infrastructure is not needed for repowered projects, but a new substation is needed due to the increase in total power of the wind park.

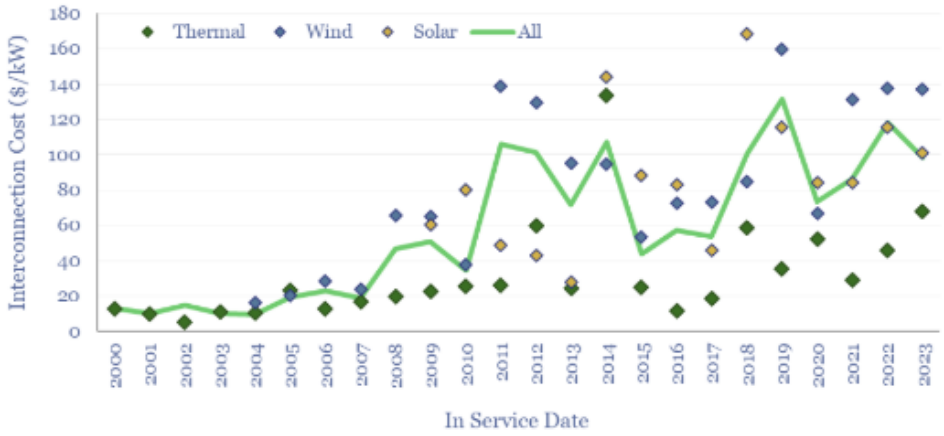

Figure 24: Cost of grid interconnection for solar and wind parks from 2000-2023 [13]

The cost of 100 $/kW is the cost of grid connection of all renewable energy sources based on Figure 24. This included the evacuation lines, the civil works and the substations. A more detailed analysis of these costs appears in the study of Antinio Colmenar-Santos et al. [45], which divided these costs into three categories. Table 13 indicates the values of each expense.

Category	Component	Cost (EUR/kW)
P&C&G grid	Civil works	11.3
	Supply and installation	4.2
Substation	High voltage level	30.7
	Medium voltage level	8.3
	Main transformer power	16.7
Evacuation line	—	34.8

Table 13: Cost breakdown by component (EUR/kW)

If the broken down costs are summed the result is 105.2 Eur/kW which is close to the study resulting in Figure 24. So the findings from Table 13 are considered as costs for the cost model.

Turbine Cost

In 2010, the total installation cost of an onshore wind turbine was USD 1,971/kW, which equates to about EUR 1,489/kW (2010 rates). By 2020, costs had fallen to USD 1,355/kW, or roughly EUR 1,192/kW (2020 rates) [14].

Figure 25 illustrates the weighted average total installed cost for onshore wind across 15 countries. Long-term IRENA data ranged between approximately USD 986/kW and USD 1,746/kW, with Japan

being a notable exception at USD 2,384/kW. Both Brazil and China reported installation costs below the global average. That same year, average wind turbine prices (excluding China) ranged from USD 706/kW to USD 1,040/kW, a significant decrease compared to 2022. By 2023, prices in most regions outside China had dropped by 41% to 64% compared to 2010 levels. In China, the decline was even more dramatic, with turbine prices falling 73% from USD 884/kW in 2010 to just USD 233/kW. So the price depends mainly on the manufacturer, classification, and country of origin, making the selection of one price for all wind turbines general.

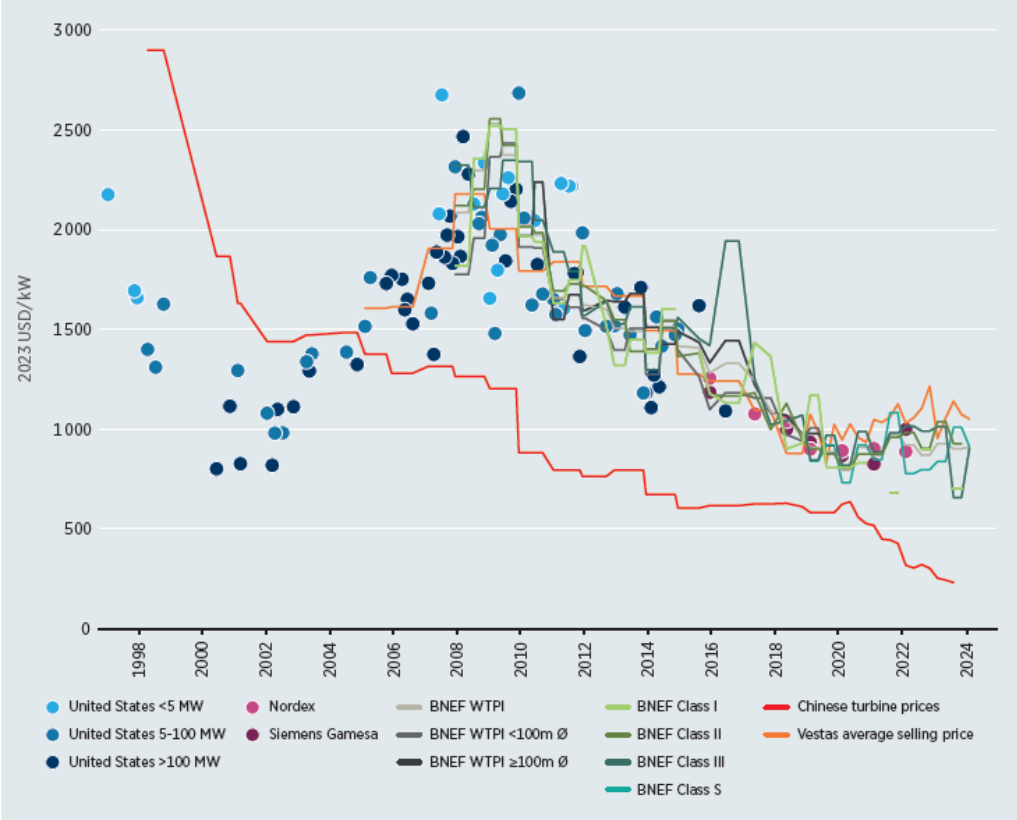

Figure 25: Wind turbine price indices and price trends, 1997-2023 [14]

Considering all of the above, the price set per KW of installed capacity in this study is set to 986 $/MW or 892,96 EUR/MW or 892,960 Eur/ MW (the conversion being done in 2025).

3.3.3 Operational Expenditure (OPEX)

According to the background study [88], wind turbine operational expenses are estimated at roughly 30 €/kW per year for the first 20 years, rising to about 60 €/kW per year during years 20–25 due to increased maintenance as turbines age. Industry sources such as Windustry and IRENA confirm that onshore wind OPEX typically falls within this range, indicating that while the initial capital outlay is high, the ongoing expenses remain relatively predictable. Furthermore, both the NREL Cost of Wind Energy Review: 2024 Edition [13] and the IEA Wind Task 26 report support these figures, and the IRENA "Renewable Power Generation Costs 2020" report [14], provides a detailed breakdown that is consistent with an average O&M of 30 €/kW per year initially, increasing to 60 €/kW per year thereafter [89]. A main assumption of this study is the operational life-time of the wind turbines, which is assumed to be 20 years; thus, the Operation and Maintenance costs are set to 30 €/kW.

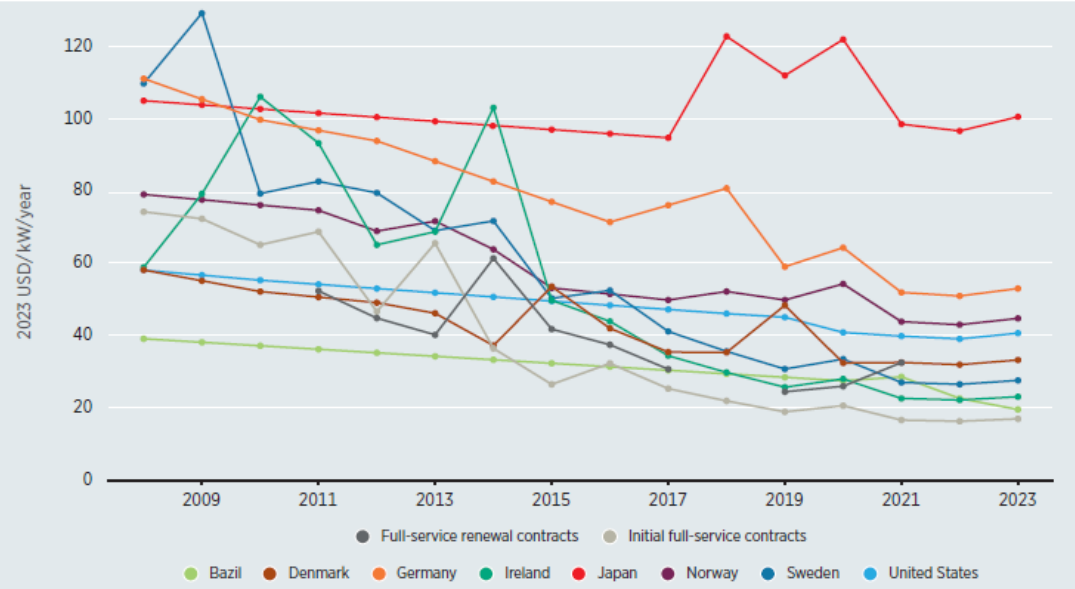

Figure 26: Full-service (initial and renewal) O&M pricing indexes and weighted average O&M costs in different Countries

In Figure 26, the O&M costs per country are presented from 2009 to 2023. Japan had the highest costs from 2010 until 2023, with an average of 105 USD/kW/year, followed by Germany and Norway. The lowest O&M costs are recorded in Brazil and Ireland, although Europe averages at 32.25 USD/kW/year or 29.67 EUR/kW/year (Conversion in Q2 of 2025). Therefore, assuming a price of 30 €/kW for this study is a reasonable estimate.

3.3.4 Costs Overview

By aggregating the cost components in Table 14, the total outlay for full decommissioning + new-build is € 1,267.1/kW, whereas repowering requires only € 1,077.4/kW, yielding a saving of €189.7 /kW. These figures assume a fixed new-turbine CAPEX of €892.96 /kW. However, the NREL 2024 Annual Technology Baseline projects that, with learning rates of 10 %, 14 % and 20% (per doubling of cumulative capacity), this baseline can be reduced by 10 % to 20 % by 2050 [19]. Table 15 shows the resulting CAPEX range for both approaches.

Table 14: Cost comparison between decommissioning + new build and repowering strategies (€/kW)

Cost category	Decomm. + New Build (€/kW)	Repowering (€/kW)	Reference(s)
Turbine dismantling	67.5	67.5	[83][38]
Material recycling	–25.9	–25.9	[87][38]
Roads	26	17.3	[87][38]
Blade disposal	15	15	[38]
Foundation construction	55	30	[33][44][45]
Grid connection	100	0	[45][84][13]
Substation	55.6	55.6	[33][84][45]
Evacuation line	34.7	0	[45]
Construction permits	47.2	25.9	[45]
New turbines CAPEX	892.96	892.96	[5][44][45]
Maintenance costs (annual)	30	30	[44][87]
Total cost	**1267.1**	**1077.4**	

Table 15: Projected onshore wind turbine CAPEX in 2050 under alternative learning-rate scenarios, with decommissioning & replacement strategy[19]

Scenario	Learning rate	2050 CAPEX (€/kW)	Decommissioning & Replacement (€/kW)
Conservative	10%	969.66	1140.3
Moderate	14%	926.5	1089.7
Advanced	20%	861.9	1013.7

3.3.5 Financial Metrics-LCOE, NPV & IRR Calculations

Financial metrics are valuable when evaluating a strategy that requires investment, which in one way or another will produce a return. This section introduces three key financial metrics, levelized cost of electricity (LCOE), internal rate of return (IRR), and net present value (NPV), widely used to evaluate the economic performance of wind turbine projects. Together, these metrics form the methodological backbone for assessing wind-energy investments. For all financial metrics, the electricity price is required, which is set to €80 /MWh, based on average historic trends (See Appendix Chapter A.1.3).

Moreover, for the selection of the discount rate, a literature review was conducted. For mature European onshore wind projects, financing costs are exceptionally low: IRENA's 2023 survey of 100 countries shows real, after-tax WACCs in 2021 of just 1.3 % for Germany, 1.5 % for Denmark, 1.8 % for France, 1.9 % for Finland, and 2.5 % for both Austria and the Netherlands (2.6 % in the UK) [90]. A fixed discount rate (DR) is therefore set at 2.5 %, reflecting the weighted average calculated, which was calculated by the following formula.

$$\mathrm{DR}_{\mathrm{wtd}} = \frac{\sum_{c \in C} \mathrm{WACC}_c \, w_c}{\sum_{c \in C} w_c} \tag{7}$$

- $\mathrm{DR}_{\mathrm{wtd}}$: The resulting weighted average discount rate (in percent).

- C: The set of countries included in the calculation.
- WACC_c: The real, after-tax weighted average cost of capital for country c (in percent).
- w_c: The weight assigned to country c, e.g. its share of total onshore-wind capacity.

Net Present Value

The net present value (NPV) measures the difference between the present-discounted value of benefits and the present-discounted value of costs over a project's life [91].

$$\text{NPV}(r) = \sum_{t=0}^{N} \frac{B_t - C_t}{(1+r)^t}$$

Where:

- NPV = Net Present Value
- B_t = Revenues in period t
- C_t = Costs in period t
- r = Discount rate
- N = Total number of periods

Levelized Cost of Electricity

The levelized cost of electricity (LCOE) is defined as the average total cost to build and operate an energy-generating asset per unit of electricity produced over its assumed lifetime. Equivalently, it represents the minimum per-unit price at which generated electricity must be sold to break even [92].

$$\text{LCOE} = \frac{\sum_{t=1}^{n} \frac{I_t + M_t + F_t}{(1+r)^t}}{\sum_{t=1}^{n} \frac{E_t}{(1+r)^t}}$$

Where:

- I_t = Capital investment cost in year t
- M_t = Operations & maintenance cost in year t
- F_t = Fuel or consumable cost in year t
- E_t = Electricity generated in year t
- r = Discount rate
- n = Project lifetime in years.

The internal rate of return (IRR) is the discount rate at which the net present value of all project cash flows equals zero. IRR does not represent a monetary value; rather, it is the annualized percentage return that makes the NPV zero [93].

$$-C_0 + \sum_{t=1}^{N} \frac{C_t}{(1+\text{IRR})^t} = 0$$

Where:

- C_0 = Initial investment
- C_t = Net cash flow in period t (inflow if positive)
- N = Total number of periods (years)

Payback Period

The Payback Period is a financial metric that measures the time required for an investment to generate cash flows high enough to recover its initial investment cost. In other words, it tells you how long it will take before an investment "pays for itself." This is especially useful for evaluating the risk and liquidity of a project.

The Payback Period is calculated using the following formula:

$$\text{Payback Period} = \frac{\text{Cost of Investment}}{\text{Average Annual Cash Flow}}$$

3.3.6 Key Assumptions

Assumption	Details
Turbine dismantling	Both repowering and decommissioning strategies involve complete dismantling and re-installation of new turbines either on the existing site or a new one
Road infrastructure	Pre-existing roads in repowered parks are fully reused and refurbished
Foundation reuse	Repowering reuses parts of the original turbine foundations
Grid connection	Grid infrastructure and evacuation lines are reused in repowering, avoiding new grid connection costs
Substation upgrade	Substation must be upgraded due to increased park capacity in repowering scenarios

Table 16: Key cost model assumptions for repowering and decommissioning strategies.

3.4 Land-use Model

Land-use efficiency can benefit from the implementation of a repowering strategy, which decreases the total space occupied by the turbines while simultaneously increasing capacity with larger and more efficient turbines. The land use efficiency of the repowering strategy was evaluated, and the land-use metrics were assessed and compared with other strategies.

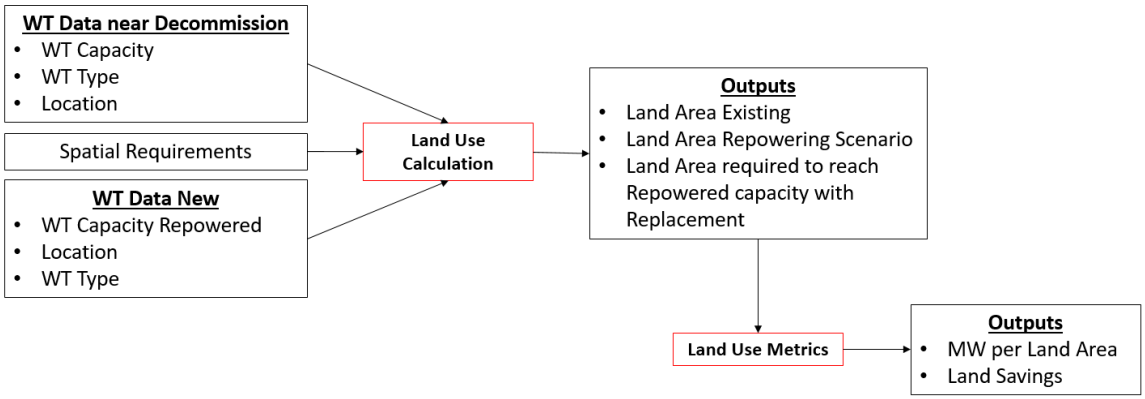

Figure 27: Environmental sub-model

Figure 27 provides an overview of the Land-use sub-model, which calculates the land usage associated with wind turbines. The model begins by estimating the land area currently occupied by existing turbines nearing decommissioning. Next, it determines the land area required for the repowered turbines, based on the potential capacity of the new installations. Additionally, the model calculates the land area needed if a decommissioning-and-replacement scenario is followed to achieve the same capacity as the repowered turbines and compares the power density of both strategies.

3.4.1 Turbine Spacing Rules & Footprint Metrics

To integrate these land-use metrics into the overall evaluation of repowering strategies, the following systematic approach is adopted:

1. **Data Acquisition:** After running the Capacity model (See 3.1.7), the results on the land use per approach are illustrated based on wind turbine specifications and locations of the park. Additionally, data for the existing wind turbines is extracted from The Wind Power - Wind energy databases [7].
2. **Land Occupancy Assessment:** As explained in the capacity model approach, if the terrain is flat, a 7D x 4D rotor diameter spacing between the turbines is followed, and 9D x 5D spacing if the terrain is complex. These results yield land use requirements for each wind turbine park, as well as the capacity of each repowered park.
3. **Metric Computation:**
   - Compute the power density for both the repowered and decommissioning-and-replacement scenarios.
   - Develop the comparative plot (decommissioning-and-replacement capacity comparison) to illustrate the extra capacity and land area required by conventional approaches to achieve the repowered strategy's capacity.

4. **Comparative Evaluation:** Finally, compare the computed metrics to highlight the benefits of repowering in terms of land-use efficiency. This evaluation serves as the quantitative basis for recommending repowering over conventional decommissioning and replacement strategies by clearly demonstrating the spatial and performance gains achieved.

By integrating these land-use metrics, the evaluation framework not only measures spatial efficiency but also connects it to operational performance. This holistic view is crucial for understanding how repowering initiatives can lead to enhanced energy production, environmental benefits, and improved overall sustainability of wind energy installations.

3.4.2 Power-Density & Land-Sparing

Power density is a critical metric that measures the amount of installed generation capacity per unit of land area. This value provides direct insight into how effectively a wind farm site converts its available land into electrical output. The power density (PD) for repowered installations is defined as:

$$PD = \frac{C_{\text{repowered}}}{A_{\text{repowered}}},$$

where:

- $C_{\text{repowered}}$ represents the total capacity of the newly installed turbines (in MW).
- $A_{\text{repowered}}$ is the land area occupied by these turbines (in km^2, hectares, or another standardized unit).

For comparative purposes, an equivalent power density is calculated for a decommissioning-and-replacement scenario using the capacities and land areas of the existing installations. A higher power density indicates a more efficient use of available land, as a greater proportion of the land is dedicated to producing electrical power. This measure facilitates a straightforward comparison of different wind turbine configurations and technologies by encapsulating both the capacity and spatial occupancy in a single value.

Instead of focusing solely on the turbine footprint reduction, the spatial allocation metric involves the development of a comparative plot. The plot represents the additional capacity—and, by extension, extra land area—that would be required under a decommissioning-and-replacement strategy to achieve the same total capacity as the repowered strategy. This visualization highlights the inherent land-use inefficiencies when repowering is not applied and underscores the spatial advantages of repowering, demonstrating quantitatively how much extra land would be needed to match the repowered scenario's output.

3.4.3 Energy Density

While power density (PD) quantifies installed capacity per unit land area, *energy density* (ED) captures the *actual annual energy* produced per unit land. This metric brings capacity factors and turbine performance into the land-use comparison. We define:

$$ED = \frac{E_{\text{repowered}}}{A_{\text{repowered}}}$$

where:

- $E_{\text{repowered}}$ is the annual energy yield of the repowered installation (in MWh or GWh per year).
- $A_{\text{repowered}}$ is the land area occupied by these turbines (in km^2, hectares, etc.).

For the decommissioning-and-replacement scenario, an equivalent energy density is

$$ED_{\text{existing}} = \frac{E_{\text{existing}}}{A_{\text{existing}}},$$

with E_{existing} and A_{existing} referring to the current turbines. A higher ED indicates that, beyond just packing more megawatts into a hectare, the repowered farm extracts more energy from the wind per hectare each year, thanks to higher hub heights, larger rotors, and improved turbine efficiencies.

3.4.4 Key Assumptions

Assumption	Details
Terrain classification	Sites are classified as *Flat* if TRI<3m and slope<5°, otherwise *Complex*.
Spacing layout	A single, uniform layout per terrain for all countries: flat terrain uses 7D×4D; complex terrain uses 9D×6D.
Rotor-diameter principle	Minimum clearances scale with rotor diameter (D), so land-take per turbine is 28D² on flat and 54D² on complex terrain.
Country homogeneity	The same terrain rules and spacing layouts apply in every country—no national adjustments.
Land availability	Decommissioned turbine footprints are assumed fully available for repowering; no competing land-use or buffer zones included.
Infrastructure reuse	Existing foundations, access roads, grid connections, and substations are *not* counted as additional land use—they are fully reused.
Onshore focus	Only onshore wind parks are modelled; offshore sites and marine constraints are excluded.
Protected areas	No explicit exclusion of protected or environmentally sensitive areas—spatial footprint is purely driven by turbine spacing.

Table 17: Key land-use assumptions in the methodology chapter.

4 Results

The results of the models and sub-models analyzed in the methods section are presented. Divided into three subsections: Capacity, Costs, and Land-use, this chapter provides insights into all three categories so conclusions can be drawn on the repowering potential.

4.1 Capacity Potential of Wind Repowering

4.1.1 Current State of Wind Farms in Europe

Figure 28 illustrates the total wind power capacity and capacity under construction of both onshore and offshore wind farms in Europe. Germany dominates the chart while Spain and the United Kingdom follow due to their significant offshore capacity. The data reveals a steep decline in offshore wind capacity as we move down the rankings, with several countries, such as Slovenia and Slovakia, contributing negligible amounts. This disparity underscores the varying levels of wind energy development across Europe, with a concentration of capacity in a few leading nations.

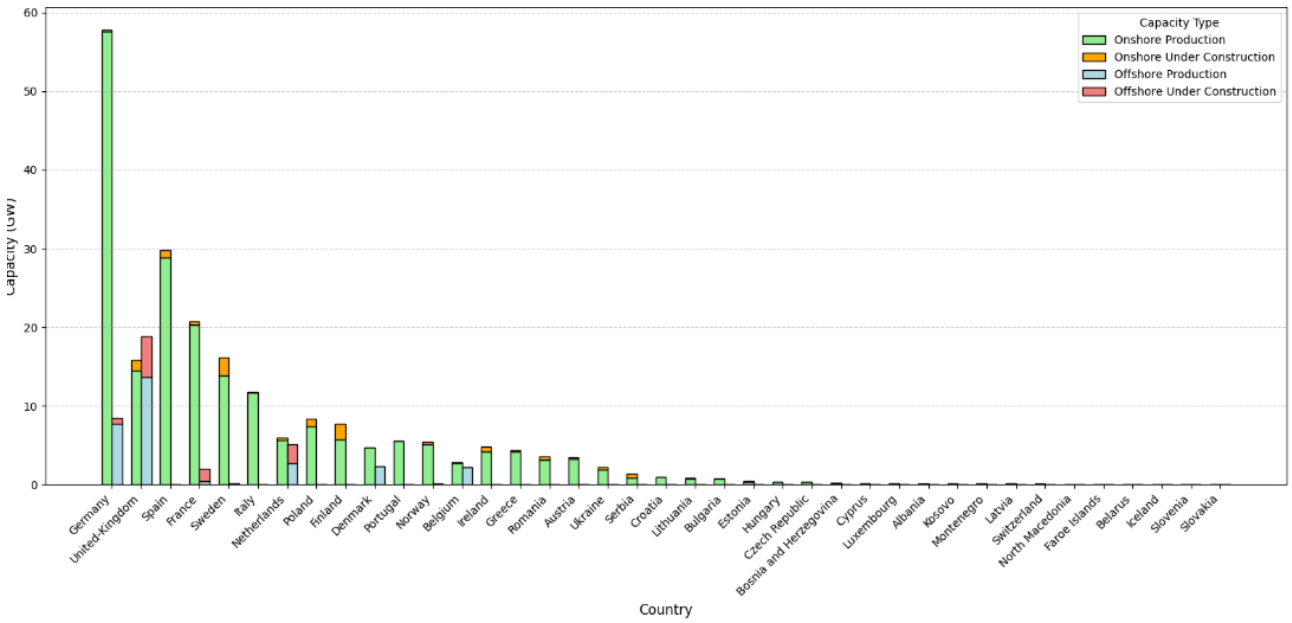

Figure 28: Wind power capacity by country in Europe originate from The Wind Power - Wind energy database [7]

Figure 28 also includes the total Offshore and Onshore capacity under construction in Europe. The United Kingdom is leading the charts, followed by the Netherlands and Sweden. This suggests that these countries prioritize future wind energy investments. Especially, despite its dominance in wind power capacity, Germany lacks ongoing project activity, potentially indicating a focus on upgrading or repowering existing infrastructure, rather than expanding their already extensive capacity. For instance, Germany led Europe in repowering efforts, contributing 1.1 GW out of the 1.4 GW of repowered wind capacity across the continent in 2023 [52].

An important parameter of the current state of the onshore wind energy sector is the size of the installed turbines. The capacity of wind turbines varies significantly depending on site-specific conditions such as wind speed, terrain, and regulatory constraints. These factors play a crucial role in determining the

optimal size and capacity of turbines for a given location. As a result, different countries have adopted diverse strategies for their wind turbine development trajectories, favoring offshore installations or various sizes to best align with their local conditions and energy goals.

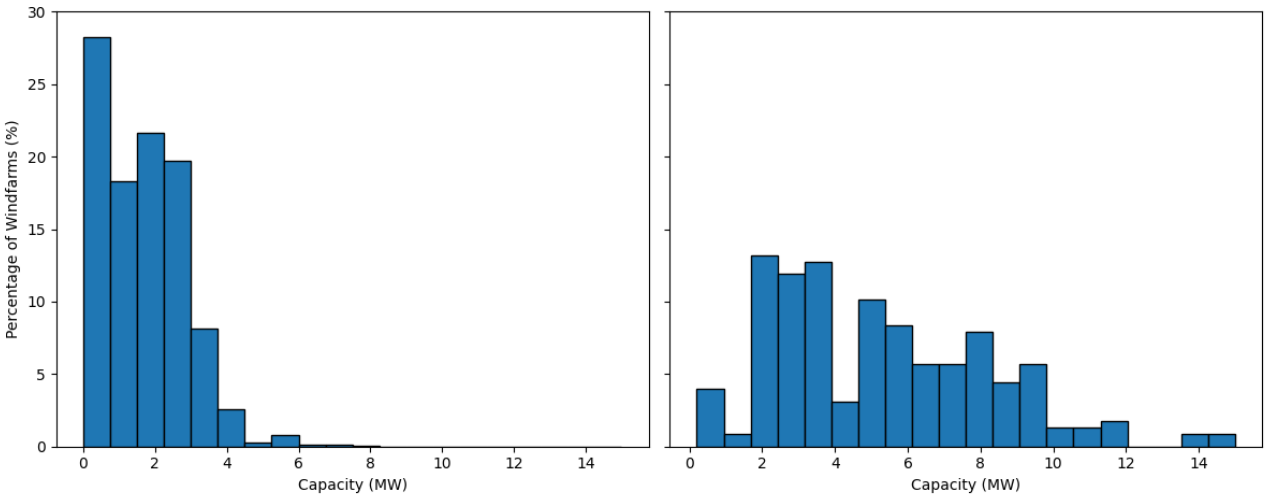

Figure 29: Onshore (left) and offshore (right) capacity distribution of wind turbines in Europe

Figure 29 illustrates the distribution of wind turbine capacities for both offshore and onshore installations. It can be observed that the majority of onshore wind turbines fall within the 0–4 MW range, whereas offshore wind turbine capacities vary from 0 to 14 MW, with noticeable gaps. This difference in capacity is primarily due to the higher wind speeds typically found at offshore sites, in contrast to the lower wind speeds encountered at onshore locations. Furthermore, as shown in Figure 28, the total offshore capacity is significantly lower than the total onshore capacity, which explains the greater dispersion in the distribution of offshore wind turbines.

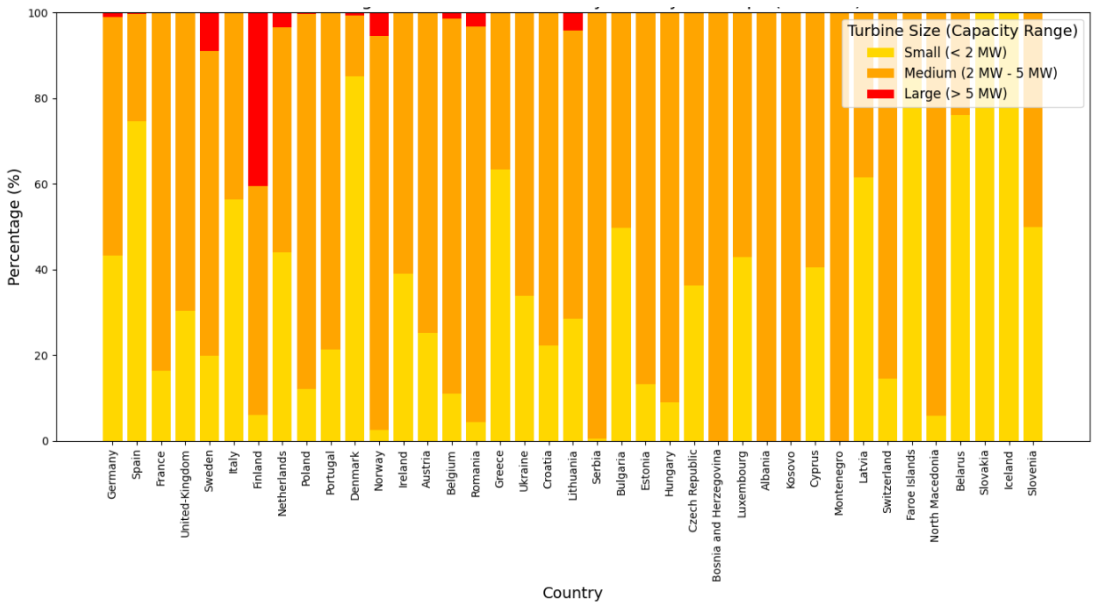

Figure 30: Distribution of onshore wind turbine sizes in Europe categorized into three categories: Small, Medium, and Large

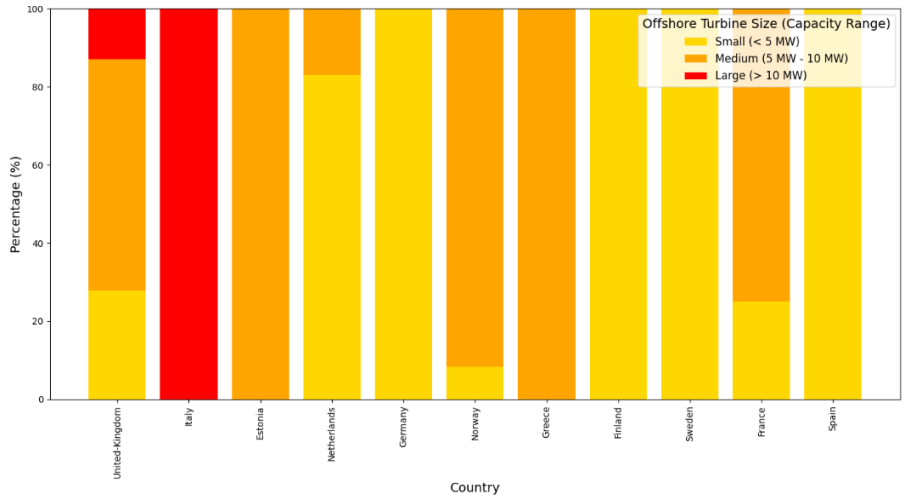

Figure 31: Distribution of offshore wind turbine sizes in Europe categorized into three categories: Small, Medium, and Large

An important factor when discussing repowering potential is the current distribution of capacities in every country. Figures 30,31 present the distribution of capacities per country, by dividing the wind turbines into small, medium, and large groups. Onshore, the bulk of Europe's newer parks (Germany, Spain, and Denmark) now deploy medium machines (2–5 MW), a clear up-sizing from older installations. In contrast, markets that built out their wind capacity earlier (e.g., Poland, Romania, and the Czech Republic) still rely heavily on small turbines (Less than 2 MW). Offshore, by comparison, is overwhelmingly dominated by large platforms (More than 10 MW) in advanced seas, most notably the United Kingdom, the Netherlands, and Belgium, reflecting both higher mean wind speeds and rapid adoption of next-generation designs when offshore terrain is accessible and can be utilized.

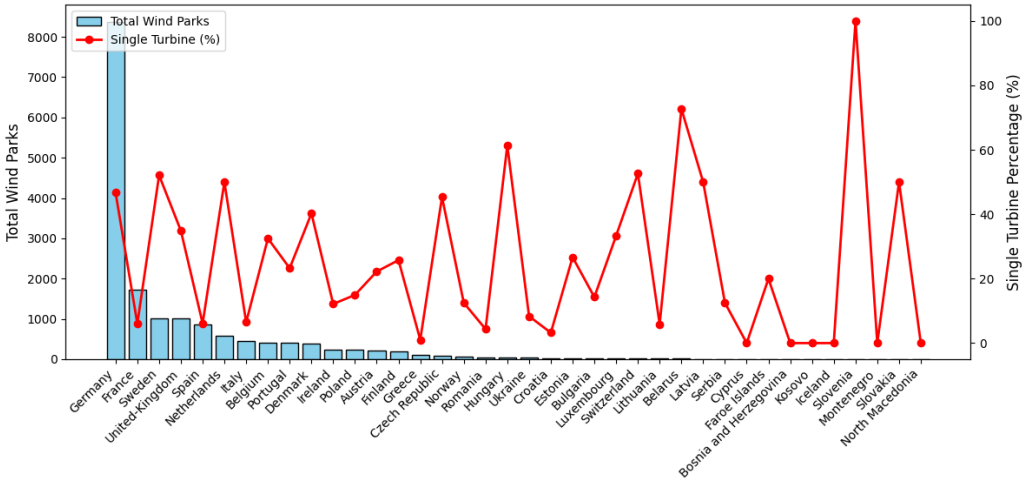

Figure 32: Total number of wind parks per country with single wind turbine parks percentages

Figure 32 illustrates that existing single-turbine parks offer very limited area for repowering. Because the available site boundary is derived solely from the rotor diameter and terrain type, parks with only one turbine have minimal expansion potential. As modern turbines of the same nominal capacity tend to have larger rotor diameters (see Chapter 3), the constrained area around a single unit results in few feasible locations for additional or larger rotors. Consequently, the repowering algorithm identifies

little to no opportunity for capacity increases when only one pre-existing turbine defines the park's footprint.

4.1.2 Projected Decommissioning Trajectory

Figure 33 shows the total onshore wind capacity in Europe from 1980 to 2050, with the red dotted line representing the release date of the database that was used to produce the plot. Data from the Database [52] were used up to 2022, and beyond that, a sensitivity analysis based on varying turbine lifespans was applied. This analysis does not take into account any additional capacities being installed after 2022.

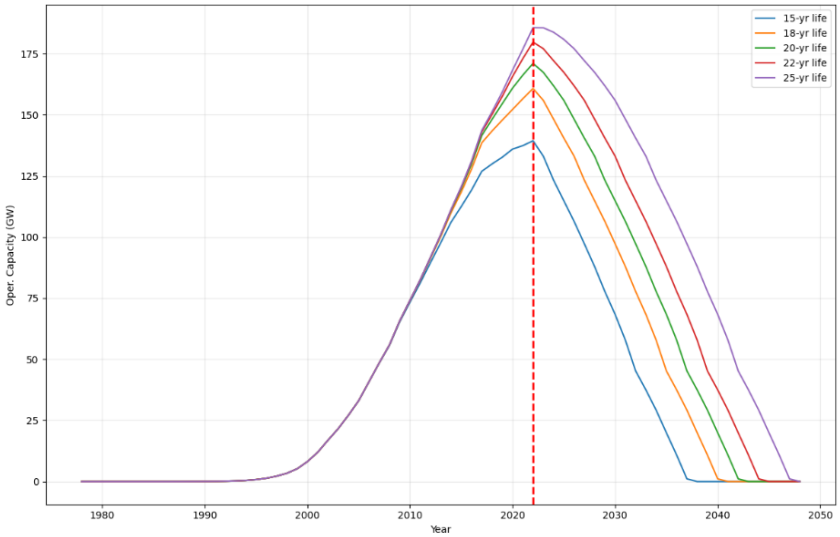

Figure 33: Total onshore wind capacity in Europe without new installations

Figure 34 presents the annual decommissioning rate for European onshore wind parks, which increases over time and peaks at 13 GW a year in 2037. This figure also reflects the repowering potential of decommissioned turbines, which can be replaced or upgraded, resulting in an overall maintenance of increase in the total capacity of each country.

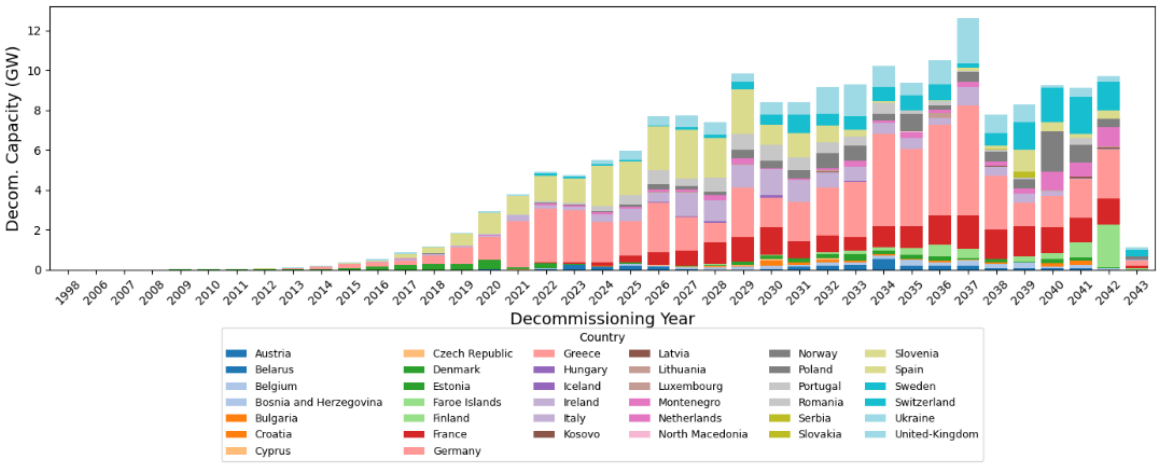

Figure 34: Annual decommissioning rate of wind parks in Europe per year and by country (Assuming 20 years of life-span)

The rising decommissioning bars after 2022 directly mirror the age profile of Europe's first-generation onshore turbines. Countries that invested in their wind fleets during the early 2000s (Spain, Germany, France, etc.) show their largest peaks in 2025-2030. Northern markets such as Denmark and the United Kingdom, which pioneered installations even earlier, begin to ramp up decommissioning slightly before 2025. In contrast, Eastern and Southern European countries (e.g., Poland, Romania, Greece) show major installations in the 2010-2015 window, creating a decommissioning uplift around 2035. Smaller markets with more recent wind-farm development, such as the Baltic, Slovakia, or North Macedonia, present modest removal rates throughout the 2020s and 2030s. Overall, the timing and magnitude of each country's annual decommissioned capacity reflect when each country invested in wind energy, underlining how fleet age drives repowering opportunities across Europe.

Overall, the figure illustrates the uneven state of wind energy development in Europe. Germany is the leader in existing capacity, especially onshore, but countries like the United Kingdom and the Netherlands are investing in wind energy, taking a lead in future developments. This shift suggests a growing focus on offshore wind projects and capacity expansion in countries that have lagged in the past. An important indicator of the data analysis thus far is the need for more balanced efforts across Europe to meet the renewable energy goals and take advantage of the wind energy potential.

4.1.3 Estimation of Repowered Capacity

This section presents the estimated repowering capacities obtained by applying the methodologies from the previous chapter. These estimates are projected to 2050, providing a perspective on how repowering strategies can affect Europe's goals in the near future. The analysis underscores the critical role of repowering in meeting future renewable energy targets, optimizing the utilization of existing wind farm sites, and assessing the potential of a high-performing wind energy sector in the coming decades.

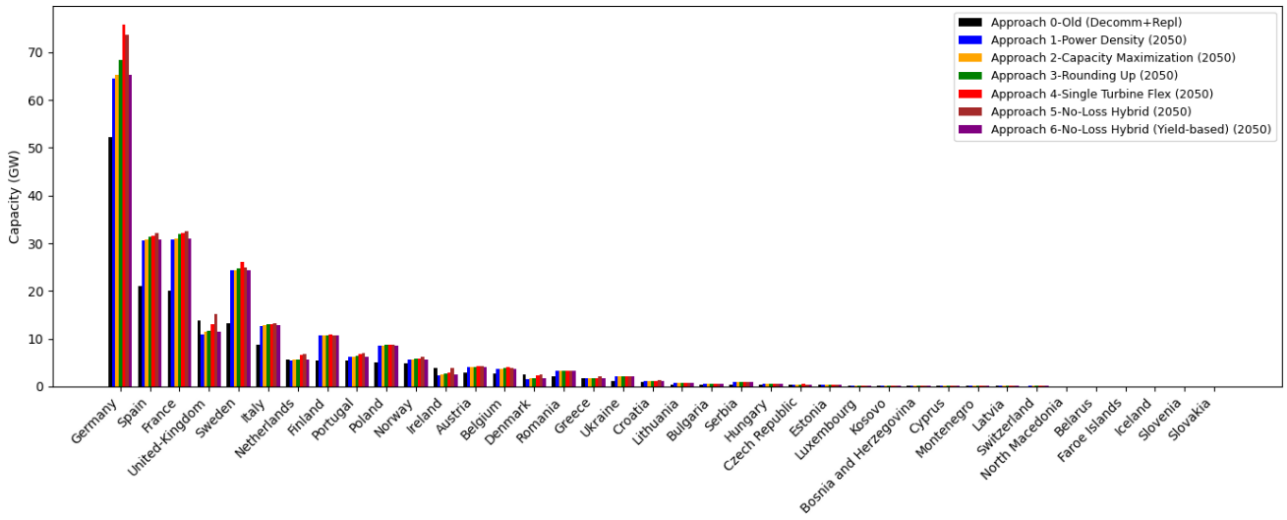

Figure 35: Repowering capacity effectiveness by country and approach against decommissioning and replacement (baseline) scenario

The results of the approaches are illustrated in Figure 35 and are more detailed in Table 18. The total capacity of the repowered wind farms indicates the total capacity that can be installed in the EU when all the wind turbines reach their operational lifetime expectancy. Although the repowering strategy increases the total capacity in every approach (from the initial 178 GW in 2022), not all wind parks can be repowered. The number of wind parks that have been repowered and successfully

increased their total capacity is presented in the table. The results highlight significant differences in repowering effectiveness depending on the approach applied.

Table 18: Wind energy repowering projection and analytics for 2050

	Approach 1 (PD) Power Density	**Approach 2 (CM)** Capacity Maximization	**Approach 3 (RU)** Rounding Up	**Approach 4 (STF)** Single Turbine Flex	**Approach 5 (NLH)** No-Loss Hybrid	**Approach 6 (NLH-Y)** No-Loss Hybrid (Yield-based)
Total Repowered Power (GW)	237.6	238.4	245.0	258.2	260.1	238.4
Number of Turbines	76,562	77,566	79,381	83,774	95,777	81,553
Number of Parks	12,291	12,291	12,291	16,684	16,684	16,684
Average Capacity per Turbine (MW)	3.10	3.07	3.09	3.08	2.72	2.92
Parks with Increased Capacity	9,161 (54.9%)	8,814 (52.8%)	8,744 (52.4%)	12,872 (77.1%)	8,814 (52.8%)	8,287 (49.7%)
Parks with Increased or Same Capacity	10,132 (60.7%)	9,950 (59.6%)	9,890 (59.3%)	14,104 (84.5%)	14,343 (85.9%)	8,957 (53.7%)

Table 18 provides a comparison of five repowering approaches by summarizing key performance indicators. The different methods are distinguished by how the algorithm upgrades to new turbine models once each park's decommissioning date is reached. The "Total Repowered Power" increases progressively from PD (237.6 GW) to NLH (260.1 GW), with the accompanying commentary indicating that NLH ultimately yields the highest capacity. This suggests that relaxing spatial constraints through forced installation, as in STF, can unlock additional output. The repowering model indicates that 33-46 % increase in nameplate capacity through full repowering—closely matching the 30 – 50 % gains observed by Prabu & Kottayil [**?**].

Additionally, while STF and NLH upgrade (by Repowering or by Decommissioning & Replacement) all 16,684 parks, their differing logic produces distinct outcomes. STF follows the least spatially restrictive strategy, yielding the second-highest total capacity (258.2 GW) and the greatest share of successful upgrades (parks whose repowered capacity exceeds the original) at 77.1 %. NLH's "no-loss" logic ensures no site falls below its existing capacity and delivers the highest overall capacity (260.1 GW), but only 52.8 % of parks are increasing in capacity. This contrast stems from STF's land-use flexibility, rounding up nearly-fitting turbines, and loosening constraints on single-turbine sites.

This section compares scenarios and approaches. The two scenarios to be compared are the repowering scenario (all 5 approaches) and the decommissioning and replacement scenario, in which the decommissioned wind turbines are replaced with the same models.

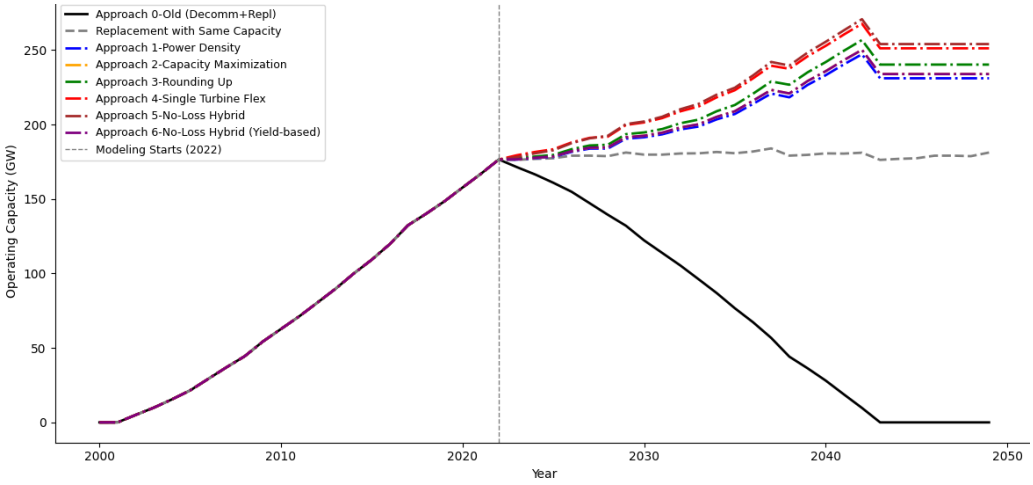

Figure 36: Total cumulative operating capacity - Repowering vs. Replacement strategy in Europe with modeling starting from 2022 (2000-2050)

This thesis examines the European Union as a whole, making it essential to consolidate the previously presented per-country figures into a single cumulative total capacity for European wind parks. Figure

36 illustrates the total EU wind capacity under different decommissioning and replacement strategy scenarios. The results demonstrate that repowering significantly enhances total capacity, with an increase of 60 GW in the worst-case scenario (PD) and up to 82 GW in the best-case scenario (STF). This comparison underscores the potential of repowering strategies to substantially expand Europe's wind energy capacity, depending on the level of strategy implementation.

Unlike decommissioning and replacement strategies, which maintain a fixed total capacity throughout the modeling process, repowering follows an upward trajectory, reflecting the benefits of deploying larger, more efficient turbines on existing wind farm sites. These findings align with the European Union's renewable energy targets, supporting efforts to increase wind energy production while minimizing land use expansion. However, large-scale repowering faces technical and regulatory challenges, including permitting constraints, grid integration issues, and capital investment requirements. Despite these obstacles, the results suggest that repowering can play a crucial role in accelerating the EU's energy transition.

Despite differences in turbine count, with NLH repowering the most turbines (95,777), the average capacity per turbine remains relatively constant (2.72 – 3.10 MW) across all approaches. This consistency suggests that gains in total capacity derive mainly from installing more turbines rather than from larger individual machines. Overall, the table demonstrates that repowering strategies incorporating flexible spatial criteria, especially RU and STF, can significantly enhance repowered capacity. In the context of the thesis, these findings highlight that while traditional and realistic methods (CM and NLH) are more conservative, RU and STF, particularly the latter, show the greatest promise for maximizing Europe's wind-park repowering potential.

Figures 37a and 37b compare the geographic distribution of repowered (blue) versus not repowered (black) onshore wind parks under the Capacity Maximization and Single Turbine Fleet approaches, respectively. Notably, Germany shows the densest cluster of repowered sites in the STF map, indicating that it benefits most from increased land-use flexibility. This observation is reinforced by Table 18, where STF (Approach 4) achieves a total repowered power of 258.GW and a 77.1% success rate—substantially higher than the 52.8% success under Capacity Maximization. Sweden and Denmark also see significant gains, but their relative improvements remain below Germany's. These results underscore that relaxing spatial constraints can unlock significant repowering potential, especially in regions with dense, legacy infrastructure, and suggest that targeted land-use policies in Germany could yield outsized capacity increases across Europe. Moreover, Figure 32 shows that more than half of Germany's onshore wind turbine fleet consists of single turbine parks, so the STF approach shows special flexibility on the single turbines, hence increasing the repowered parks substantially.

Despite the noticeable changes in installed capacities, the geographical distribution of wind energy infrastructure remains largely unchanged. Both maps highlight Northern Germany, the Netherlands, Denmark, and the United Kingdom as key regions of wind energy deployment. This consistency suggests that repowering has primarily focused on enhancing the capacity of existing sites rather than expanding into new regions. In this way, land use is optimized without increasing spatial footprint, aligning with the Sustainable Development Goals.

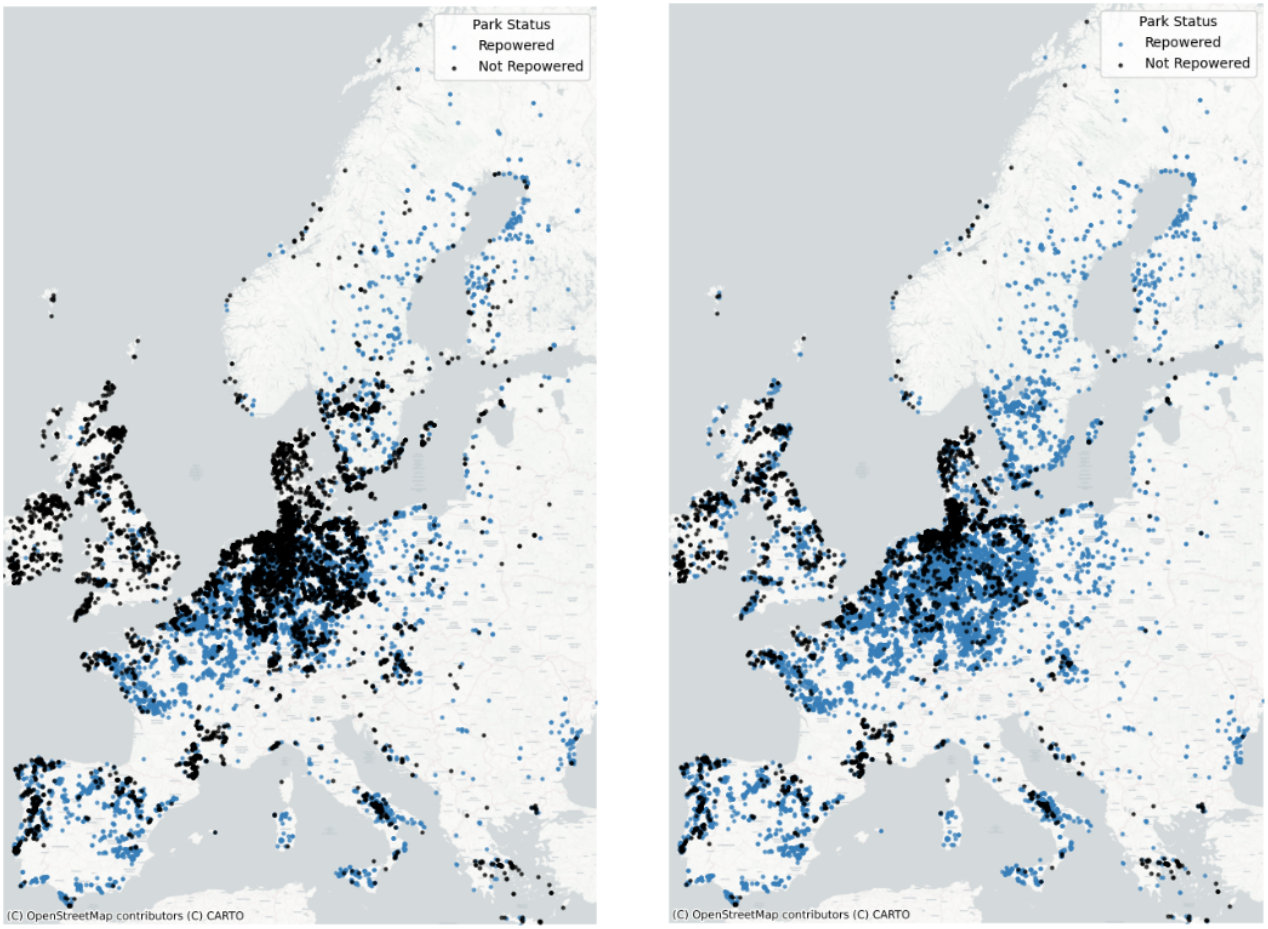

(a) Capacity maximization approach

(b) Single wind turbine flex approach

Figure 37: Installed repowered and non-repowered onshore wind turbine capacity per country in the region of Europe for two approaches with different degrees of flexibility

4.2 Energy Yield Potential of Wind Repowering

4.2.1 Capacity Factor: The True Driver of Energy Yield

Annual energy production must be assessed across scenarios to enable another perspective of the repowering evaluation. It is important to mention that the repowered results (Approaches 1-4) refer only to the wind parks that could be repowered based on the repowering strategy presented in 3 section. The rest of the approaches include parks that followed the decommissioning and replacement strategy. Moreover, an energy yield comparison took place between the six different approaches to evaluate the impact of repowering on capacity increase and the energy produced.

Figure 38 was created to assess the annual energy production while considering the total repowered capacity per country. On the left y-axis, the annual energy production per country is illustrated, and on the right y-axis, the installed capacity per country in MW is presented. The results were produced by calculating the capacity factor of the Capacity Maximization approach (Approach 2), and due to the different locations of the wind parks, each wind park shared a different capacity factor from the rest.

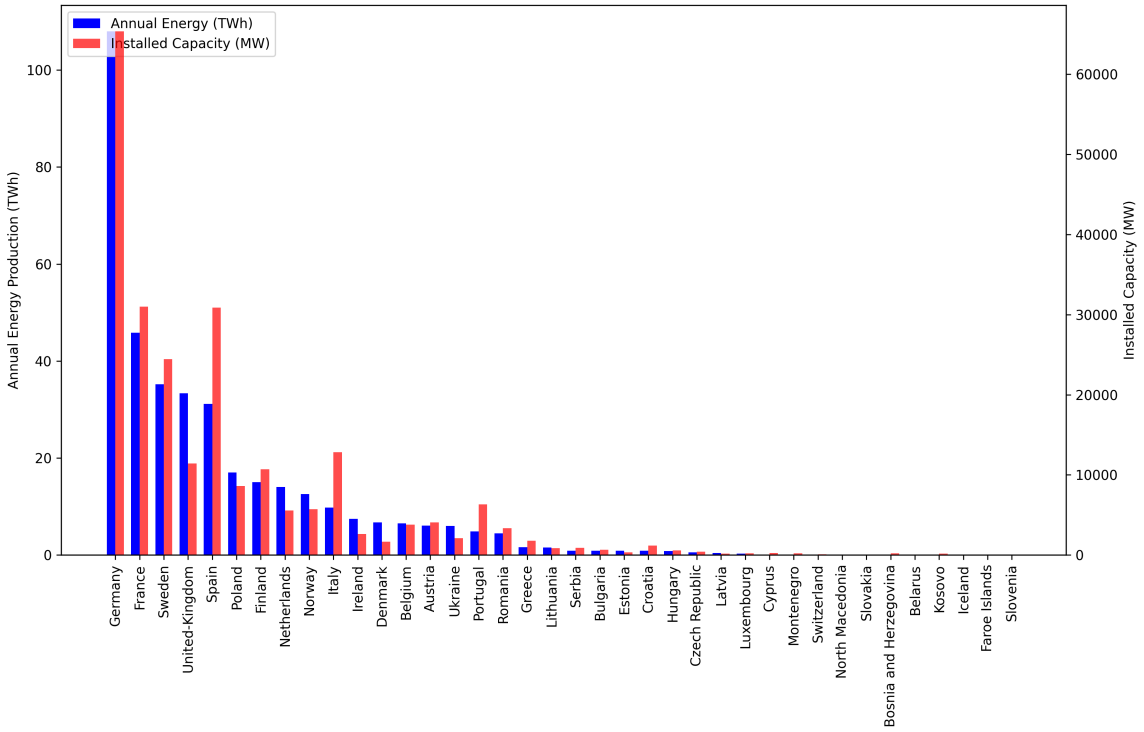

Figure 38: Total installed wind turbine capacity (MW) vs energy yield (TWh) per Country for capacity maximization repowering approach (approach 2)

Figure 38 shows that Germany leads in annual wind-energy production, exceeding 100 TWh, with France, Sweden, and the UK following in descending order. Importantly, however, installed capacity alone does not guarantee proportional output: variations in wind resource quality, turbine technology, and site selection mean that two countries with similar capacities can yield different energy production. For example, France and Spain both have roughly 34 GW of repowered wind capacity; yet, France achieves nearly 47 TWh of generation, while Spain remains below 40 TWh.

From the capacity results in Section 4.1.3, it is clear that repowering can boost the EU's total installed wind capacity. However, the gains are uneven: in some countries, overall capacity increases, while in others it remains the same or even declines because post-repowering capacity factors fall (see Appendix Figure 62). This disparity highlights that repowering is about more than installing higher-capacity turbines—it also requires careful optimization of turbine design, hub height, and siting to local wind regimes to preserve or improve capacity factors and maximize real energy output.

4.2.2 Yield per Country and Strategy

Figure 39 plots each country's old and repowered energy production for all scenarios. For some countries, even with a capacity increase, the energy yield decreased. Therefore, another method of choosing which farm to repower was applied. An energy yield-based approach was used to calculate both the old and the repowered energy yield (Approach 6 No-Loss Hybrid-Yield Based), and the wind park with the highest overall energy yield, between the old and the repowered (Approach 2 Capacity Maximization), was ultimately selected. With this methodology, the annual energy production results increased significantly for all countries.

An insight from the results is that the total capacity sometimes is disproportional to the energy yield, due to the inefficiency of the repowered turbines in specific locations to produce higher energy

than the existing parks. In total, **16,684** existing wind parks were evaluated for repowering. Under the capacity-based NLH selection rule, **12,239** parks were repowered, whereas the yield-based rule repowered **9,240** parks. This demonstrates that prioritizing energy yield over total installed capacity allows repowering efforts to deliver greater system-wide annual production, offsetting the inefficiencies of repowered turbines in specific locations. Furthermore, the layout is now more efficient, with larger wind turbines occupying more space on the one hand, but fewer are needed to produce the same capacity on the other hand.

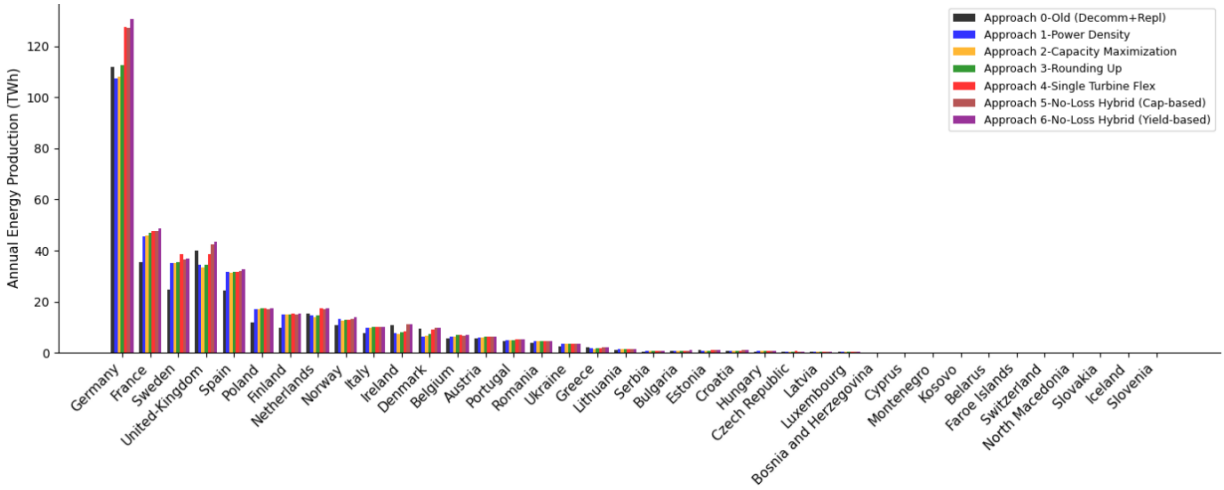

Figure 39: Energy production per country Old vs. repowering approaches in the EU

Figure 40 illustrates that repowering significantly enhances annual energy production across nearly all European countries, although the extent of the gains varies depending on the existing wind energy infrastructure. Countries like Finland, Sweden, Ukraine, Serbia, and Hungary experience substantial increases in energy yield across all approaches, indicating that the lack of spatial restrictions has little impact on the trajectory of wind repowering potential in these nations. Conversely, countries where energy increases vary by approach (as spatial constraints are relaxed) highlight the importance of expanding land use to maximize energy production growth. Overall, the estimate of the annual energy yield increase is around 20% with repowering, in line with Verma & Ahmed's [44] WAsP-based analysis, which reported 25 – 35 % improvements (and up to 70 % in high-resource sites) within the same footprint.

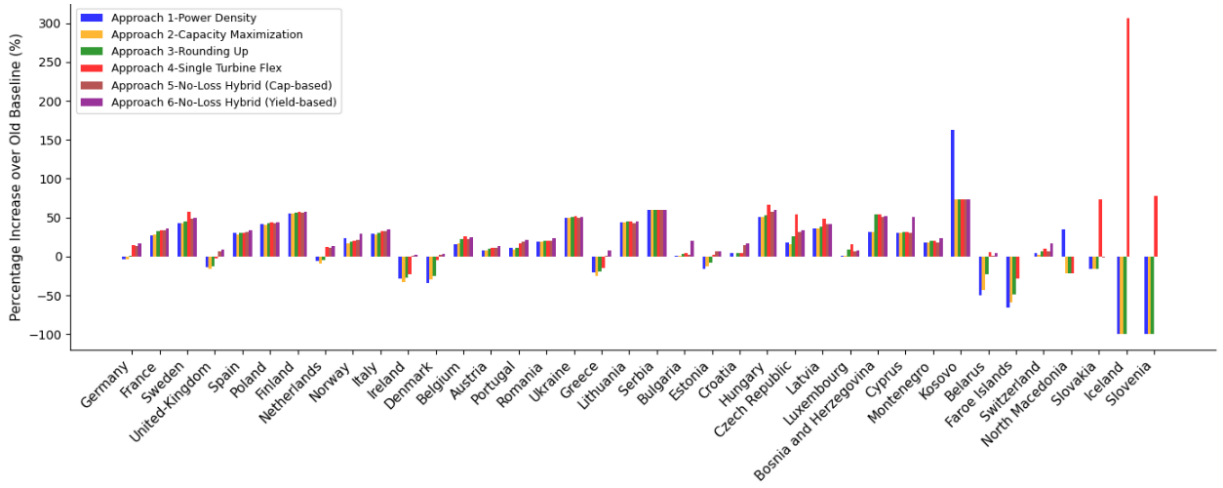

Figure 40: Energy production per country old vs. repowering approaches in the EU

There are also many countries presenting negative gains through the strategy of repowering. The UK, the Netherlands(when the land constraints are strict), Ireland, Denmark, Greece, and other countries decrease when implementing every strategy except the LH-Yield Based Approach, which doesn't allow energy yield decrease. Reflecting on Figure 30, dozens of low-yield machines are replaced by fewer, much higher-yield units in countries with small fleets. Countries with medium-sized fleets (e.g., Germany and France) also consolidate parks and increase output by tens of TWh, thanks to much higher post-repowering capacity factors. By contrast, regions already dominated by large machines (such as parts of the UK) exhibit only minimal improvements—or in some cases slight declines—because there is less room for capacity-factor gains. In all cases, however, replacing many under-performing turbines with a smaller number of modern, high-efficiency models maximizes both land-use efficiency and total generation.

4.2.3 Energy Yield GIS Comparison & Demand Coverage

Figures 41a and 41b depict the repowered parks of Europe as well as the energy increase from that repowering strategy, respectively. The red dots describe the repowered parks of Europe, after the implementation of the Approach 2 model, and with black dots the parks that were not able to be upgraded, thus fostering the decommissioning and repowering strategy so that no capacity is lost. Repowered cites cluster overwhelmingly along the North Sea coast, southern England, Denmark, and into northern Germany and the Baltic states, exactly the regions with the strongest, most consistent wind resources.

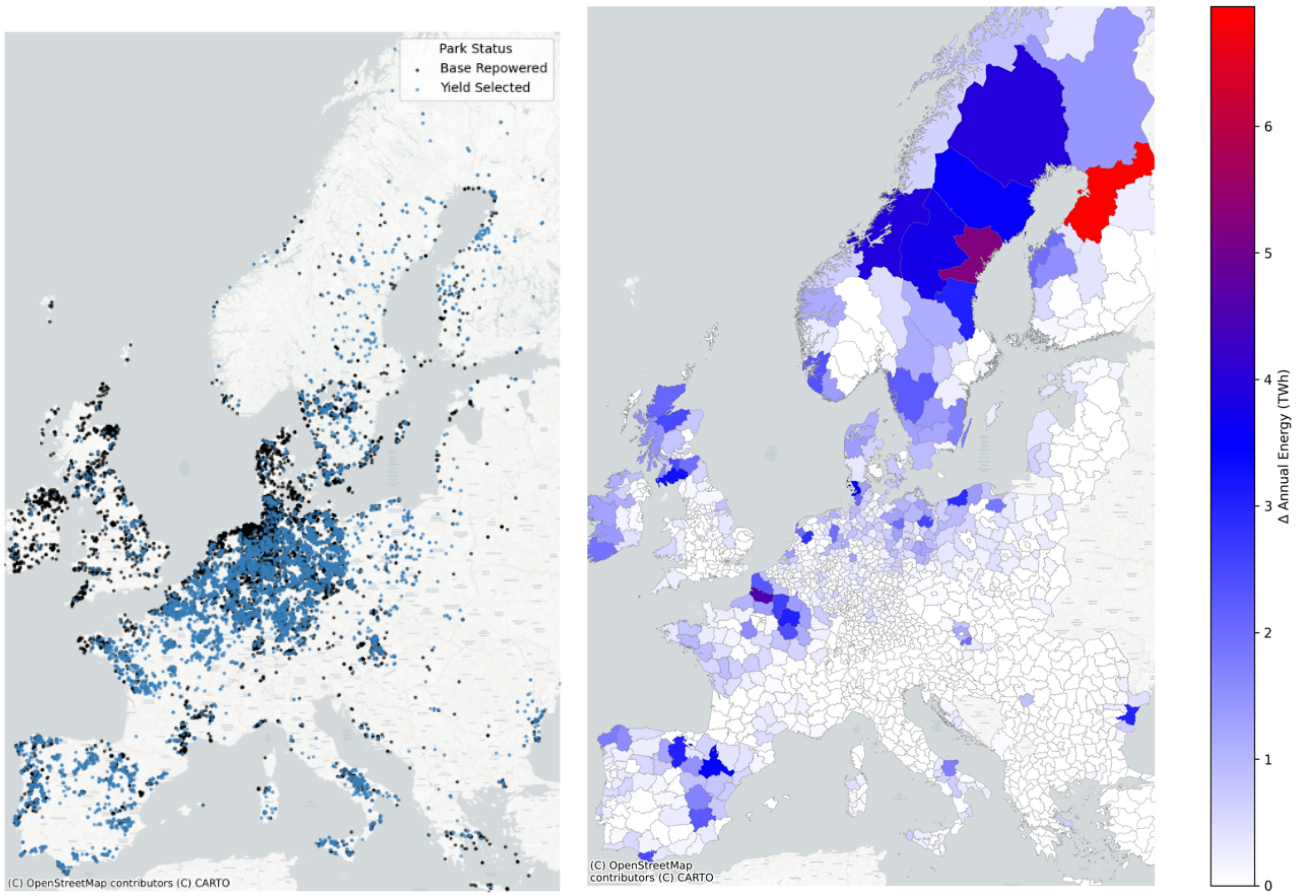

(a) Repowered vs. non-repowered sites vs. Yield Selected

(b) Energy Production Difference Decommissioning and Replacement (2022) vs. NLH (Yield-based)(2050)

Figure 41: (a) No-Loss Hybrid (Yield-Based) approach locations and capacity difference.

For the energy production map, NUTS Level 3 region bounds were assigned to each park, and the No-Loss Hybrid Yield-Based approach was selected due to the high energy yield gains. Most regions see relatively modest gains of under 500 GWh per year because their existing parks were already well sited or offered limited scope for larger rotors and higher hub heights. In areas with high capacity density, regions appear purple and red, indicating yearly increases between 1-2.5 TWh. A key takeaway from Figure 41 is that repowering can boost energy yield across many European locations but not in all of them. To maximize returns and overall energy production, implementation should be selective. The old energy production, as well as the repowered, can be found in Appendix 63

The last step is to estimate and assess the wind energy coverage of repowered wind energy in Europe. The amount of electricity that was generated in 2022 was around 2884.81 TWh in total [94], which is the number used as consumption across all EU countries (See Figure 64).

Table 19: Total annual energy production and relative gains by repowering approach

Approach	Total Energy (TWh)	Relative Gain (%)
Approach 0 (Baseline)	342.87	0.0
Approach 1 (Power Density)	373.13	8.8
Approach 2 (Capacity Maximization)	370.80	8.3
Approach 3 (Rounding Up)	382.62	11.6
Approach 4 (Single Turbine Flex)	411.90	20.1
Approach 5 (No-Loss Hybrid, cap-based)	416.60	21.5
Approach 6 (No-Loss Hybrid, yield-based)	425.34	24.1

Approaches 1 and 2 yield only modest improvements (8–9 %) over the existing wind energy fleet, whereas Approach 3-Rounding Up achieves an intermediate gain of 11.6 %. By contrast, strategies that combine repowering with land flexibility or hybrid optimization deliver far larger uplifts: Approach 4-single-turbine flexibility increases output by 20.1 %, the Approach No-Loss Hybrid (Capacity based) by 21.5 %, and Approach 6 No-Loss Hybrid (Yield-focused) by +24.1 %. These results illustrate that embedding repowering within a no-loss framework, especially optimizing for energy yield, maximizes the sum wind production in Europe as a whole.

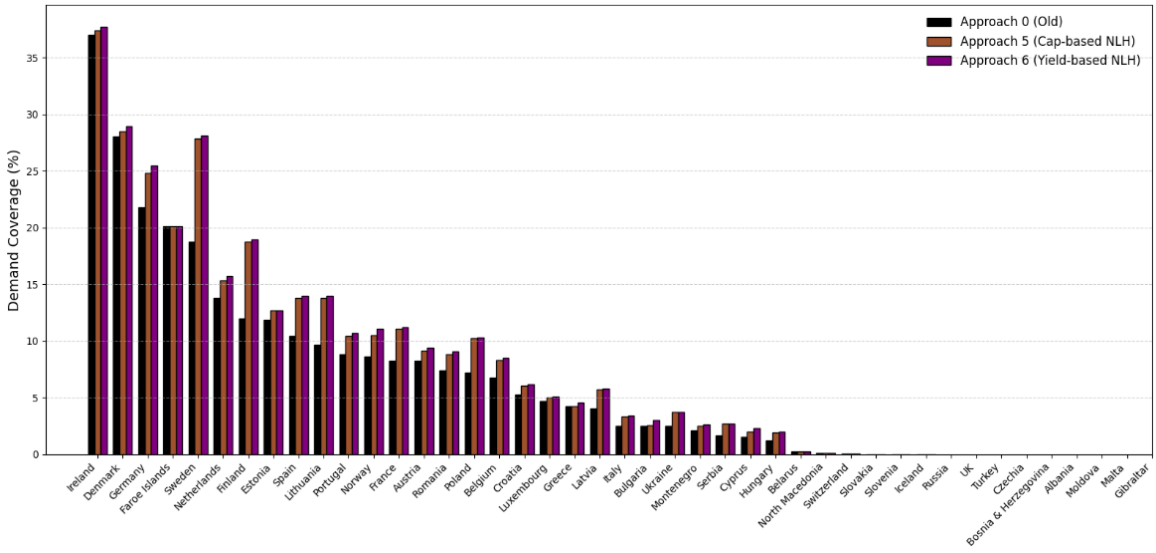

Figure 42: Yield-based and Capacity-Based Demand Coverage of Repowered Wind Turbines (NLH Approach)

Relative to the baseline existing wind fleet (Approach 0), both hybrid repowering schemes (Approach 5: capacity-based; Approach 6: yield-based) substantially raise demand coverage in every country. On

average, Approach 5 contributes an uplift of approximately +7–10 percentage points across markets, while the yield-optimized Approach 6 adds 0.5–1 % on top of that. High-resource regions (e.g., the Netherlands, Ireland) benefit most, with gains of 9–10 %, whereas lower-resource countries see smaller absolute improvements (2–4 %), remaining below 8 % even after repowering. Consistently, Approach 6 outperforms Approach 5 by a narrow margin, underscoring the incremental value of targeting energy yield rather than capacity alone.

4.3 Cost Comparison

The financial performance of repowering was compared to the decommissioning and replacement strategy implemented across Europe. Based on a detailed breakdown of cost components for both approaches, cash flow analyses at the wind park level and aggregated financial metrics are presented. It is essential to note that the comparisons made are between all wind parks, even if they could be repowered based on Approach 2 (Capacity Maximization), which disallows any spatial expansion of the park's currently occupied space. It should be noted that not all repowered parks yield higher energy in this approach compared to Approach 6, the NLH-Yield Based Approach.

4.3.1 Repowering vs. Replacement Financial Metrics

By summing the cost per method, derived from literature, the Eur per KW expenses are estimated at **€1,267.1 /kW** for the decommissioning and replacement of a turbine. In contrast, repowering costs are of lower magnitude at €1,077.4 /kW, yielding a savings of €189.7 /kW under the repowering strategy. For the cost results, a moderate **(14%** learning rate) is assumed for the calculations, lowering the total capital expenses of repowering to **€953.34/kW** and **€1089.9/kW** for repowering and decommissioning, respectively.

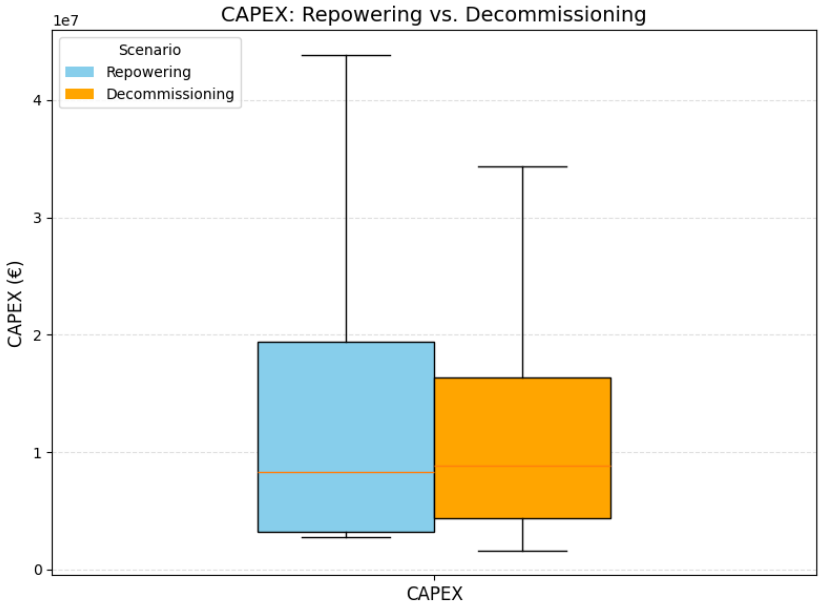

Figure 43: Box-and-whisker plot comparing CAPEX for the repowering versus decommissioning + replacement scenarios. Boxes span the interquartile range (25th–75th percentiles), the bold line marks the median CAPEX, and whiskers extend to the minimum and maximum observed values.

The box-plot presented in Figure 43 reveals two apparently contradictory but ultimately complementary insights. On the one hand, the mean capital outlay for repowering (€18.0 M) exceeds that of full decommissioning and replacement (€15.0 M), owing to a handful of extensive repowering projects that push the upper whisker out to nearly €44 M (versus €34 M for replacement). These extreme values reflect large wind parks where new, high-capacity machines and upgraded foundations drive absolute expenses well above the baseline. On the other hand, the median CAPEX is lower under the repowering strategy—€8.34 M compared to €8.83 M—indicating that for a typical project, the investment is smaller. Although repowering can become capital-intensive for very large sites (inflating the mean), it consistently lowers the typical project CAPEX, shifting the median downward and concentrating most investments in a narrower, more cost-efficient band. This dual behavior underscores repowering's ability to deliver robust per-kW savings in the majority of cases, even as flagship large-scale conversions command higher absolute budgets.

4.3.2 Levelized Cost of Electricity Comparison

Figure 44 applies three onshore-wind learning rates (10%, 14%, and 20%) to the baseline LCOE, highlighting how technological learning can further reduce long-term costs. Across all learning-rate scenarios decommissioning and replacement strategy consistently achieves lower median LCOE's than repowering. At the Baseline (0%) case, replacement's median LCOE sits around €60/MWh versus roughly €65/MWh for repowering, and as CAPEX falls under Conservative (10%), Moderate (14%), and Advanced (20%) learning rates, both strategies see their LCOEs drop, but replacement retains a clear edge. By the Advanced scenario, median LCOE for replacement falls to just over €50/MWh compared with about €55/MWh for repowering, and its lower quartile is several euros cheaper too. This mirrors earlier findings on NPV per MW and IRR: while repowering can boost returns at the very top end, replacement delivers consistently lower-than-replacement generation costs, making it the more cost-efficient choice across the majority of sites (53.4%).

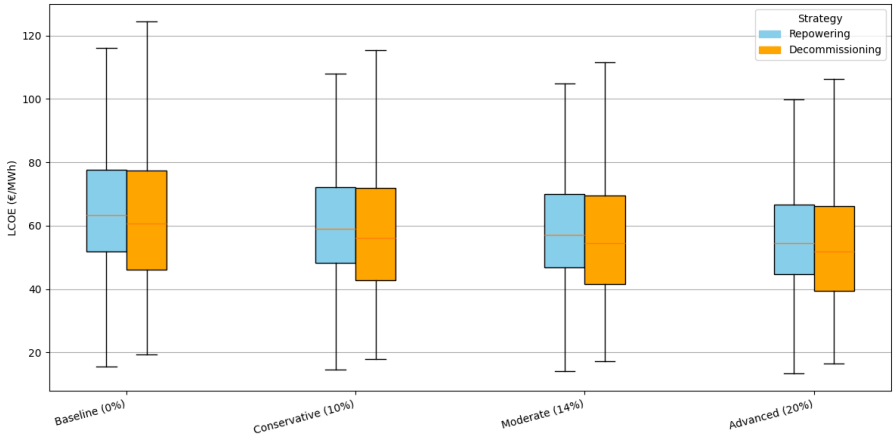

Figure 44: Box-and-whisker plot of average EU LCOE for onshore wind under three learning-rate scenarios (10 %, 14 %, 20 %). Boxes span the interquartile range (25th–75th percentiles), the bold line indicates the median LCOE, and whiskers extend to the minimum and maximum observed values.

What was presented in Figure 44 was the overall comparison of all 12,210 (The wind parks that could be repowered successfully under the no-expansion approach 2) wind parks to illustrate the effect of repowering. Figure 45 then breaks down the average LCOE by country and strategy for approach 2 (Capacity Maximization and 6 the No-loss Hybrid-Yield based approach). Although only 4,491 out of 12,210 sites (36.8 %) see an improved capacity factor after repowering, a significantly larger

share, 7,444 sites (61.0 %), delivers higher annual energy yield once larger turbines are installed. Under the Moderate (14 %) learning-rate assumption, the overall mean LCOE is virtually flat at 67.4 €/MWh for repowering versus 68.0 €/MWh for full decommissioning and replacement, showing that the incremental energy gains generally offset the somewhat higher CAPEX. The pronounced cross-country differences in LCOE stem directly from each site's wind regime and from how larger rotors shift operations into different regions of their turbine power curves.

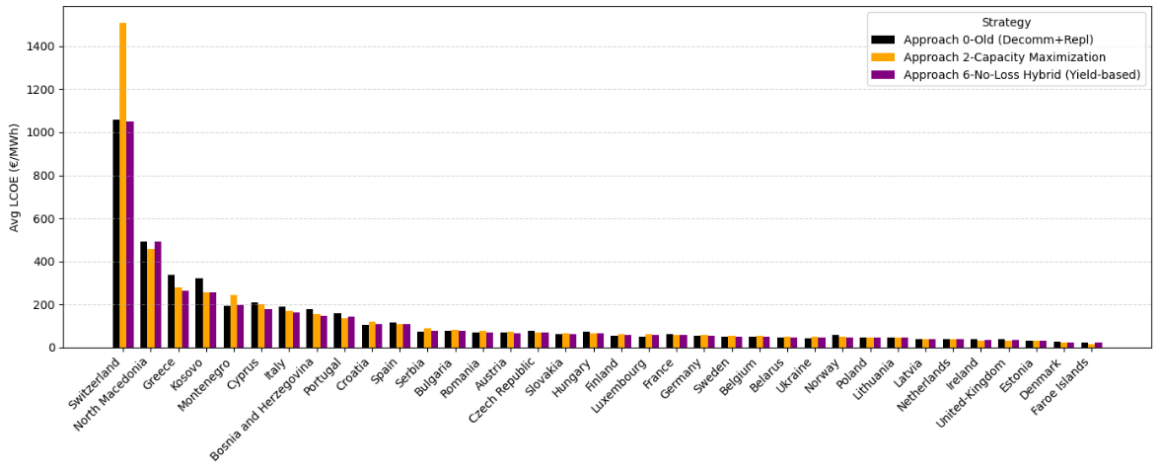

Figure 45: Repowering (Approach 2 and 6) vs. Decommissioning and Replacement LCOE comparison per country

In the Faroe Islands, full repowering under the Moderate (14 %) assumption cuts average LCOE from 21.7 €/MWh down to 15.4 €/MWh, driven by the dramatic yield boost. The No-Loss Hybrid design then holds LCOE at 15.4 €/MWh, matching pure repowering but avoiding over-investment where wind resources are marginal. Denmark sees repowering lower LCOE from 26.6 to 21.5 €/MWh, while the hybrid achieves 24.7 €/MWh, capturing most of the benefit with less upfront CAPRX. In the U.K., repowering trims LCOE from 36.8 to 30.2 €/MWh versus 34.4 €/MWh under the hybrid. Spain's more variable regime yields an 8.2 €/MWh reduction for pure repowering and 9.3 €/MWh under the hybrid. France, by contrast, sees a more modest 2.0 €/MWh cut with repowering and 1.7 €/MWh via the hybrid. These cases demonstrate that the hybrid approach generally yields almost the same LCOEs while capping capital risk in lower-wind installations.

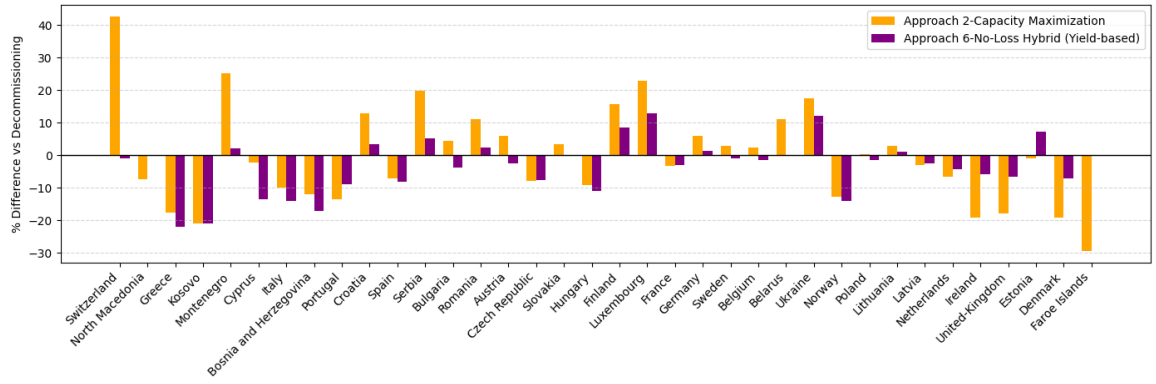

Figure 46: Relative repowering (Approach 2 and 6) vs. Decommissioning and Replacement LCOE comparison per country

Figure 46 isolates the percentage reduction in LCOE delivered by two strategies—Approach 2 (standard repowering) and Approach 6 (no-loss hybrid)—relative to the baseline decommissioning-and-replacement

case, for every country in the study. Under our Moderate (14 %) learning-rate assumption, pure repowering cuts LCOE by anywhere from about 3.3 % in France up to roughly 29.0 % in the Faroe Islands. The no-loss hybrid variant, which only replaces under-performing machines, closely matches those gains, delivering reductions of 2.8 % in France and about 28–29 % in the Faroe Islands. Meanwhile, Denmark and the U.K. each see 19 % and 18 % drops under full repowering, with the hybrid still capturing 7 % and 6 % of where the biggest wins are, respectively. Spain's more variable regime yields 7.1 % savings via standard repowering and 8.0 % under the hybrid, while France shows the more modest 3.3 %/2.8 % splits. In nearly every market, the no-loss approach tracks within 1–2 percentage points of the full-repowering curve, underscoring its ability to lock in most of the unit-cost improvement while reducing the capital risk.

4.3.3 IRR-NPV and Electricity Price Sensitivity Analysis

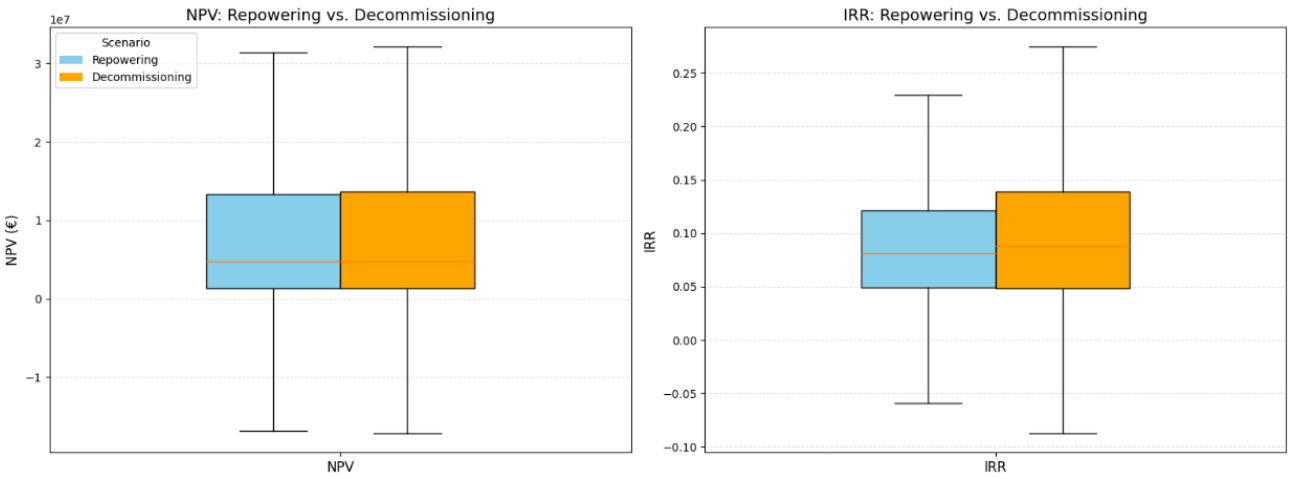

Figure 47: Box-and-whisker comparison of Net Present Value (NPV) and Internal Rate of Return (IRR) between the repowering (Approach 2: Capacity Maximization, no spatial expansion) and decommissioning scenarios for the 6,850 active European onshore wind parks (12 210 park–scenario pairs). Boxes span the interquartile range (25th–75th percentiles), the orange line marks the median, and whiskers extend to the minimum and maximum observed values.

Figure 47 presents side-by-side box and whisker plots comparing two different financial metrics across the analyzed wind parks for both scenarios explored. The From the 6,850 active European onshore wind parks in 2022 that were analyzed, 12,210 could be compared between scenarios because repowering was not always possible for all wind parks. The results of repowering were acquired from Approach 2 (Capacity Maximization), which did not allow any spatial expansions.

The two-panel box-plot Figure 47 reveals insights on the economic side of wind repowering and decommissioning strategy. On average, repowering with larger turbines commands a higher upfront investment cost compared to straightforward decommissioning and replacement. When it comes to value creation, decommissioning edges out repowering on mean NPV (€11.8 M vs. €10.7 M), but medians are almost identical (€4.8 M each), indicating that half of all projects perform similarly under either strategy. Furthermore, repowering shows a slightly higher average IRR (9.62 % vs. 9.19 %), though the median IRR is a bit higher for replacement (8.85 % vs. 8.13 %), again suggesting that the very best repowering sites boost the mean, while most projects yield comparable returns. Payback periods cluster around ten years for both options, with decommissioning recovering costs marginally faster on median (9 years vs. 10 years).

Taken together, these results imply that, in most cases, simply replacing turbines delivers a marginally higher(or at least more consistent) NPV and slightly shorter paybacks, whereas repowering can unlock higher IRRs at the cost of greater upfront investment and a few projects that aren't feasible or fall below financial thresholds. In practice, the best approach is to repower where site conditions favor larger machines—i.e., where the additional complexity and CAPEX can be justified by superior returns at your strongest wind-resource locations.

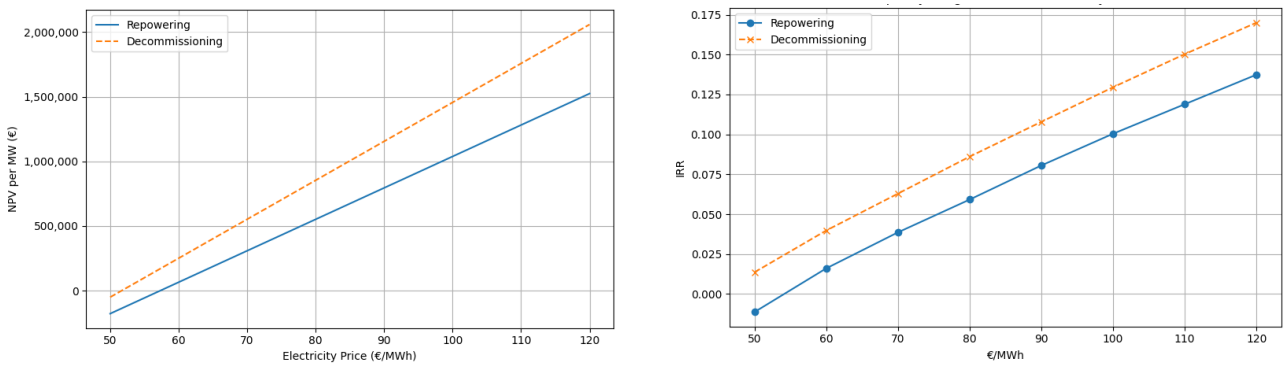

(a) NPV per MW as a function of electricity price

(b) IRR as a function of electricity price

Figure 48: Comparison of key financial metrics vs. electricity price for repowering and decommissioning scenarios.

Figure 48a shows the per-megawatt curves revealing that across the entire price range of 50 to 120 €/MWh of wholesale electricity price, decommissioning and straight replacement systematically outperforms repowering on a per-MW basis. At low prices, repowering yields slightly negative NPVs per MW, whereas replacement remains marginally positive, underscoring its lower break-even threshold. As prices rise, both strategies improve linearly, but the decommissioning and replacement strategy sees a steeper slope, which translates into higher NPVs at every price point. In practical terms, replacement unlocks more value per unit of capacity in almost all market conditions, while repowering only narrows the gap at the highest prices but never fully catches up.

Figure 48b on the right presents the weighted IRR versus the electricity price. At the lowest prices, decommissioning again leads, with a positive IRR even at €50/MWh—while repowering hovers around zero. However, repowering's IRR rises almost as quickly as replacement's, and by roughly €100/MWh, the gap narrows to just a few percentage points. Above that threshold, repowering delivers double-digit IRRs approaching 15 % at €120/MWh, compared with about 17 % for replacement. Thus, although replacement offers higher returns per euro invested under most scenarios, repowering can achieve competitive IRRs in high-price environments, making it an attractive option where market conditions support premium power prices.

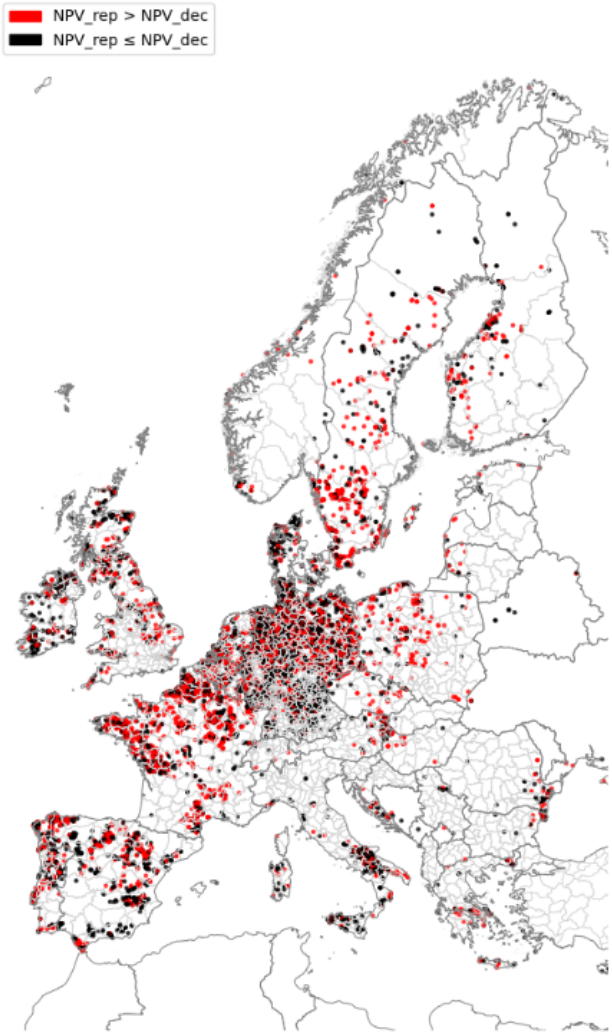

Figure 49: Decommissioning and replacement, and repowering NPV comparison map of Europe (NPV_{rep} = $the NPV of repowered turbines and NPV_{dec}$ = the NPV of the decommissioning and replacement)

Of the 12,210 sites analyzed, only 5,688 (46.6 %) showed higher NPV under repowering versus decommissioning and replacement. Figure 49 highlights that repowering (red) clusters in the highest-wind regions—Atlantic Spain, the North Sea coast, and southern France—where the extra CAPEX of larger machines is most readily recovered. It's important to weigh both percentage and scale: for example, France alone accounts for 984 repowering-viable sites out of 1,608 (61 %), whereas smaller markets may show higher percentages but involve very few parks. Conversely, Germany—with the largest cohort of 5,914 sites—sees only 2,433 (41 %) favoring repowering, underscoring that sheer volume can tilt the balance toward replacement even where a substantial minority benefits from new turbines. In practice, repowering delivers the greatest financial upside in both the strongest wind-resource zones and in markets where a critical mass of parks can justify the upfront investment, while in lower-resource or heavily saturated areas, simple replacement remains the more reliable strategy.

4.3.4 Example Wind Park Case Study

Figure 50 illustrates how four key financial indicators for a single repowering site in the United Kingdom respond as the assumed wholesale electricity price is varied from €50 to €120 /MWh.

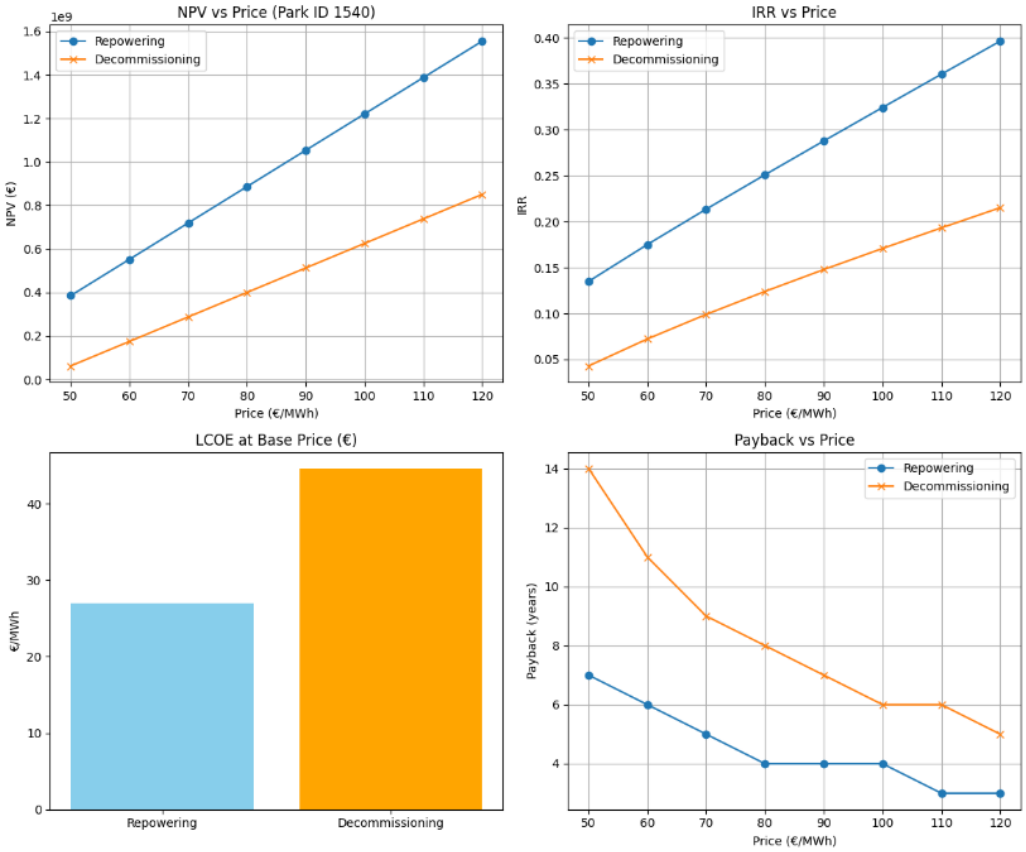

Figure 50: ensitivity analysis of financial metrics (NPV, IRR, payback period) and LCOE to wholesale electricity price for a representative UK onshore wind park under two scenarios—repowering (Approach 2: Capacity Maximization, no spatial expansion) versus decommissioning + replacement. Each box spans the interquartile range (25th–75th percentiles) of metric values across the price sweep, the bold line marks the median, and whiskers extend to the minimum and maximum observed values.

Park ID 1540 in the U.K. originally comprised 140 × 2.3 MW Siemens SWT 2.3-101 turbines (322 MW). Under a decommissioning and replacement strategy (322 MW of new 2.3 MW machines), the park would incur a CAPEX of €350.95 M, produce 722,995 MWh/yr (CF 25.6 %), and deliver an NPV of €400.1 M at a 12.4 % IRR, with an eight-year payback and an LCOE of €44.50/MWh for a fixed electricity price of €80 /MWh. By contrast, repowering with 49 × 6.6 MW Siemens SWT 6.6-170 units (323.4 MW on the same footprint) carries a lower CAPEX of €299.63 M, yet boosts output to 1,072,470 MWh/yr (CF 37.9 %), yielding an NPV of €886.6 M at a 25.1 % IRR, a four-year payback and an LCOE of just €26.97/MWh for the same electricity price.

These dramatic gains arise because the SWT 6.6-170's larger rotors and higher hub height shift its power curve into a far more productive wind-speed range—delivering nearly 50 % more energy—while its lower specific CAPEX (€/kW) drives down unit costs. The result is a roughly 40 % reduction in LCOE, more than double the NPV, and a halved payback period. This case underscores that, at sites with strong wind regimes and suitable terrain, repowering can unlock financial and operational value compared to simple replacement.

4.4 Land Use Comparison

A land-use comparison between decommissioning with capacity addition elsewhere and repowering was necessary for a complete assessment of the two strategies. To this end, various figures were used to illustrate key aspects when evaluating wind repowering as a potential method for reducing the spatial footprint of wind energy. The primary metrics for assessing land occupation were power and energy density, measured in MW and TWh per unit of land area (km^2). This metric reflected the effectiveness of wind turbine deployment concerning the land area utilized

The following graphs present land-use-affiliated results that can provide insights into the spatial utilization strategies for wind energy in each European country. Figure 51 shows the percentage of Land occupied by onshore wind parks for each country of Europe. The regional area of each country in Europe was collected from the European Health Information Gateway [95], while the wind turbine spatial requirements for each wind park are acquired from the Capacity Model in Chapter 3.1.7.

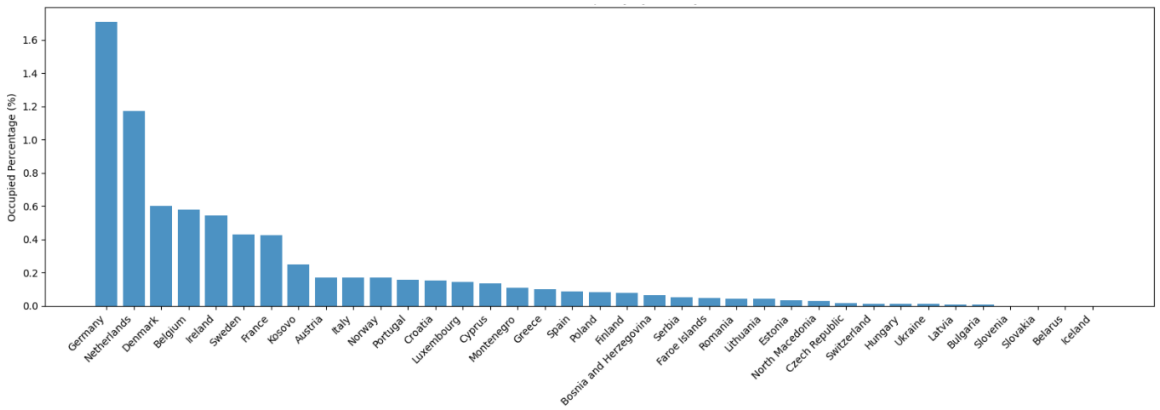

Figure 51: Land-use of wind parks in EU countries

Germany leads with the highest percentage of land occupied by wind turbines, followed by the Netherlands, Belgium, and Luxembourg. An analytical table with the total areas of each country and the total area wind parks occupy can be found in Appendix 29. This indicates that, in absolute terms, Germany devotes more physical land area to wind farms than the rest of the countries in Europe, with a total area of 357,590 km^2 and 6,441 km^2 devoted to wind energy generation. At the same time, smaller countries have significantly less spatial occupation by wind turbines, simply because the total capacity of the turbines is much less than the top countries, or since the sector of onshore wind energy is underdeveloped, or lastly because the terrain does not fit the requirements for the installation of turbines.

4.4.1 Power Density Comparison

The capacity model's output consists of the new wind turbines, the number of new wind turbines at a specific location, and the land area used. All strategies are compared with each other on power density impacts after repowering. Decommissioning and replacement have the same power density as the existing parks since the capacity of each park remains the same. For approaches 1,2,5,6, the area is not flexible, but approaches 3,4 allow limited area expansion; this effect can be seen in Table 20. Figure 52 illustrates the difference in Power density for every country, as every approach is applied.

Approach	Total Land (km^2)	Δ vs Baseline (km^2)	% Expansion vs Baseline
1	90 164.0	0.0	0.0
2	90 565.2	-401.2	-0.4
3	91 446.1	1 282.1	1.4
4	93 168.7	3 004.7	3.3
5	93 516.3	3 352.3	3.7
6	90 565.2	401.2	0.0

Table 20: Global land-use summary by approach number.

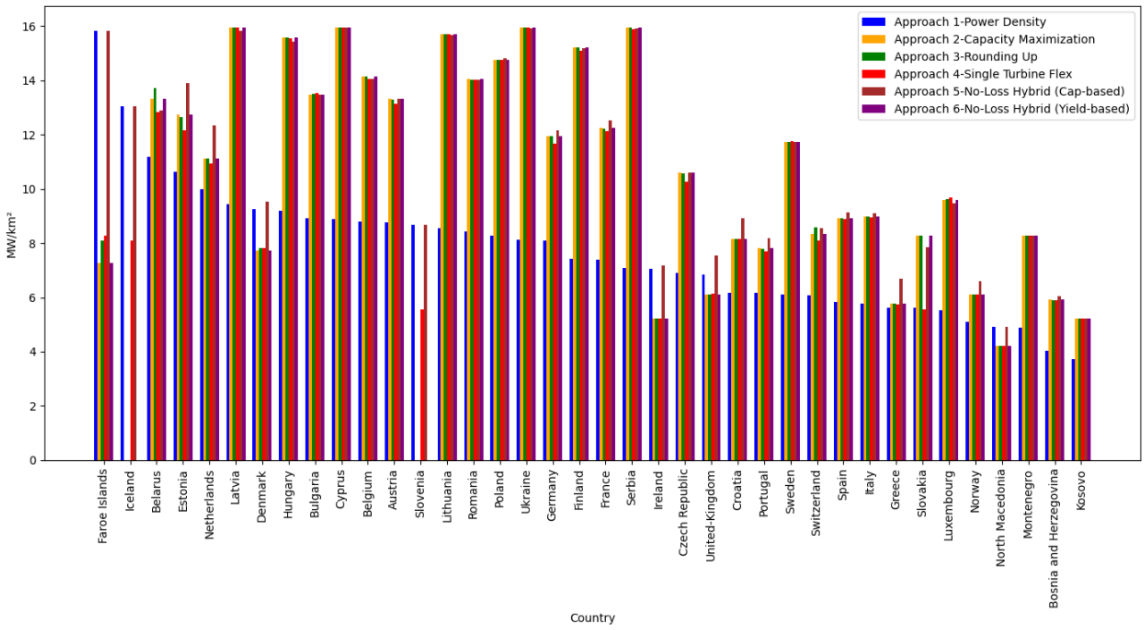

Figure 52: Power density (MW/km^2)*percountryandapproach*

Most countries see their power density rise when older turbines are swapped out for modern machines, confirming that repowering is effective at squeezing more megawatts onto the same land footprint. Approach 2 (Capacity Maximization) consistently delivers the largest density gains, with the no-loss hybrid (Approach 6) almost matching its performance while offering a more conservative capital outlay, making those two the clear "best" strategies. The least impactful methods tend to be the incremental upgrades or age-based replacements (Approaches 3 and 5), which improve density only modestly.

High-resource, large-scale markets like Germany, the Netherlands, Spain, and France regularly post the biggest absolute increases, thanks to both abundant wind potential and extensive existing park area. Conversely, very small or highly constrained countries (Slovenia, Iceland, the Faroe Islands) often register flat or even negative "potential" under strict spatial limits; there simply isn't enough onshore real estate to accommodate larger rotors without encroaching on other land uses. Denmark and the U.K. also achieve zero or negative returns when you assume that repowering must stay within existing farm boundaries, implying that many sites there have already optimized their layout long ago. In short, full repowering and its hybrid variant are the most universally beneficial, with a few high-constraint markets as the notable exceptions, where land availability, not technology, becomes the limiting factor.

4.4.2 Energy Density Comparison

Apart from the power density, the energy density is assessed across all scenarios and countries. The increase of capacity in a wind park does not always translate to higher energy yield, as reported in the energy yield results. The following Figure 53 is created to present the energy density effects of repowering compared to the decommissioning and replacement scenario.

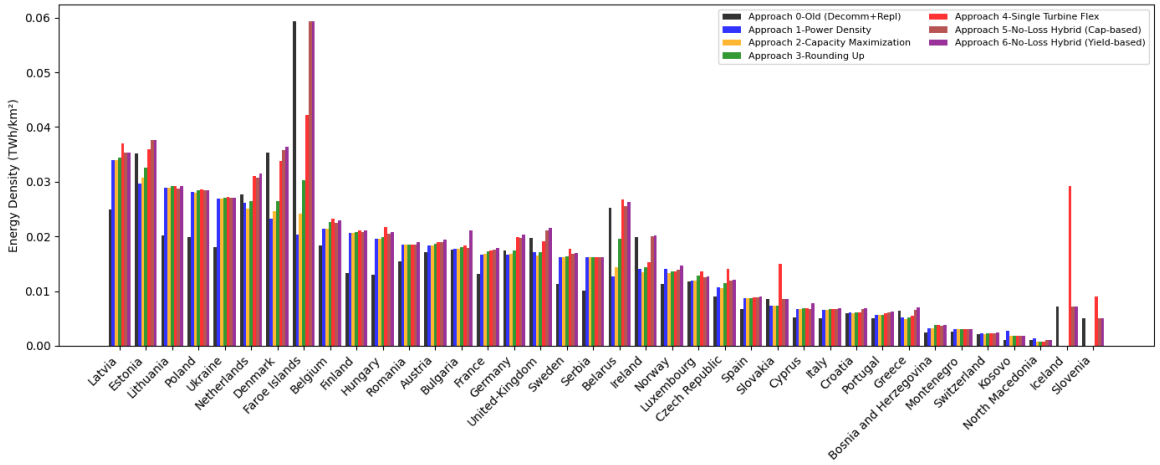

Figure 53: Energy density (TWh/km^2) per country and approach

Across all EU countries, the no-loss hybrid variants deliver the highest energy density (TWh per km^2), closely followed by the single-turbine-flex strategy. In most cases, the yield-based hybrid edges out the capacity-based hybrid by a small margin, confirming that selectively keeping the best-performing old machines can boost annual output per km^2 without expanding the footprint. For example, Latvia or Estonia: baseline energy density sits at roughly 0.02–0.03 TWh/ km^2, yet the hybrids raise that to around 0.035–0.038 TWh/ km^2,an uplift of 20–30 %.

These energy-density gains mirror the power-density improvements presented earlier. Countries that saw the largest jump in MW/ km^2 (Latvia, Cyprus, Ukraine, Serbia) also rank near the top for TWh/km² after repowering, since both metrics scale with the combination of higher nameplate capacity and improved capacity factors. Conversely, nations with already-dense wind farms or very constrained land, like Iceland and Slovenia, show up with modest or even zero gains in both power and energy density. This strong one-to-one correspondence tells us that repowering not only raises instantaneous power output in MW per area but also translates into real, measurable increases in annual energy yield per km^2.

4.4.3 Land Savings Assessment

Figure 54 indicates for each country, how much land would be needed to match the repowered capacity if one strictly followed a decommissioning-and-replacement approach rather than a repowering approach. In other words, each stacked bar represents the total land area that would be required to achieve the same final capacity that repowering achieves more efficiently. The bar graphs describe both the extremes (minimum and maximum) of each country and all approaches. If the baseline scenario is followed, the green and orange bars show how much additional capacity each country will require when repowering capacity is reached. A more detailed plot with each approach's land savings can be found in Appendix Figure 65. Each approach has a different capacity per country, but it's always larger than the decommissioning and replacement scenario.

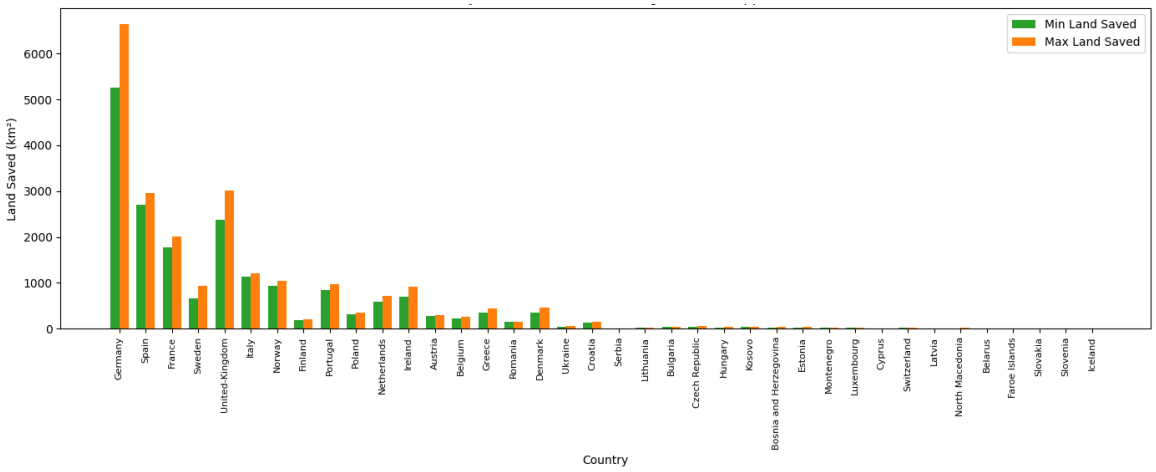

Figure 54: Minimum and maximum land saved from the implementation of repowering against the baseline (Decommissioning and replacement) scenario, considering all approaches

Germany stands out with the highest total land, mainly because it dedicates almost 1.8% of the total land to wind energy production based on Figure 51, reflecting its substantial installed and projected wind capacity. Overall, Figure 54 demonstrates that repowering can avoid 37–41 % (resulting from table 21) of the additional land demand compared to a straight decommission-and-replacement baseline, considering most of the countries, if the decommissioning and replacement scenario is followed, countries would need almost twice the land to match the repowered strategy capacity goals. Even modest expansions in turbine size and technology under repowering can yield substantial capacity gains without requiring proportionally larger land footprints, underscoring the spatial efficiency advantages of repowering.

Approach	Land Saved (km^2)	Baseline Density (MW/km^2)	Repowered Density (MW/km^2)
Approach 1	33 522	7.08	10.41
Approach 2	33 924	7.08	10.41
Approach 3	34 804	7.08	10.41
Approach 4	36 527	7.08	10.32
Approach 5	36 875	7.08	10.79
Approach 6	33 924	7.08	10.08

Table 21: Land area saved and power-density improvements under each repowering approach.

Even the most conservative repowering scenario (Approach 1) would free up over 33,522 km^2 of land compared to a straight decommission-and-replace strategy, while more ambitious strategies (Approaches 4 and 5) can save upwards of 36,500 km^2. At the same time, average power density increases from about 7 MW/km^2 in today's fleet to roughly 10–10.8 MW/km^2 once repowered. In particular, Approach 5 achieves the greatest land savings (36,875 km^2) alongside the highest repowered density (10.8 MW/km^2), highlighting how incremental improvements in turbine size and technology yield substantial spatial-efficiency gains.

5 Conclusion and Discussion

5.1 Conclusion

This analysis rests on several simplifying assumptions that introduce uncertainty into our estimates. We apply a uniform 20-year operational lifetime to all turbines, glossing over real-world variations in component degradation. We assume full availability of decommissioned land without accounting for environmental protections, buffer-zone regulations, or competing land-use pressures that could constrain actual repowering. Turbine layouts are generated with fixed spacing rules across both complex and flat terrains, so site-specific wake-loss interactions are not captured in our yield estimates. National permitting processes, cultural land-access norms, and grid-connection bottlenecks are held constant across countries to enable a continent-wide screening, but this overlooks critical local nuances.

1. **What is the total power capacity potential of wind turbines reaching the end of their operational lifetime in Europe, categorized by region, year, and how big is the maximum capacity and energy yield achievable through wind repowering?**

   This thesis's results have demonstrated that repowering Europe's aging onshore wind turbines offers a powerful pathway to increasing total installed capacity, reducing costs, and conserving land at the same time. Yet, its benefits display uneven efficiency across geographies and technical contexts. Under the all scenarios (allowing site-by-site optimization of turbine layouts), repowering unlocks an additional 60 GW to 82 GW of nameplate capacity by 2050, corresponding to a 33–46 % total nominal power increase of the turbines relative to a straight decommissioning and replacement strategy. These capacity gains are most pronounced in smaller or emerging wind markets (Latvia, Cyprus, Ukraine, Serbia), where replacing numerous low-capacity machines with fewer, high-capacity turbines can more than double power density. On the other hand, in countries that already have a high power density combined with minimal wind park footprints (Slovenia, Iceland, the Faroe Islands), the capacity increase is negligible or even negative in most cases, indicating that repowering serves more to a shift to newer and more reliable technologies that an expansion.

   However, increases in nominal capacity do not always translate into proportional energy-output gains. Across Europe as a whole, repowering uplifts annual generation from 342.9 TWh under the baseline to 425.3 TWh under the yield-focused no-loss hybrid (a 24.1 % gain). Yet in the United Kingdom, several repowering strategies actually delivered power below the baseline—a reflection of its already large turbines and the limited pool of repowerable sites. For instance, the pure capacity-maximization rule (Approach 2) boosted nameplate capacity by 8.3 % but reduced UK output by a few percent, while only the yield-based no-loss hybrid (Approach 6) preserved and slightly improved generation there. Because this is a system-level modeling study, not a site-specific analysis, the results can only be as accurate as the aggregate inputs allow. With a restricted set of repowering turbines and without detailed CFD-based wake-loss and yield assessments at each site, our findings remain first-order estimates. Only by coupling the repowering framework to high-resolution, local wind-flow simulations can planners ensure that theoretical capacity uplifts materialize as generation increases, avoiding "bigger is not always better" outcomes.

2. **What are the estimated costs of decommissioning versus repowering aging wind turbines, and how do these compare in terms of economic feasibility**?

   From an economic standpoint, repowering performs differently than greenfield replacement. The average capital expenditure is higher for repowering (€18.0 M vs. €15.0 M), yet its median CAPEX is slightly lower (€8.34 M vs. €8.83 M), reflecting savings in site preparation and

infrastructure. In terms of value creation, replacement wins on mean NPV (€11.8 M vs. €10.7 M), though both approaches share the same median NPV (€4.8 M). Repowering delivers a marginally higher average IRR (9.62 % vs. 9.19 %), even if replacement shows a higher median IRR (8.85 % vs. 8.13 %). Under a moderate learning-rate assumption, repowering slightly undercuts replacement on the levelized cost of electricity (median €67.4/MWh vs. €68.0/MWh). Payback periods cluster around 10 years for repowering and 9 for replacement.

However, repowering's lower capital intensity per megawatt (unit-capacity cost of € 1,077.4/kW vs. € 1,267.1/kW, saving €189.7/kW) and its improved cash-flow profile over the project lifetime makes it more affordable to finance. Although its payback is roughly one year longer, the combination of slightly higher average IRR and reduced LCOE enhances long-run profitability on a risk-adjusted basis, providing a clear incentive for investors seeking durable returns over a 20-year horizon.

3. **What are the avoided environmental impacts, particularly regarding land use, by choosing repowering over constructing new wind farms?**

   Spatially, repowering delivers substantial land-use savings by reusing existing foundations, roads, and grid connections. Across Europe, average power density increases from 7.08 MW/km² under greenfield or straight replacement scenarios to 10.4–10.8 MW/km², representing a 25–40 % uplift (and up to nearly 100 % in high-resource markets). This improvement in spatial efficiency frees up 33,522 km² to 36,875 km² of land—an area larger than Belgium—that would otherwise be consumed by decommissioning-and-replacement strategies, effectively avoiding 37–41 % of the extra land demand.

   Moreover, annual energy output per unit area rises from 0.02–0.03 TWh/km² to 0.035–0.038 TWh/km², an absolute uplift of roughly 0.008–0.015 TWh per km² (i.e., an extra 8–15 GWh per square kilometer each year). In other words, repowering not only halves the land needed per megawatt but also delivers significantly more electricity per hectare, making it a clear environmental win for conserving land while maximizing renewable output.

5.2 Future Research Directions

Based on the results and conclusions of this report, the following recommendations are offered:

- **Developing a Yield-Maximization Algorithm.** Create and benchmark an optimization routine that selects turbine models and layouts to maximize annual MWh per park, using site-specific wind distributions, wake interactions, and availability data.
- **Expand Turbine Model Library.** Incorporate a comprehensive, manufacturer-verified pool of turbine power curves and technical specifications—especially emerging large-rotor, low-wind-speed machines and next-generation drive-trains—to improve the fidelity of capacity and yield matching.
- **Enrich Spatial Planning Module.** Augment the land-use algorithm with wake-loss modeling, variable row staggering, and terrain- or setback-specific rules (e.g., protected habitats, residential buffers) to refine area requirements and energy-production forecasts.
- **Leverage High-Performance Computing.** Deploy parallelized CFD and wake-interaction simulations across the full turbine dataset to generate accurate, continent-wide energy forecasts under repowering scenarios, addressing the computational intensity of detailed flow modeling.
- **Integrate Dynamic Market & Policy Frameworks.** Couple the financial model to stochastic electricity-price forecasts that evolve year-to-year, carbon-tax trajectories, and sliding-scale

support mechanisms (e.g., repowering-specific CfDs) to quantify and de-risk investment under changing market conditions.

- **Develop a GIS-Enabled Feasibility Toolkit.** Create an open-access software platform that combines high-resolution spatial data (wind resources, terrain), turbine databases, and repowering algorithms to rapidly identify and rank candidate parks—complete with interactive statistical dashboards and bankable feasibility reports.

5.3 Discussion

5.3.1 Methodological Reflections and Limitations

This analysis uses a modular framework but relies on simplifying assumptions. Turbine lifetimes are set uniformly to 20 years while actual retirements vary based on maintenance and component performance. As for the approaches that allow some extension of the wind park land, the availability derives from global terrain and land cover datasets that may overlook protected areas or zoning restrictions. Decommissioned sites are assumed immediately available for repowering, excluding possible environmental remediation or community objections for larger turbines. Permitting and grid connection delays are held constant across countries, enabling a pan-European assessment, but smoothing local fast-track procedures or bottlenecks. For a more realistic approach, future work should incorporate variable decommissioning timelines high high-resolution land use constraints, and stochastic permitting delay models. moreover, the selection of the repowered turbines was from a small list of 18 turbines, which does not describe the market status with complete accuracy.

Finally, it's important to remember that the ultimate goal for every country is not simply to install the highest capacity, but to maximize actual energy yield. In the analysis presented, turbine selection was driven by capacity-maximization logic, without accounting for annual yield due to computational constraints, although a hybrid approach of selecting to or not to repower the park based on energy yield was applied. Ideally, an algorithm would evaluate each turbine by its expected yearly output and then select the model that delivers the greatest energy production for each site. By prioritizing annual yield over nameplate capacity alone, such an approach would unlock the full potential of repowering.

5.3.2 Park Size & Configuration

The existing state analysis of Europe's onshore wind turbine fleet shows that a large part of the parks consists of a small number of turbines, indicating that the land there is restricted in use. Under strict layout rules, these small parks inherently offer little room for additional machines or spacing optimization. The Single-Turbine Flex (STF) approach specifically addresses this by relaxing footprint constraints on single-turbine sites, boosting their repowering success (increasing the total capacity) from 52.8 % to 77.1 % of all eligible parks. This highlights how repowering potential is correlated to the original park configuration: larger, multi-unit wind farms enjoy more potential in repowering under any approach, while small parks require a more tailored approach with flexible spatial restrictions for smaller turbines to unlock meaningful gains.

5.3.3 Energy and Economic Performance

Our analysis reveals a clear link between technical performance and economic outcomes in repowered wind parks. Specifically, we find a strong inverse relationship between energy-yield uplift and changes

in LCOE: sites that capture the biggest increases in annual generation tend to see the largest unit-cost reductions. In practical terms, parks in the top energy-uplift quartile achieve nearly twice the LCOE savings of those in the bottom quartile, highlighting how improved wind capture directly drives down levelized costs. Equally compelling is the positive correlation between energy yield gains and net present value improvements. The higher output parks translate into larger cash flows, so parks with the strongest generation uplifts consistently deliver the most attractive NPVs. This relationship underscores that repowering is fundamentally a performance-driven investment: by prioritizing sites with the greatest wind resource and spacing potential, developers and policymakers can maximize financial returns.

Together, these correlations show that the technical and economic benefits of repowering reinforce one another. Better turbine performance lowers per-megawatt costs, which in turn enhances project viability and spurs further investment, creating a virtuous cycle. This insight simplifies subsidy design: targeting support toward parks with the highest expected energy gains will simultaneously optimize both cost-efficiency and investor appeal.

5.3.4 Regional Heterogeneity

Although continental results highlight widespread benefits, national outcomes vary substantially. Germany achieves about 120 TWh of annual repowered generation due to high average wind speeds and large park clusters, as well as an outdated infrastructure of medium-sized and small turbines. In France and Spain, repowering approximately 20 GW of old turbines to 32 GW produces about 47 TWh and 40 TWh respectively, which indicates a significant increase to the local network. In contrast, countries with already compact footprints (e.g., Slovenia, Iceland, and the Faroe Islands) often register negligible or even negative capacity uplifts under strict spacing constraints, meaning repowering there primarily modernizes technology rather than expands output . Even in mature markets like the United Kingdom, deploying larger rotors can reduce delivered energy despite increased nameplate capacity.

In short, there's no one-size-fits-all solution for repowering. In tightly packed, high-yield areas, replacing with larger turbines with bigger rotor diameters that can harness the wind more efficiently can unlock the biggest gains. In contrast, regions dotted with small, standalone turbines get the most yield gains as they are, so decommissioning and replacement can only modernize the turbine, not adding any substantial amount the the net energy gains. Ultimately, each country needs its own game plan: pick the turbine sizes and models that work best for local wind conditions, optimize park layouts, and decide whether to repower with larger, more efficient machines—or simply replace in kind when repowering gains are minimal—so that every upgrade truly delivers more clean energy to the grid.

5.3.5 Site-Specific Constraints on Repowering Potential

Repowering eligibility is strongly tied to equipment age and turbine dimensions rather than simply the amount of available land or theoretical uplift. Parks that have reached or exceeded a 20-year operational life with relatively small rotor diameters generally meet the spacing and age criteria for turbine replacement, allowing them to install higher-capacity machines without infringing on adjacent units. In contrast, newer installations equipped with large-diameter rotors and high-capacity turbines are already modern and typically fall outside repowering rules: they are not due for decommissioning and offer little net capacity gain, and strict spacing requirements can even necessitate removing units to fit replacements. Total park footprint, while relevant, does not by itself predict repowering feasibility. Notably, both eligible and ineligible sites display similar modeled capacity uplifts, underscoring that it is the combination of turbine age and existing machine scale—not raw land area or projected gains—

that ultimately determines whether a park can be repowered.

5.3.6 Outlook

Looking ahead, wind repowering offers a truly win-win proposition: by replacing aging turbines with modern and larger machines on existing sites, projects can unlock higher capacity and energy output without ever touching new land, safeguarding habitats and community landscapes. Financially, repowered parks deliver stronger returns and shorter payback horizons than greenfield builds, thanks to lower permitting hurdles, reduced infrastructure costs, and improved turbine performance. The fully open-source workflow (https://github.com/AngelosChatz/Evaluating_Wind_Repowering) gives planners and investors the tools to adapt these strategies in the EU, ensuring repowering continues to drive clean, affordable power while minimizing environmental and economic risks.

References

[1] Working towards a European standard for decommissioning wind turbines, July 2020. URL: https://windeurope.org/newsroom/news/working-towards-a-european-standard-for-decommissioning-wind-turbines/.

[2] Share of energy consumption from renewable sources in Europe, October 2024. URL: https://www.eea.europa.eu/en/analysis/indicators/share-of-energy-consumption-from.

[3] Eduardo Martínez, Juan Latorre-Biel, Emilio Jiménez, Félix Sanz, and Julio Blanco. Life cycle assessment of a wind farm repowering process. *Renewable and Sustainable Energy Reviews*, 93:260–271, October 2018. doi:10.1016/j.rser.2018.05.044.

[4] Leonie Grau, Christopher Jung, and Dirk Schindler. Sounding out the repowering potential of wind energy – A scenario-based assessment from Germany. *Journal of Cleaner Production*, 293:126094, April 2021. URL: https://www.sciencedirect.com/science/article/pii/S0959652621003140, doi:10.1016/j.jclepro.2021.126094.

[5] IRENA – International Renewable Energy Agency, December 2024. URL: https://www.irena.org/.

[6] Mladen Bošnjaković, Marko Katinić, Robert Santa, and Dejan Marić. Wind Turbine Technology Trends. *Applied Sciences*, 12(17):8653, January 2022. Number: 17 Publisher: Multidisciplinary Digital Publishing Institute. URL: https://www.mdpi.com/2076-3417/12/17/8653, doi:10.3390/app12178653.

[7] About - The Wind Power - Wind energy Market Intelligence. URL: https://www.thewindpower.net/about_en.php.

[8] Global Wind Atlas v3, October 2019. URL: https://data.dtu.dk/articles/dataset/Global_Wind_Atlas_v3/9420803/2, doi:10.11583/DTU.9420803.v2.

[9] Open Maps for Europe | Eurogeographics. URL: https://www.mapsforeurope.org/datasets/euro-dem.

[10] James Sherwood, Gerardo Tun Gongora, and Anne P. M. Velenturf. A circular economy metric to determine sustainable resource use illustrated with neodymium for wind turbines. *Journal of Cleaner Production*, 376:134305, November 2022. URL: https://www.sciencedirect.com/science/article/pii/S095965262203877X, doi:10.1016/j.jclepro.2022.134305.

[11] Wind Characteristics and Resources. In *Wind Energy Explained*, pages 23–89. John Wiley & Sons, Ltd, 2009. Section: 2 _eprint: https://onlinelibrary.wiley.com/doi/pdf/10.1002/9781119994367.ch2. URL: https://onlinelibrary.wiley.com/doi/abs/10.1002/9781119994367.ch2, doi:10.1002/9781119994367.ch2.

[12] Home page – ADEME, the French Agency for Ecological Transition. URL: https://www.ademe.fr/en/frontpage/.

[13] Eric Lantz, Edward Baring-Gould, and Michael Leventhal. Wind Power Project Repowering: Financial Feasibility, Decision Drivers, and Supply Chain Effects. 2013. URL: https://research-hub.nrel.gov/en/publications/wind-power-project-repowering-financial-feasibility-decision-driv-2, doi:10.2172/1117058.

[14] Renewable Power Generation Costs in 2020, June 2021. URL: https://www.irena.org/publications/2021/Jun/Renewable-Power-Costs-in-2020.

[15] European Wholesale Electricity Price Data. URL: https://ember-energy.org/data/european-wholesale-electricity-price-data.

[16] IEC 61400-1:2019. URL: https://webstore.iec.ch/en/publication/26423.

[17] Wind energy database. URL: https://www.thewindpower.net/index.php.

[18] Lucas Bauer. Welcome to wind-turbine-models.com. URL: https://en.wind-turbine-models.com/.

[19] Index | Electricity | 2024 | ATB | NREL. URL: https://atb.nrel.gov/electricity/2024/index.

[20] Publications. URL: https://iea-wind.org/iea-publications/.

[21] Evdokia Tapoglou, Jacopo Tattini, Andreas Schmitz, Aliki Georgakaki, Michał Długosz, Simon Letout, Anna Kuokkanen, Aikaterini Mountraki, Ela Ince, Drilona Shtjefni, ORDONEZ Geraldine Joanny, Olivier Daniel Eulaerts, and Marcelina Grabowska. Clean Energy Technology Observatory: Wind energy in the European Union - 2023 Status Report on Technology Development, Trends, Value Chains and Markets, October 2023. ISBN: 9789268080641 ISSN: 1831-9424. URL: https://publications.jrc.ec.europa.eu/repository/handle/JRC135020, doi:10.2760/618644.

[22] Patrik Söderholm, Kristina Ek, and Maria Pettersson. Wind power development in Sweden: Global policies and local obstacles. *Renewable and Sustainable Energy Reviews*, 11(3):365–400, April 2007. URL: https://www.sciencedirect.com/science/article/pii/S136403210500047X, doi:10.1016/j.rser.2005.03.001.

[23] United Nations. *World Population Prospects 2019: Highlights*. United Nations, June 2019. URL: https://www.un-ilibrary.org/content/books/9789210042352, doi:10.18356/13bf5476-en.

[24] Eva Topham, David McMillan, Stuart Bradley, and Edward Hart. Recycling offshore wind farms at decommissioning stage. *Energy Policy*, 129:698–709, June 2019. URL: https://www.sciencedirect.com/science/article/pii/S0301421519300618, doi:10.1016/j.enpol.2019.01.072.

[25] Hugo Díaz and Carlos Guedes Soares. An integrated GIS approach for site selection of floating offshore wind farms in the Atlantic continental European coastline. *Renewable and Sustainable Energy Reviews*, 134:110328, August 2020. doi:10.1016/j.rser.2020.110328.

[26] Pablo Del Rio, Anxo Calvo Silvosa, and Guillermo Gómez. Policies and design elements for the repowering of wind farms: A qualitative analysis of different options. *Energy Policy*, 39:1897–1908, April 2011. doi:10.1016/j.enpol.2010.12.035.

[27] JustWind4All - Home. URL: https://justwind4all.eu/.

[28] The European Green Deal - European Commission, July 2021. URL: https://commission.europa.eu/strategy-and-policy/priorities-2019-2024/european-green-deal_en.

[29] Delivering the European Green Deal - European Commission, July 2021. URL: https://commission.europa.eu/strategy-and-policy/priorities-2019-2024/european-green-deal/delivering-european-green-deal_en.

[30] L. Buchsbaum and S. Patel. Wind turbine repowering is on the horizon. 160, November 2016.

[31] Wind energy A gender perspective, January 2020. URL: https://www.irena.org/publications/2020/Jan/Wind-energy-A-gender-perspective.

[32] Siyu Tao, Chaohai Zhang, Andrés Feijóo, and Victor Kim. Wind farm repowering optimization: a techno-economic-aesthetic approach. *IET Renewable Power Generation*, 17(8):2137–2147, 2023. _eprint: https://onlinelibrary.wiley.com/doi/pdf/10.1049/rpg2.12756. URL: https://onlinelibrary.wiley.com/doi/abs/10.1049/rpg2.12756, doi:10.1049/rpg2.12756.

[33] Laura Serri, Ettore Lembo, Davide Airoldi, Camilla Gelli, and Massimo Beccarello. Wind energy plants repowering potential in Italy: technical-economic assessment. *Renewable Energy*, 115:382–390, January 2018. URL: https://www.sciencedirect.com/science/article/pii/S0960148117307863, doi:10.1016/j.renene.2017.08.031.

[34] Isabel C. Gil García, Ana Fernández-Guillamón, M. Socorro García-Cascales, and Ángel Molina-García. Multi-factorial methodology for Wind Power Plant repowering optimization: A Spanish case study. *Energy Reports*, 11:179–196, June 2024. URL: https://www.sciencedirect.com/science/article/pii/S235248472301569X, doi:10.1016/j.egyr.2023.11.044.

[35] Jéssica Ceolin de Bona, Joao Carlos Espindola Ferreira, and Julian Fernando Ordoñez Duran. Analysis of scenarios for repowering wind farms in Brazil. *Renewable and Sustainable Energy Reviews*, 135:110197, January 2021. URL: https://www.sciencedirect.com/science/article/pii/S1364032120304871, doi:10.1016/j.rser.2020.110197.

[36] Christopher Jung, Leon Sander, and Dirk Schindler. Future global offshore wind energy under climate change and advanced wind turbine technology. *Energy Conversion and Management*, 321:119075, December 2024. URL: https://www.sciencedirect.com/science/article/pii/S0196890424010161, doi:10.1016/j.enconman.2024.119075.

[37] T. Prabu and S.K. Kottayil. Repowering a windfarm - A techno-economic approach. *Wind Engineering*, 39(4):385–397, 2015. doi:10.1260/0309-524X.39.4.385.

[38] Aubryn Cooperman, Annika Eberle, and Eric Lantz. Wind turbine blade material in the United States: Quantities, costs, and end-of-life options. *Resources, Conservation and Recycling*, 168:105439, May 2021. URL: https://linkinghub.elsevier.com/retrieve/pii/S092134492100046X, doi:10.1016/j.resconrec.2021.105439.

[39] Redirecting wind energy in India. URL: https://ember-energy.org/latest-insights/redirecting-wind-in-india.

[40] M. Verma, S. Ahmed, and J.L. Bhagoria. An analysis for repowering prospects of jamgodarani wind farm using WASP. *International Journal of Control Theory and Applications*, 9(21):155–161, 2016.

[41] Chris Stetter, Henrik Wielert, and Michael H. Breitner. Hidden repowering potential of non-repowerable onshore wind sites in Germany. *Energy Policy*, 168:113168, September 2022. URL: https://www.sciencedirect.com/science/article/pii/S0301421522003901, doi:10.1016/j.enpol.2022.113168.

[42] Jan Frederick Unnewehr, Eddy Jalbout, Christopher Jung, Dirk Schindler, and Anke Weidlich. Getting more with less? Why repowering onshore wind farms does not always lead to more wind power generation – A German case study. *Renewable Energy*, 180:245–257, December 2021. URL: https://www.sciencedirect.com/science/article/pii/S0960148121012167, doi:10.1016/j.renene.2021.08.056.

[43] Rebecca Windemer. Considering time in land use planning: An assessment of end-of-life decision making for commercially managed onshore wind schemes. *Land Use Policy*, 87:104024, September 2019. URL: https://www.sciencedirect.com/science/article/pii/S026483771831915X, doi:10.1016/j.landusepol.2019.104024.

[44] Faraedoon Ahmed, Aoife Foley, Carole Dowds, Barry Johnston, and Dlzar Al Kez. Assessing the engineering, environmental and economic aspects of repowering onshore wind energy. *Energy*, 301:131759, August 2024. URL: https://www.sciencedirect.com/science/article/pii/S0360544224015329, doi:10.1016/j.energy.2024.131759.

[45] Antonio Colmenar-Santos, Severo Campíñez-Romero, Clara Pérez-Molina, and Francisco Mur-Pérez. Repowering: An actual possibility for wind energy in Spain in a new scenario without feed-in-tariffs. *Renewable and Sustainable Energy Reviews*, 41:319–337, January 2015. URL: https://www.sciencedirect.com/science/article/pii/S1364032114007175, doi:10.1016/j.rser.2014.08.041.

[46] Peng Hou, Peter Enevoldsen, Weihao Hu, Cong Chen, and Zhe Chen. Offshore wind farm repowering optimization. *Applied Energy*, 208:834–844, December 2017. URL: https://www.sciencedirect.com/science/article/pii/S030626191731348X, doi:10.1016/j.apenergy.2017.09.064.

[47] Sebastian Himpler and Reinhard Madlener. Repowering of Wind Turbines: Economics and Optimal Timing, July 2012. URL: https://papers.ssrn.com/abstract=2236265, doi:10.2139/ssrn.2236265.

[48] Ben Hoen, Ryan Darlow, Ryan Haac, Joseph Rand, and Ken Kaliski. Effects of land-based wind turbine upsizing on community sound levels and power and energy density. *Applied Energy*, 338:120856, May 2023. URL: https://www.sciencedirect.com/science/article/pii/S0306261923002209, doi:10.1016/j.apenergy.2023.120856.

[49] Osservatorio Balcani e Caucaso. Solar energy in Europe's countryside: huge potential, complex challenges. URL: https://www.balcanicaucaso.org/eng/Areas/Europe/Solar-energy-in-Europe-s-countryside-huge-potential-complex-challenges-236101.

[50] High-resolution large-scale onshore wind energy assessments: A review of potential definitions, methodologies and future research needs - ScienceDirect. URL: https://www.sciencedirect.com/science/article/pii/S0960148121014841.

[51] Jackson G. Njiri, Nejra Beganovic, Manh H. Do, and Dirk Söffker. Consideration of lifetime and fatigue load in wind turbine control. *Renewable Energy*, 131:818–828, February 2019. URL: https://www.sciencedirect.com/science/article/pii/S0960148118309078, doi:10.1016/j.renene.2018.07.109.

[52] Wind Farm Layout Upgrade Optimization. URL: https://www.mdpi.com/1996-1073/12/13/2465.

[53] IER. Wind Turbines and Solar Panels are Aging Prematurely, February 2024. URL: https://www.instituteforenergyresearch.org/renewable/wind-turbines-and-solar-panels-are-aging-prematurely/.

[54] Begoña Guezuraga, Rudolf Zauner, and Werner Pölz. Life cycle assessment of two different 2 MW class wind turbines. *Renewable Energy*, 37(1):37–44, January 2012. URL: https://www.sciencedirect.com/science/article/pii/S0960148111002254, doi:10.1016/j.renene.2011.05.008.

[55] S. Tegen, E. Lantz, M. Hand, B. Maples, A. Smith, and P. Schwabe. 2011 Cost of Wind Energy Review, March 2013. Number: NREL/TP-5000-56266 Publisher: National Renewable Energy Laboratory (U.S.). URL: https://digital.library.unt.edu/ark:/67531/metadc830372/, doi:10.2172/1072784.

[56] C. Bak. 3 - Aerodynamic design of wind turbine rotors. In Povl Brøndsted and Rogier P. L. Nijssen, editors, *Advances in Wind Turbine Blade Design and Materials*, Woodhead Publishing Series in Energy, pages 59–108. Woodhead Publishing, January 2013. URL: https://www.sciencedirect.com/science/article/pii/B9780857094261500039, doi:10.1533/9780857097286.1.59.

[57] Resource Library. URL: https://www.nyserda.ny.gov/All-Programs/Offshore-Wind/Resource-Library.

[58] Javier González and Roberto Lacal Arantegui. Technological evolution of onshore wind turbines—a market-based analysis. *Wind Energy*, 19, February 2016. doi:10.1002/we.1974.

[59] Douglas C. Montgomery, Elizabeth A. Peck, and G. Geoffrey Vining. *Introduction to Linear Regression Analysis*. John Wiley & Sons, April 2012. Google-Books-ID: 0yR4KUL4VDkC.

[60] Johan Meyers and Charles Meneveau. Optimal turbine spacing in fully developed wind farm boundary layers. *Wind Energy*, 15(2):305–317, 2012. _eprint: https://onlinelibrary.wiley.com/doi/pdf/10.1002/we.469. URL: https://onlinelibrary.wiley.com/doi/abs/10.1002/we.469, doi:10.1002/we.469.

[61] Enrico G. A. Antonini, David A. Romero, and Cristina H. Amon. Optimal design of wind farms in complex terrains using computational fluid dynamics and adjoint methods. *Applied Energy*, 261:114426, March 2020. URL: https://www.sciencedirect.com/science/article/pii/S0306261919321130, doi:10.1016/j.apenergy.2019.114426.

[62] Bukurije Hoxha, Igor K. Shesho, and Risto V. Filkoski. Analysis of Wind Turbine Distances Using a Novel Techno-Spatial Approach in Complex Wind Farm Terrains. *Sustainability*, 14(20):13688, January 2022. Number: 20 Publisher: Multidisciplinary Digital Publishing Institute. URL: https://www.mdpi.com/2071-1050/14/20/13688, doi:10.3390/su142013688.

[63] L. J. Vermeer, J. N. Sørensen, and A. Crespo. Wind turbine wake aerodynamics. *Progress in Aerospace Sciences*, 39(6):467–510, August 2003. URL: https://www.sciencedirect.com/science/article/pii/S0376042103000782, doi:10.1016/S0376-0421(03)00078-2.

[64] K. Foster and S. Wharton. Winds of Change: Assessing Wind Energy Efficiency in Complex Terrain. Technical Report LLNL-TR-788155, Lawrence Livermore National Lab. (LLNL), Livermore, CA (United States), August 2019. URL: https://www.osti.gov/biblio/1559401, doi:10.2172/1559401.

[65] Pramod Jain. *Wind Energy Engineering*. McGraw-Hill Education, 2nd edition edition, 2016. URL: https://www.accessengineeringlibrary.com/content/book/9780071843843.

[66] Mahmoud Elgendi, Maryam AlMallahi, Ashraf Abdelkhalig, and Mohamed Y. E. Selim. A review of wind turbines in complex terrain. *International Journal of Thermofluids*, 17:100289, February 2023. URL: https://www.sciencedirect.com/science/article/pii/S2666202723000113, doi:10.1016/j.ijft.2023.100289.

[67] Shawn Riley, Stephen Degloria, and S.D. Elliot. A Terrain Ruggedness Index that Quantifies Topographic Heterogeneity. *Internation Journal of Science*, 5:23–27, January 1999.

[68] R. J. Barthelmie, K. Hansen, S. T. Frandsen, O. Rathmann, J. G. Schepers, W. Schlez, J. Phillips, K. Rados, A. Zervos, E. S. Politis, and P. K. Chaviaropoulos. Modelling and measuring flow and wind turbine wakes in large wind farms offshore. *Wind Energy*, 12(5):431–444, 2009. _eprint: https://onlinelibrary.wiley.com/doi/pdf/10.1002/we.348. URL: https://onlinelibrary.wiley.com/doi/abs/10.1002/we.348, doi:10.1002/we.348.

[69] GWEC Global Wind Report - WindEnergy Hamburg. URL: https://www.windenergyhamburg.com/news-themen/reports-market-updates/gwec-global-wind-report.

[70] V110-2.0 MW™, February 2025. URL: https://www.vestas.com/content/vestas-com/global/en/pages/backup-2-mw-platform/V110-2-0-mw.html.

[71] 2mw-platform | GE Vernova. URL: https://www.gevernova.com/wind-power/onshore-wind/2mw-platform?utm_source=chatgpt.com.

[72] Peter Enevoldsen and George Xydis. Examining the trends of 35 years growth of key wind turbine components. *Energy for Sustainable Development*, 50:18–26, June 2019. URL: https://www.sciencedirect.com/science/article/pii/S097308261831353X, doi:10.1016/j.esd.2019.02.003.

[73] R. McKenna, P. Ostman v. d. Leye, and W. Fichtner. Key challenges and prospects for large wind turbines. *Renewable and Sustainable Energy Reviews*, 53(C):1212–1221, 2016. Publisher: Elsevier. URL: https://ideas.repec.org//a/eee/rensus/v53y2016icp1212-1221.html.

[74] (PDF) An Optimization Framework for Wind Farm Design in Complex Terrain. *ResearchGate*, October 2024. URL: https://www.researchgate.net/publication/328536112_An_Optimization_Framework_for_Wind_Farm_Design_in_Complex_Terrain, doi:10.3390/app8112053.

[75] Offshore wind turbine rotor diameter globally 2030. URL: https://www.statista.com/statistics/1085674/offshore-wind-turbines-average-rotor-diameter-globally/?utm_source=chatgpt.com.

[76] admin. The Sky's The Limit - Why Wind Turbines Blades Are Becoming Longer and Longer, October 2023. URL: https://windpowerlab.com/longer-blades-bigger-rotor-diameter/.

[77] World's largest onshore wind turbine spins up 430 ft blades to deliver 15 MW, October 2024. Section: Energy. URL: https://newatlas.com/energy/sany-world-largest-onshore-wind-turbine/.

[78] China completes building world's largest 26-MW offshore wind turbine | REVE News of the wind sector in Spain and in the world, October 2024. URL: https://www.evwind.es/2024/10/14/china-completes-building-worlds-largest-26-mw-offshore-wind-turbine/101752.

[79] Fabian Hofmann, Johannes Hampp, Fabian Neumann, Tom Brown, and Jonas Hörsch. atlite: A Lightweight Python Package for Calculating Renewable Power Potentials and Time Series, June 2021. URL: https://github.com/PyPSA/atlite, doi:10.21105/joss.03294.

[80] Helen Setchell. ECMWF Reanalysis v5, February 2020. URL: https://www.ecmwf.int/en/forecasts/dataset/ecmwf-reanalysis-v5.

[81] Territorial units for statistics (NUTS) - GISCO - Eurostat. URL: https://ec.europa.eu/eurostat/web/gisco/geodata/statistical-units/territorial-units-statistics.

[82] vwf/power_curves at master · renewables-ninja/vwf. URL: https://github.com/renewables-ninja/vwf/tree/master/power_curves.

[83] Luis M. Abadie and Nestor Goicoechea. Old Wind Farm Life Extension vs. Full Repowering: A Review of Economic Issues and a Stochastic Application for Spain. *Energies*, 14(12):3678, January 2021. Number: 12 Publisher: Multidisciplinary Digital Publishing Institute. URL: https://www.mdpi.com/1996-1073/14/12/3678, doi:10.3390/en14123678.

[84] NREL 2013 Renewable Energy Data Book includes biopower statistics | Biomass Magazine. URL: https://biomassmagazine.com//articles/nrel-2013-renewable-energy-data-book-includes-biopower-statistics-11562.

[85] hhHWStowersUU, Author at HWS Towers, December 2020. URL: https://www.hwstowers.com/author/hhHWStowersUU/.

[86] Retrofitting wind and solar energy property: Key considerations. URL: https://www.cohnreznick.com/insights/retrofitting-wind-solar-energy-property-key-considerations.

[87] Wind Farms: Reach Renewable electricity targets, March 2025. URL: https://www.sia-partners.com/en/insights/publications/wind-farms-reach-renewable-electricity-targets.

[88] BIOWIND | Sustainable Approaches to Wind Turbine Decommissioning | Interreg Europe, December 2024. URL: https://www.interregeurope.eu/biowind/news-and-events/news/sustainable-approaches-to-wind-turbine-decommissioning.

[89] Infographic: Renewable Power Generation Costs Continue to Fall Despite Inflation, September 2024. URL: https://www.irena.org/News/articles/2024/Sep/Infographic-Renewable-Power-Generation-Costs-in-2023.

[90] The cost of financing for renewable power, May 2023. URL: https://www.irena.org/Publications/2023/May/The-cost-of-financing-for-renewable-power.

[91] Net Present Value (NPV). URL: https://corporatefinanceinstitute.com/resources/valuation/net-present-value-npv/.

[92] Levelized Cost of Energy (LCOE). URL: https://corporatefinanceinstitute.com/resources/valuation/levelized-cost-of-energy-lcoe/.

[93] Internal Rate of Return (IRR): Formula and Examples. URL: https://www.investopedia.com/terms/i/irr.asp.

[94] [nrg_ind_peh] Gross and net production of electricity and derived heat by type of plant and operator. URL: https://ec.europa.eu/eurostat/databrowser/view/nrg_ind_peh/default/table?lang=en.

[95] WHO European health information at your fingertips. URL: https://gateway.euro.who.int/en/indicators/hfa_28-0161-area-km2/.

[96] Bias—Variance Trade-off. ISBN: 9781119439868. URL: https://www.researchgate.net/publication/324271509_Bias-Variance_Trade-off.

[97] Trevor Hastie, Robert Tibshirani, and Jerome Friedman. Model Assessment and Selection. In Trevor Hastie, Robert Tibshirani, and Jerome Friedman, editors, *The Elements of Statistical Learning: Data Mining, Inference, and Prediction*, pages 219–259. Springer, New York, NY, 2009. doi:10.1007/978-0-387-84858-7_7.

[98] Gareth James, Daniela Witten, Trevor Hastie, and Robert Tibshirani. Statistical Learning. In Gareth James, Daniela Witten, Trevor Hastie, and Robert Tibshirani, editors, *An Introduction to Statistical Learning: with Applications in R*, pages 15–57. Springer US, New York, NY, 2021. doi:10.1007/978-1-0716-1418-1_2.

[99] Yun Wang, Qinghua Hu, Linhao Li, Aoife M. Foley, and Dipti Srinivasan. Approaches to wind power curve modeling: A review and discussion. *Renewable and Sustainable Energy Reviews*, 116:109422, December 2019. URL: https://www.sciencedirect.com/science/article/pii/S1364032119306306, doi:10.1016/j.rser.2019.109422.

[100] Zhiming Wang, Xuan Wang, and Weimin Liu. Genetic least square estimation approach to wind power curve modelling and wind power prediction. *Scientific Reports*, 13(1):9188, June 2023. Publisher: Nature Publishing Group. URL: https://www.nature.com/articles/s41598-023-36458-w, doi:10.1038/s41598-023-36458-w.

[101] Francisco Bilendo, Angela Meyer, Hamed Badihi, Ningyun Lu, Philippe Cambron, and Bin Jiang. Applications and Modeling Techniques of Wind Turbine Power Curve for Wind Farms—A Review. *Energies*, 16(1):180, January 2023. Number: 1 Publisher: Multidisciplinary Digital Publishing Institute. URL: https://www.mdpi.com/1996-1073/16/1/180, doi:10.3390/en16010180.

[102] The Wind Resource. In *Wind Energy Handbook*, pages 9–38. John Wiley & Sons, Ltd, 2011. Section: 2 _eprint: https://onlinelibrary.wiley.com/doi/pdf/10.1002/9781119992714.ch2. URL: https://onlinelibrary.wiley.com/doi/abs/10.1002/9781119992714.ch2, doi:10.1002/9781119992714.ch2.

[103] Khurram Mushtaq, Asim Waris, Runmin Zou, Uzma Shafique, Niaz B. Khan, M. Ijaz Khan, Mohammed Jameel, and Muhammad Imran Khan. A comprehensive approach to wind turbine power curve modeling: Addressing outliers and enhancing accuracy. *Energy*, 304:131981, September 2024. URL: https://www.sciencedirect.com/science/article/pii/S0360544224017547, doi:10.1016/j.energy.2024.131981.

[104] C. G. Justus, W. R. Hargraves, A. Mikhail, and D. Graber. Methods for estimating wind speed frequency distributions. *J. Appl. Meteorol.; (United States)*, 17:3, March 1978. Institution: School of Aerospace Engineering, Georgia Institute of Technology, Atlanta 30332. URL: https://www.osti.gov/biblio/5127748, doi:10.1175/1520-0450(1978)017<0350:MFEWSF>2.0.CO;2.

[105] Huanyu Shi, Zhibao Dong, Nan Xiao, and Qinni Huang. Wind Speed Distributions Used in Wind Energy Assessment: A Review. *Frontiers in Energy Research*, 9, November 2021. Publisher: Frontiers. URL: https://www.frontiersin.orghttps://www.frontiersin.org/journals/energy-research/articles/10.3389/fenrg.2021.769920/full, doi:10.3389/fenrg.2021.769920.

[106] Assoc.Prof.Dr.Jompob Waewsak, Chana Chancham, Mathieu Landry, and Yves Gagnon. An Analysis of Wind Speed Distribution at Thasala, Nakhon Si Thammarat, Thailand. *Journal of Sustainable Energy and Environment*, 2, January 2011.

[107] Kidmo D., Doka Serge, Raidandi Danwe, and Noël Djongyang. Performance Assessment of Two-parameter Weibull Distribution Methods for Wind Energy Applications in the District of Maroua in Cameroon. *International Journal of Sciences: Basic and Applied Research (IJSBAR)*, 17:39–59, July 2014.

[108] Mohammad Golam Mostafa Khan and Mohammed Rafiuddin Ahmed. Bayesian method for estimating Weibull parameters for wind resource assessment in a tropical region: a comparison between two-parameter and three-parameter Weibull distributions. *Wind Energy Science*,

8(8):1277–1298, August 2023. Publisher: Copernicus GmbH. URL: https://wes.copernicus.org/articles/8/1277/2023/, doi:10.5194/wes-8-1277-2023.

[109] Windenergie-Daten der Schweiz. URL: https://wind-data.ch/tools/weibull.php?lng=en.

[110] Susanna Twidale. Explainer: Why Russia drives European and British gas prices. *Reuters*, June 2022. URL: https://www.reuters.com/business/energy/why-russia-drives-european-gas-prices-2022-01-21/.

[111] Joanna Sitarz, Michael Pahle, Sebastian Osorio, Gunnar Luderer, and Robert Pietzcker. EU carbon prices signal high policy credibility and farsighted actors. *Nature Energy*, 9(6):691–702, June 2024. Publisher: Nature Publishing Group. URL: https://www.nature.com/articles/s41560-024-01505-x, doi:10.1038/s41560-024-01505-x.

[112] Droughts rattle Europe's hydropower market, intensifying energy crisis, May 2022. URL: https://www.spglobal.com/commodity-insights/en/news-research/latest-news/electric-power/080522-droughts-rattle-europes-hydropower-market-intensifying-energy-crisis.

A Appendix

A.1 Methods

A.1.1 Capacity Model

Rotor Diameter Estimation

Linear regression models the relationship between the wind turbine capacity (x) and the rotor diameter (y) using the equation:

$$y = mx + b$$

Where:

- y: Predicted rotor diameter (m),
- x: Wind turbine capacity (MW),
- m: Slope of the regression line, representing the change in rotor diameter per MW of capacity,
- b: Intercept of the regression line, representing the rotor diameter when capacity is 0.

For this analysis:

$$\text{Predicted Rotor Diameter (m)} = m \cdot \text{Capacity (MW)} + b$$

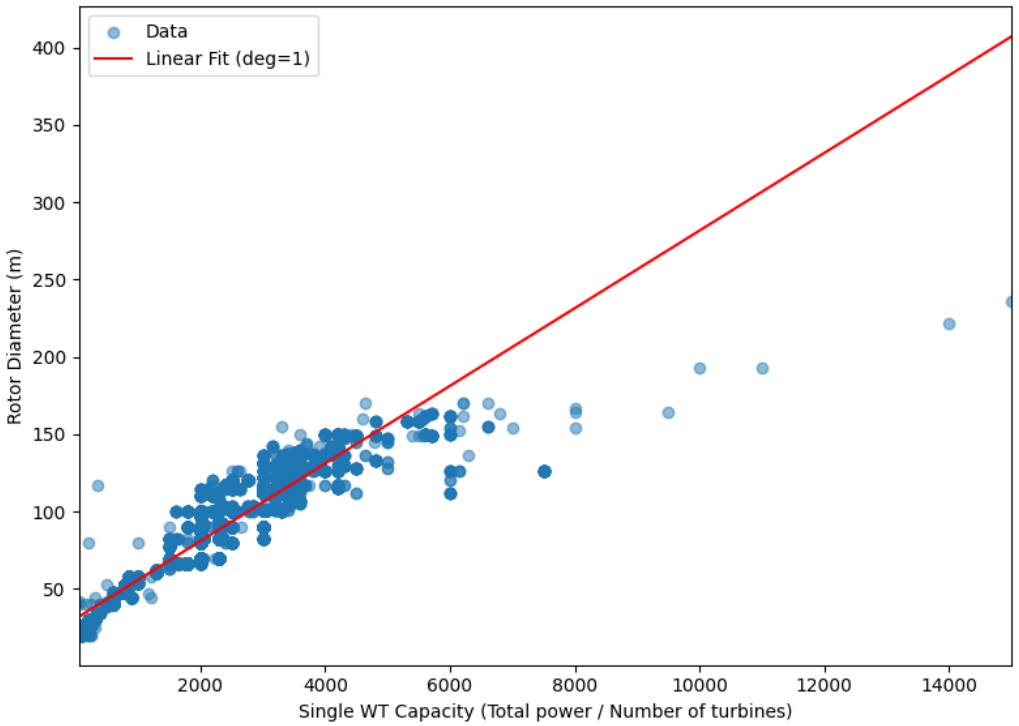

Figure 55: Linear regression of turbine's capacity vs. rotor diameter

From the plot, the linear regression line captures the general upward trend, but there appear to be non-linear patterns, especially a slight curvature in the lower capacity range and a flattening or spread in rotor diameter at higher capacities. But it is clear that for larger capacities, the rotor diameter does not increase linearly like the lower capacities.

This preference is due to the bias-variance trade-off: simpler models(with fewer parameters) tend to have lower variance and are less prone to overfitting, while higher-order models might capture noise rather than the true relationship between the variables [96].

Hastie, Tibshirani, and Friedman (2009) discuss that as model complexity increases, the reduction in bias is frequently offset by an increase in variance, which is especially problematic when data are limited [97]. James et al. (2013) explain that with few data points, higher-order polynomials are prone to fitting the noise rather than the true underlying relationship, thereby resulting in overfitting. Moreover, linear models are not only easier to interpret but also provide a more stable prediction when no strong non-linear trends are evident in the data [98].

The Dataset of 16,195 turbines is quite significant, and overfitting is not a problem. It can be seen in Figure 55 that with linear regression, turbines up to 5MW have accurate estimations, but for larger capacities, the estimation deviates from the real data. Hence, a higher-degree regression technique is examined.

A.1.2 Energy Yield Model

To estimate the energy yield of repowered wind turbines, the power curve of the turbine must be approximated. When manufacturer data are not available, a modeling approach is used to estimate the capacity factor and, subsequently, the annual energy yield based on wind speed data.

Wind Turbine Parameters

Each turbine is defined by several parameters that directly influence its energy production:

1. Rated Capacity (MW): The maximum power output under optimal wind conditions.
2. Cut-In Speed (m/s): The minimum wind speed at which the turbine begins generating power.
3. Rated Speed (m/s): The wind speed at which the turbine reaches its nominal power output.
4. Cut-Out Speed (m/s): The wind speed beyond which the turbine is shut down to avoid mechanical damage.
5. Hub Height: The height of the rotor above ground.

These specifications, typically obtained from manufacturer data or literature, serve as the fundamental inputs to the energy yield model.

Power Curve Approximation

In the literature, a wide range of methods has been suggested for approaching power curves with high accuracy. Parametric approaches, such as logistic functions and piecewise polynomial techniques, are commonly used to capture the S-shaped relationship between wind speed and power output. Similarly, piecewise polynomial techniques—such as the cubic and quadratic approaches—provide simple yet effective means to model the ramp-up region (between cut-in and rated speeds) using power law

scaling. More recently, an exponential ramp model has been introduced to offer a smooth, adjustable transition in this region [99].

For example, a piecewise cubic ramp function can be employed to approximate the turbine power output $P(v)$ as a function of wind speed v. The resulting idealized power curve has an S-shape: a cubic ramp up, a plateau, then a cutoff. This piecewise model (sometimes called the ideal or theoretical power curve) is widely used in simulations and preliminary energy calculations because of its simplicity and physical basis. It closely resembles actual manufacturer power curves in shape, especially in the initial cubic climb[100, 101]. Textbook sources (e.g., Burton et al. 2011 [102]) and IEC guidelines (IEC 61400-12-1 [16], power performance testing) acknowledge this standard form: it provides a reasonable approximation for predicting annual energy production and understanding turbine performance with varying wind speeds. The following formula [101] was used to estimate the power output of the turbines at specific wind speeds of the cubic approach:

$$P(v) = \begin{cases} 0, & \text{if } v < v_{ci}, \\ P_{\text{rated}} \cdot \dfrac{v^3 - v_{ci}^3}{v_r^3 - v_{ci}^3}, & \text{if } v_{ci} \leq v < v_r, \\ P_{\text{rated}}, & \text{if } v_r \leq v < v_{co}, \\ 0, & \text{if } v \geq v_{co}, \end{cases}$$

where:

- $P(v)$ is the power output (in kW) at wind speed v.
- P_{rated} is the rated (maximum) power of the turbine.
- v_{ci}, v_r, and v_{co} are the cut-in, rated, and cut-out wind speeds, respectively.

Table 22 summarizes several approaches that rely solely on the cut-in, rated, and cut-out speeds, along with their key characteristics and corresponding references. In our study, we compare four parametric, piecewise the logistic model, the cubic power law, the quadratic approach, and the exponential ramp model, to illustrate their relative performance under idealized conditions.

Table 22: Summary of Ramp-up Region Modeling Approaches Using Only Rated, Cut-in, and Cut-out Speeds.

Method	**Formula** ($v_{ci} \leq v < v_r$)	**Notes**	**Reference**
Logistic Function	$P(v) = \frac{P_{\text{rated}}}{\left(1 + Q\exp\left(-B\left(v - c\right)\right)\right)^{1/g}}$	$c = \frac{v_{ci}+v_r}{2}$. Captures the typical S-shaped ramp-up from zero to rated power.	[103]
Cubic Approach	$P(v) = P_{\text{rated}}\frac{v^3 - v_{ci}^3}{v_r^3 - v_{ci}^3}$	Implements a cubic power law ramp-up using v^3 scaling, smoothly transitioning from zero to rated power.	[101]
Quadratic Approach	$P(v) = P_{\text{rated}}\left(\frac{v - v_{ci}}{v_r - v_{ci}}\right)^2$	Uses squared scaling for a nonlinear ramp-up alternative that gradually increases power.	[101]
Exponential Approach	$P(v) = P_{\text{rated}}\frac{1 - \exp\left(-k\left(v - v_{ci}\right)\right)}{1 - \exp\left(-k\left(v_r - v_{ci}\right)\right)}$	Provides a smooth ramp-up with adjustable steepness via parameter k (set to 0.5 by default).	[103]

Legend of Symbols:

Symbol	**Definition**
v_{ci}	Cut-in wind speed – the minimum wind speed at which the turbine starts generating power.
v_r	Rated wind speed – the wind speed at which the turbine reaches its rated power.
$P(v)$	Power output at a given wind speed v.
P_{rated}	Rated power of the wind turbine.
Q, B, g	Parameters in the logistic function that control the shape of the ramp-up curve.
k	Parameter in the exponential approach that adjusts the steepness of the ramp-up curve.

While many other methods, such as spline interpolation, support vector machines, and quintile regression–based models, have been proposed in the other literature, these techniques typically require additional input variables or more in-depth datasets. For scenarios where only the rated, cut-in, and cut-out speeds are known, the parametric methods summarized above provide a robust and practical solution. Recent studies also suggest that integrating pre-processing with these parametric models can further enhance accuracy in real-world applications [103].

This approximation captures the essential physics of wind energy conversion and has been validated for large-scale energy yield assessments.

Table 23: Error metrics for the uphill slope (Cut-in to Rated Speed)

Turbine	Model	MAE (kW, %)	RMSE (kW, %)	Max Error (kW, %)
E-82 EP2 E4	Logistic	141.61 (4.72%)	179.21 (5.97%)	318.47 (10.62%)
	Cubic	457.19 (15.24%)	573.33 (19.11%)	941.02 (31.37%)
	Quadratic	342.50 (11.42%)	431.52 (14.38%)	714.40 (23.81%)
	Exponential	1162.70 (38.76%)	1391.17 (46.37%)	2161.95 (72.06%)
Vestas V90-3.0 MW	Logistic	71.00 (2.37%)	83.56 (2.79%)	144.00 (4.80%)
	Cubic	508.01 (16.93%)	613.02 (20.43%)	992.30 (33.08%)
	Quadratic	489.13 (16.30%)	578.71 (19.29%)	913.22 (30.44%)
	Exponential	854.16 (28.47%)	1077.75 (35.93%)	1759.17 (58.64%)
Vestas V105-3.5	Logistic	451.55 (13.09%)	589.00 (17.07%)	1100.38 (31.90%)
	Cubic	137.04 (3.97%)	216.79 (6.28%)	438.82 (12.72%)
	Quadratic	90.77 (2.63%)	150.66 (4.37%)	345.50 (10.01%)
	Exponential	1394.44 (40.42%)	1665.97 (48.29%)	2485.33 (72.04%)
Vestas-v136-3.45	Logistic	143.50 (4.16%)	204.47 (5.93%)	445.69 (12.92%)
	Cubic	427.56 (12.39%)	552.76 (16.02%)	996.71 (28.89%)
	Quadratic	412.12 (11.95%)	516.79 (14.98%)	913.38 (26.47%)
	Exponential	906.53 (26.28%)	1170.53 (33.93%)	1880.21 (54.50%)
vestas_v150-4200	Logistic	155.11 (3.69%)	230.37 (5.49%)	501.97 (11.95%)
	Cubic	524.62 (12.49%)	658.02 (15.67%)	1166.96 (27.78%)
	Quadratic	505.83 (12.04%)	615.91 (14.66%)	1065.50 (25.37%)
	Exponential	1110.73 (26.45%)	1403.57 (33.42%)	2253.73 (53.66%)
_nordex_n149-4.0-4.	Logistic	241.99 (5.38%)	354.73 (7.88%)	765.69 (17.02%)
	Cubic	461.05 (10.25%)	585.79 (13.02%)	1077.45 (23.94%)
	Quadratic	440.92 (9.80%)	540.38 (12.01%)	968.75 (21.53%)
	Exponential	1282.77 (28.51%)	1593.73 (35.42%)	2511.14 (55.80%)
Nordex N131/3600 Delta	Logistic	216.11 (6.00%)	319.38 (8.87%)	666.55 (18.52%)
	Cubic	337.44 (9.37%)	434.83 (12.08%)	788.96 (21.92%)
	Quadratic	321.33 (8.93%)	397.72 (11.05%)	702.00 (19.50%)
	Exponential	1054.55 (29.29%)	1309.05 (36.36%)	2043.91 (56.78%)
Enercon E-126 7.58 EP8	Logistic	238.89 (3.15%)	309.32 (4.08%)	603.11 (7.96%)
	Cubic	1169.67 (15.43%)	1486.16 (19.61%)	2581.27 (34.05%)
	Quadratic	955.44 (12.60%)	1207.46 (15.93%)	2116.98 (27.93%)
	Exponential	2654.56 (35.02%)	3297.43 (43.50%)	5314.03 (70.11%)

Wind Speed Characterization via the Weibull Distribution

The statistical behavior of wind speeds is typically modeled using the Weibull distribution due to its simplicity and flexibility. Justus et al. (1978) showed that the Weibull curve produced smaller errors in modeling wind speed distributions compared to other models [104]. This approach is now standard in wind resource assessment and is discussed in leading textbooks (e.g., Wind Energy Handbook, Burton et al.[102] and Wind Energy Explained, Manwell et al.[11]). Modern studies confirm that Weibull is "the most widely used" probability distribution for wind speeds [105], thanks to its flexibility in matching the observed wind variability in many regions.

Its probability density function (PDF) is defined as:

$$f(v;k,\lambda) = \frac{k}{\lambda}\left(\frac{v}{\lambda}\right)^{k-1} \exp\left[-\left(\frac{v}{\lambda}\right)^{k}\right],$$

where:

- k is the shape parameter.
- λ is the scale parameter, closely related to the mean wind speed.

Weibull Parameters Calculation

Traditionally, the shape factor k can be estimated from the turbulence intensity I by the empirical relation

$$k = \left(\frac{1}{I}\right)^{1.086},$$

as proposed by Justus et al. [104]. However, this method may lead to wide variations in k depending on the measured turbulence intensity.

Studies consistently show that shape factors for onshore wind usually range roughly from 1.5 up to 3 under normal conditions[106]. For example, a comprehensive analysis of 38 UK weather stations (1981–2018) found k values between 1.63 and 2.97 across diverse sites [107, 108]. This study assumes a constant shape parameter of $k = 2$, corresponding to the Rayleigh distribution for simplicity and in line with many onshore wind assessments. Under this assumption, the scale parameter λ is determined by matching the theoretical mean wind speed of the Weibull distribution to the observed average wind speed. The following formula gives the mean of a Weibull distribution [102]:

$$\bar{v} = \lambda\,\Gamma\Big(1 + \frac{1}{k}\Big),$$

where $\Gamma(\cdot)$ denotes the Gamma function,

$$\Gamma(x) \;=\; \int_0^\infty e^{-t}\,t^{x-1}\,dt.$$

Thus, for a given average wind speed v_{avg} (after adjusting to the turbine hub height), the scale parameter is

$$\lambda = \frac{v_{\text{avg}}}{\Gamma\Big(1 + \frac{1}{k}\Big)}.$$

With $k = 2$, we have $\Gamma(1.5) \approx 0.8862$, so that

$$\lambda = \frac{v_{\text{avg}}}{0.8862}.$$

In our implementation, the average wind speed v_{avg} is derived from a raster dataset that provides the wind speed at a reference height (100 m). A power-law correction is applied to adjust this speed to the turbine's hub height h_{hub} [102]:

$$v_{\text{hub}} = v_{\text{ref}}\left(\frac{h_{\text{hub}}}{h_{\text{ref}}}\right)^{\alpha},$$

where:

- v_{ref} is the wind speed at the reference height $h_{\text{ref}} = 100$ m,
- h_{hub} is the turbine hub height, and
- α is the shear exponent

The shear exponent varies depending on the terrain type as presented in Table 24. Offshore smooth terrains have a shear exponent of 0.1, and it can increase up to 0.6 for onshore turbines installed in cities with tall buildings. For this study, the terrain types are simplified and divided into two categories as presented in 3.1.4; the shear exponent values are assumed to be 0.2 and 0.3 for flat and complex terrains, respectively.

Table 24: Wind Shear by Terrain Features, Surface Roughness, and Obstacles (IEA Expert Group Report on Recommended Practices [20]

Site Type	**Wind Shear Exponent** α
Sea	0.10
Coast with onshore winds	0.10
Snow-covered crop stubble	0.12
Open, smooth surface (i.e., concrete)	0.20
Cut grass	0.25
Short-grass prairie	0.25
Open agriculture without hedges/fences	0.30
Crops, tall-grass prairie	0.30
Agriculture with homes, hedges at 1,250 m	0.35
Scattered trees and hedges	0.35
Agriculture with homes, hedges at 250 m	0.40
Trees, hedges, a few buildings	0.45
City suburbs, villages, scattered forests	0.31
Larger cities with tall buildings	0.60
Woodlands	0.50

In general, high-turbulence wind regimes tend to have a broader spread of wind speeds (more variability), corresponding to a lower Weibull shape factor k. Conversely, low-turbulence sites have more consistently steady winds, yielding a higher k value (narrower distribution) based on the Swiss Federal Office of Energy [109]. For instance, in very turbulent environments (IEC Class A or A+ sites, such as complex terrain or stormy areas), k might be around 1.5 or even approaching 1 in extreme cases [109]. Empirical surveys in temperate regions show most sites falling in between, with k roughly 1.7–2.5 for typical mid-latitude winds.

Figure 56 shows Weibull distribution curves for various site classifications. Random database entries were used to generate these curves. Higher-classification sites exhibit a probability density that is more concentrated around the mean wind speed, indicating more consistent conditions, while increased turbulence results in broader curves, reflecting a wider range of wind speeds.

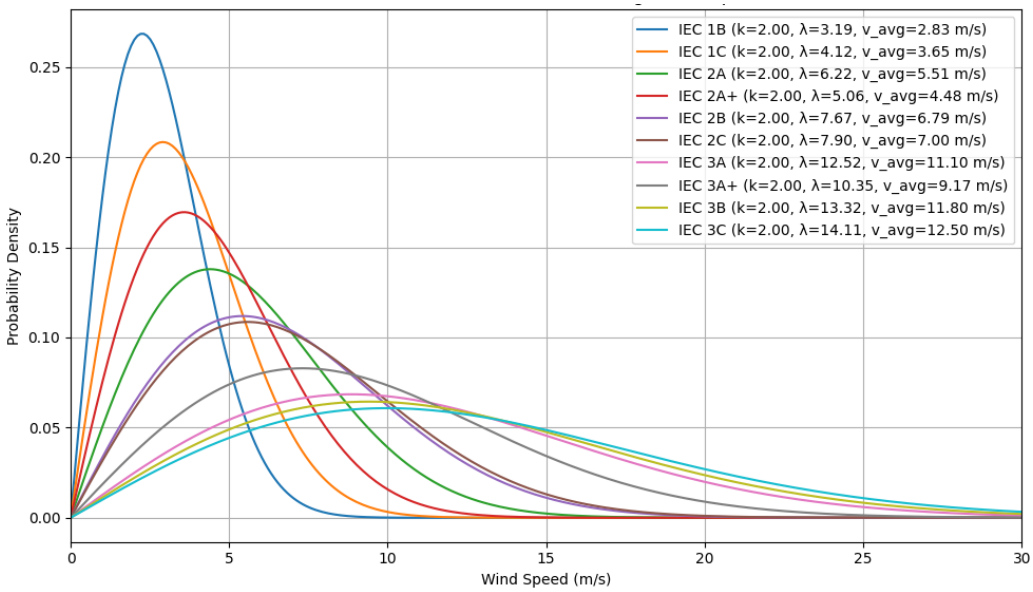

Figure 56: Weibull distribution curves

Table 25: Representative turbine model for each unique capacity

Model	Capacity (kW)	Model	Capacity (kW)
XANT.M21.100	100	Enercon.E66.1800	1800
Bonus.B23.150	150	Enercon.E66.2000	2000
Vestas.V27.225	225	Suzlon.S88.2100	2100
Nordex.N29.250	250	Bonus.B82.2300	2300
Bonus.B33.300	300	Enercon.E92.2350	2350
Bonus.B37.450	450	GE.2.5xl	2500
Bonus.B41.500	500	GE.2.75.103	2750
Bonus.B44.600	600	Alstom.Eco.110	3000
Gamesa.G47.660	660	Nordex.N131.3300	3300
Enercon.E48.800	800	REpower.3.4M	3400
Gamesa.G52.850	850	Siemens.SWT.3.6.107	3600
Enercon.E44.900	900	Wind.World.W3700	3700
Bonus.B54.1000	1000	Siemens.SWT.4.0.130	4000
Bonus.B62.1300	1300	Wind.World.W4200	4200
Acciona.AW77.1500	1500	Enercon.E112.4500	4500
GE.1.6	1600	REpower.5M	5000
Vestas.V66.1650	1650	REpower.6M	6000
Alstom.Eco.74	1670	Enercon.E126.6500	6500
GE.1.7	1700	Enercon.E126.7000	7000
Vestas.V66.1750	1750	Enercon.E126.7500	7500

A.1.3 Costs Model

Electricity Price

To gain some results on financial metrics and assess the repowering strategy against decommissioning and replacement, a constant price for electricity needs to be set. All of the metrics presented above,

except LCoE, consider wholesale electricity price in their formulas to calculate the integrity of the wind park investments. Apart from the metrics presented, the payback period and cash flow stream are examined for both scenarios, thus making the electricity price a necessary input.

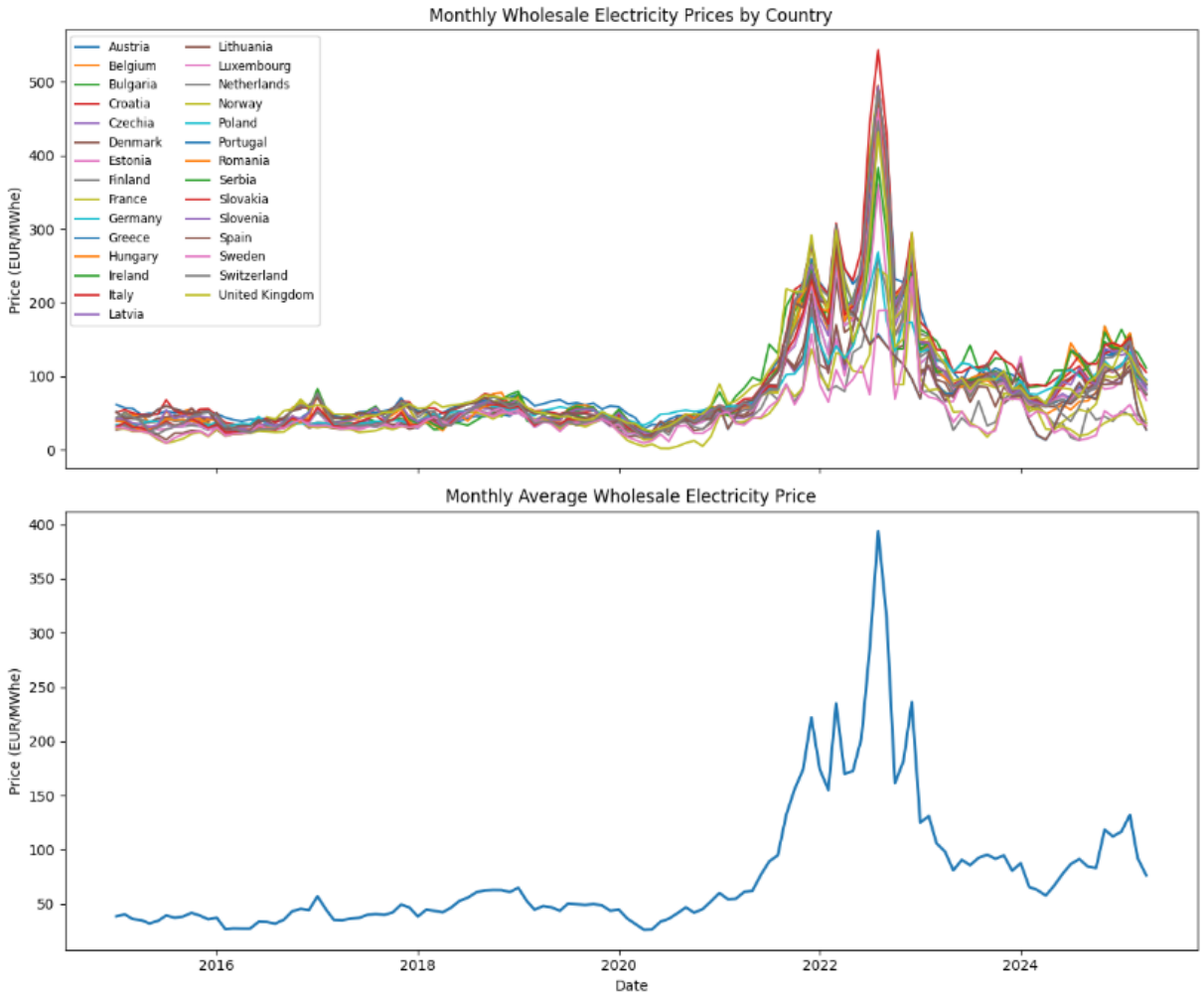

Figure 57: Electricity wholesale prices per country in Europe and average prices in Europe (2005-2025)[15]

Figure 57 presents the monthly wholesale electricity prices for all European countries from 2005 to 2025, together with the annual European average. From 2005 to 2021, prices remained relatively stable, fluctuating between €30 and €50 /MWh, but then, driven by factors such as the COVID-19 pandemic, the Russia affecting the gas prices [110], carbon-permit inflation [111], and weather-induced supply tightness [112], they became highly volatile, spiking to around €400 /MWh. After 2022, volatility eased, although the average price settled at a level higher than in 2005–2021. For this study, we therefore adopt a representative price of **€80 /MWh**, which closely matches the 20-year average.

A.2 Results

A.2.1 Capacity Model

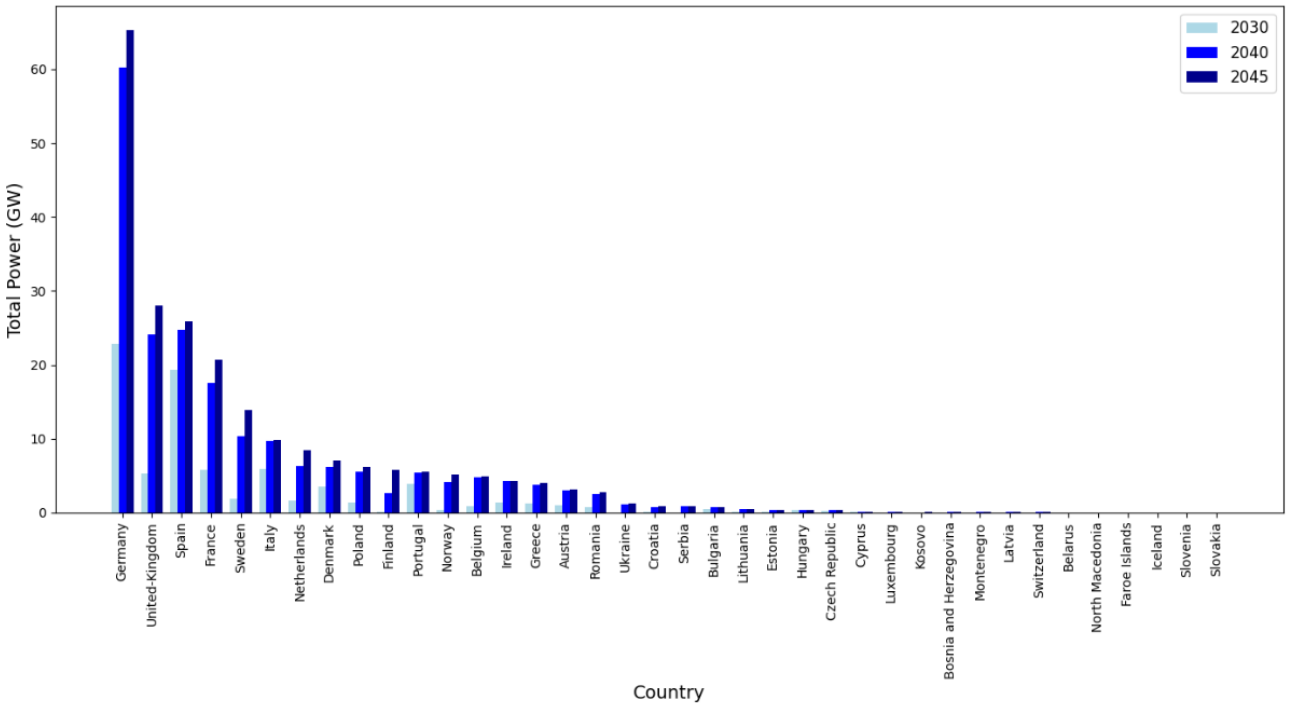

Figure 58: Decommissioned capacity by country total

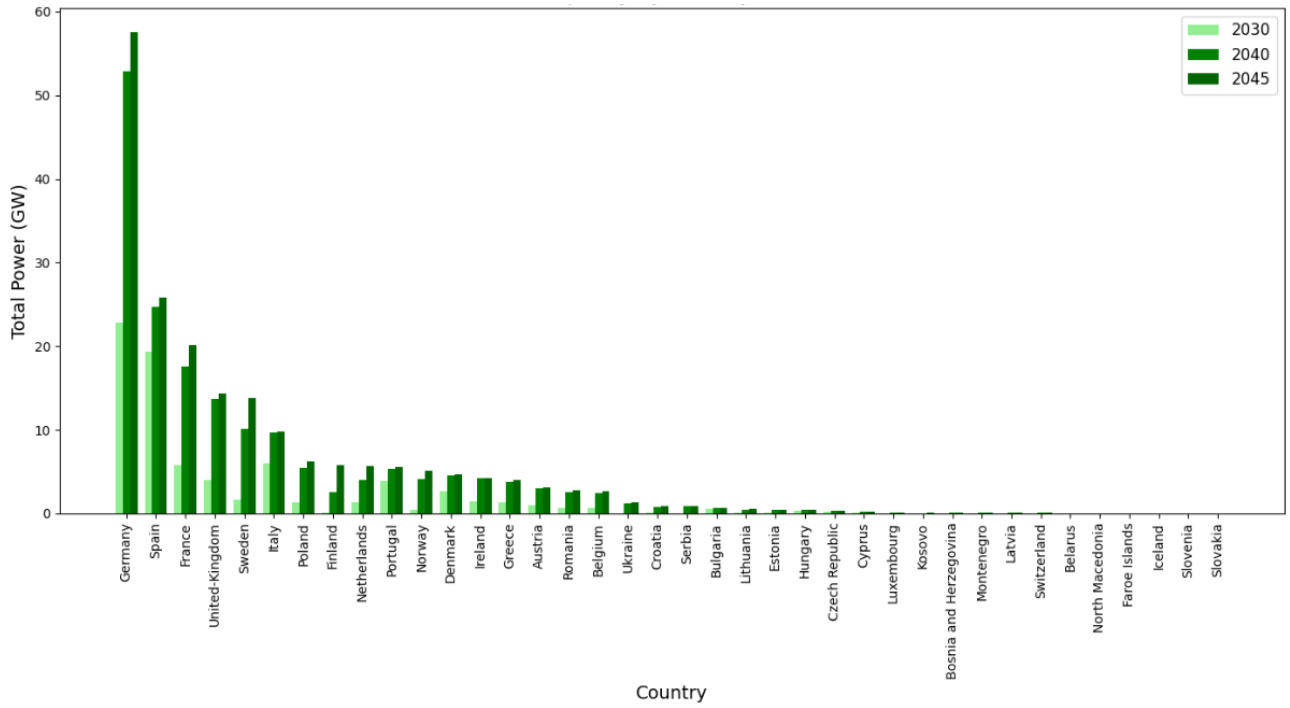

Figure 59: Decommissioned capacity by country Onshore

Supplier Data Analysis

Many different manufacturers can supply wind turbines; Siemens Gamesa, Vestas, and Enercon are some of the largest wind turbine manufacturers in Europe. Moreover, there are plenty of different types and sizes of wind turbines installed all over Europe. This section analyzes the data provided by The Wind Power [7] database on manufacturing and wind turbine type to gain valuable insights into the most used wind turbines and manufacturers across Europe.

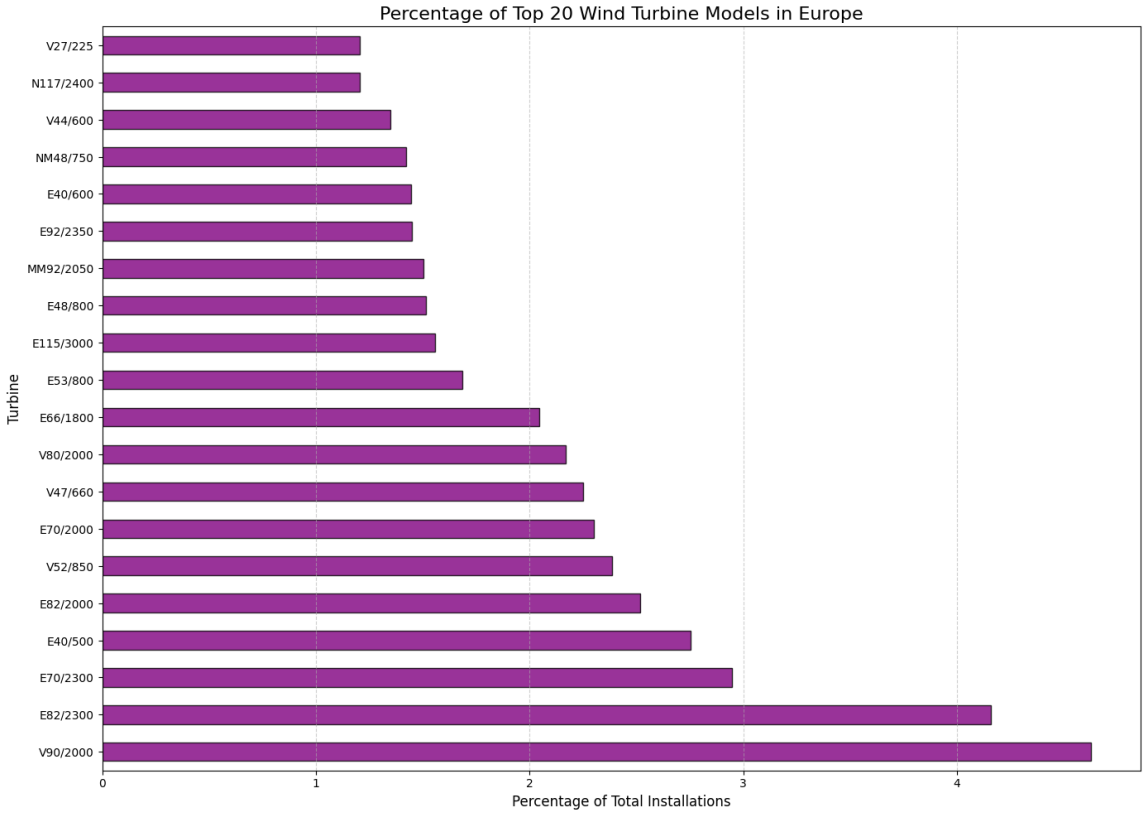

Figure 60: Top 20 wind turbine models used in Europe by percentage of installations

Chart 60 shows the distribution of the top 20 wind turbine models by the percentage of total installations on the continent of Europe. The Vestas model V90/2000 dominates installation with more than 4% occurrence, accounting for the largest share of wind turbines chosen to be used in wind parks. Models like Enercon E82/2300 and E70/2300 are frequently used, reflecting their popularity. The distribution suggests that particularly mid-range capacities (2-3 MW) dominate the European wind energy market.

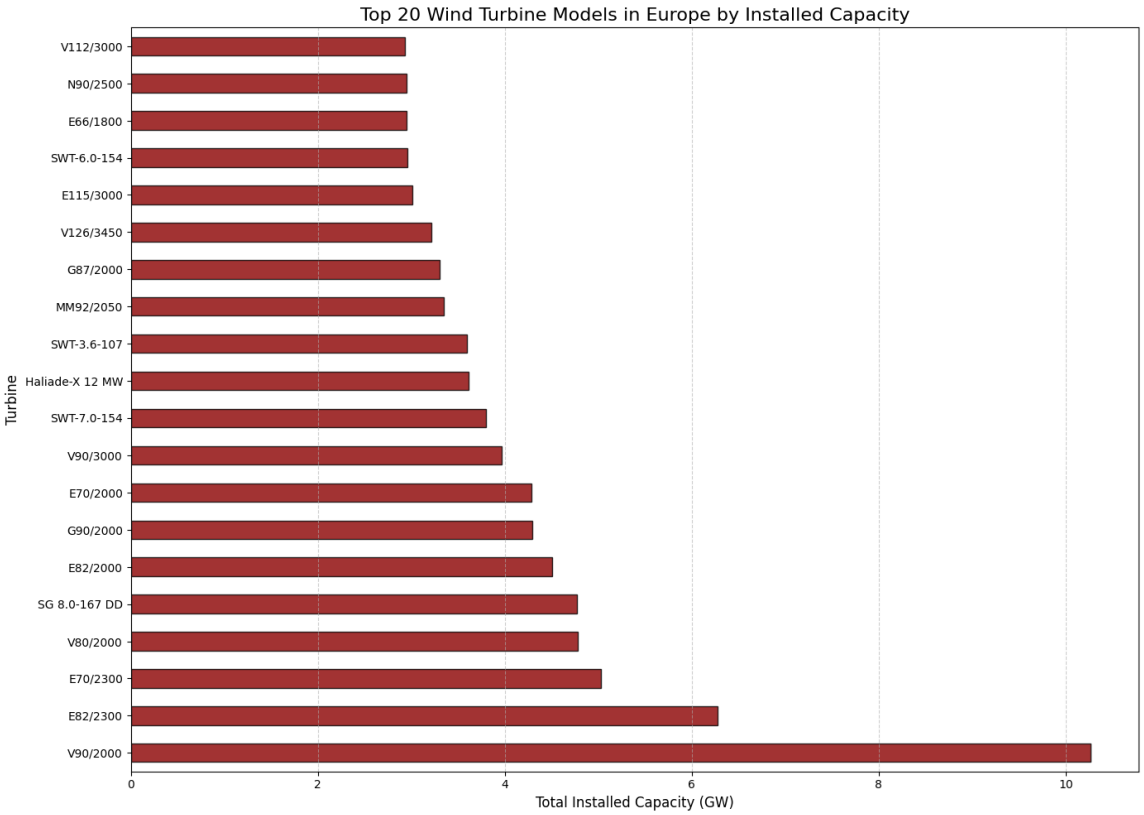

Figure 61: Top 20 wind turbine types in Europe evaluated by installed capacity

Figure 61 illustrates the top 20 wind turbine types and their total installed capacity in the region of Europe. Firstly, the Vestas model V90/2000 again leads the charts with the highest installed capacity of 10.26 GW, showing its market dominance. Modern high-capacity offshore models such as G 8.0-167 DD and Halide-X 12 MW are also prominent, emphasizing a shift toward larger and more efficient turbines in recent years. Furthermore, models like E70/2300 and E82/2300 remain relevant due to their consistent performance and deployment across various sites.

Table 27 and Table 26 present the top 10 manufacturers and wind turbine types for onshore and offshore installations in Europe, based on their percentage of installations. A clear distinction can be observed in the manufacturing trends: Siemens dominates offshore wind turbine installations, accounting for more than half of the market, followed by Vestas and GE Energy. In contrast, Vestas leads in the onshore segment, followed by Enercon and Nordex, with Siemens Gamesa ranking fourth.

Table 26: Offshore top 10 manufacturers and turbines with their percentage of installations

Top 10 Manufacturers

Manufacturer	**Capacity (%)**
Siemens	37.0896
Siemens-Gamesa	24.8600
Vestas	13.8838
GE Energy	11.1310
MHI Vestas Offshore	5.1096
Senvion	2.9752
Areva	1.5160
Bard	0.9746
Adwen	0.8930
Bonus	0.5897

Top 10 Turbines

Turbine	**Capacity (%)**
SG 8.0-167 DD	11.4671
SWT-7.0-154	9.1320
Haliade-X 12 MW	8.6628
SWT-3.6-107	8.4202
SWT-6.0-154	7.0552
V164/9500	6.7895
SG 11.0-200	5.9027
SWT-3.6-120	4.3353
V164/8000	4.2149
SWT-8.0-154	3.8915

Table 27: Onshore top 10 manufacturers and turbines with their percentage of installations

Top 10 Manufacturers

Manufacturer	**Capacity (%)**
Vestas	29.1252
Enercon	22.0293
Nordex	10.1832
Gamesa	9.2004
GE Energy	5.9037
Senvion	4.9570
Siemens	4.6631
Siemens-Gamesa	2.0254
Neg Micon	1.8929
Repower	1.5793

Top 10 Turbines

Turbine	**Capacity (%)**
V90/2000	5.4761
E82/2300	3.3467
E70/2300	2.6829
E82/2000	2.4024
V80/2000	2.3290
G90/2000	2.2885
E70/2000	2.2840
V90/3000	2.0546
MM92/2050	1.7832
G87/2000	1.7602

A.2.2 Energy Yield Comparison

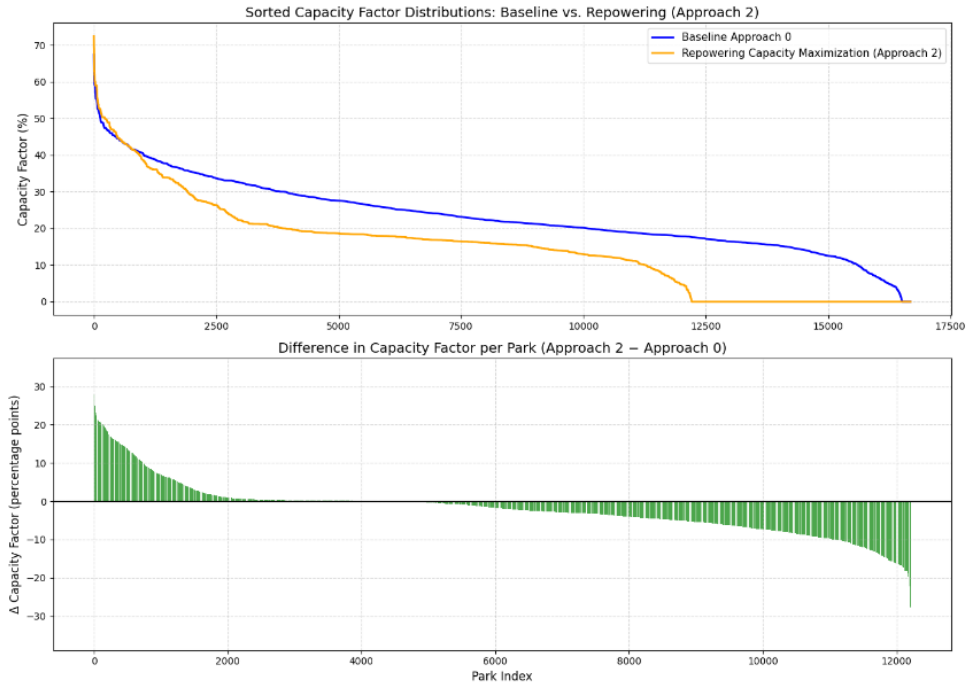

Figure 62: Capacity factor difference between baseline and repowering (Capacity Maximization approach 2) scenarios

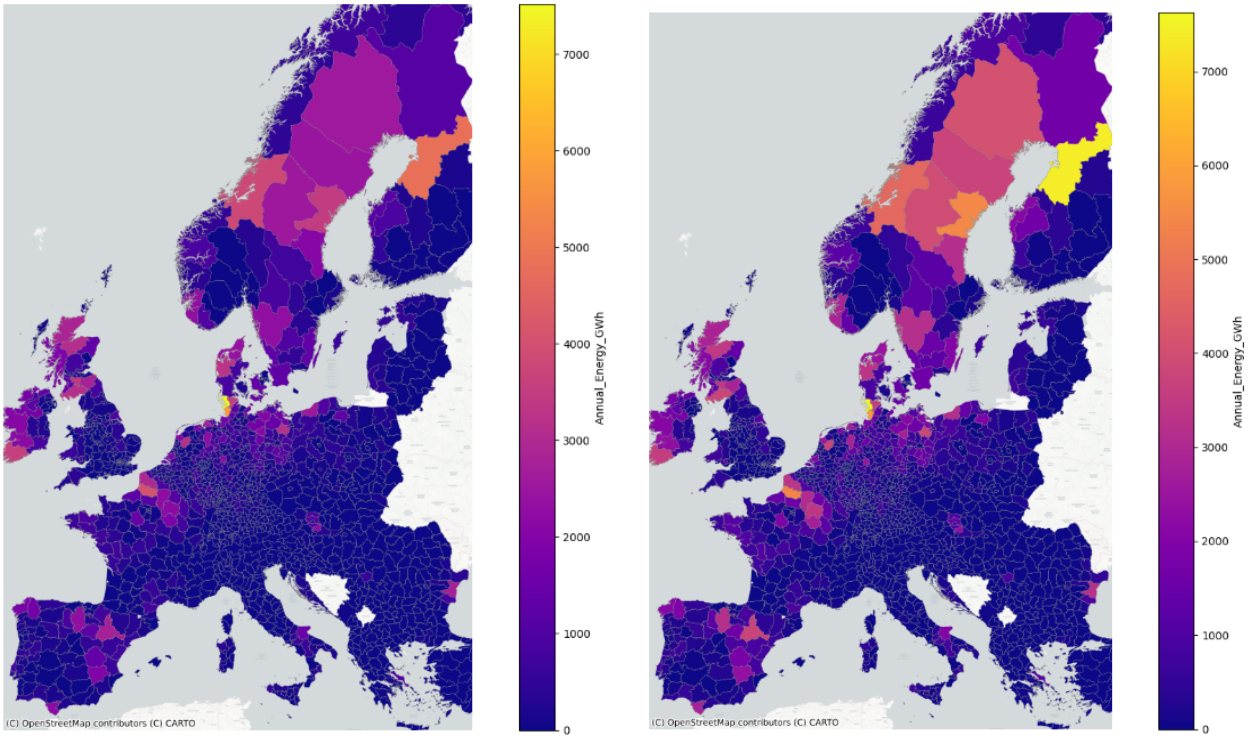

(a) Baseline energy production

(b) Repowered-only energy production

Figure 63: Comparison of annual energy production before and after repowering.

A.2.3 Cost Comparison

Country	Total Wind Parks	Wind Parks with 1 Turbine	% of 1 wt Parks
North Macedonia	1	0	0%
Iceland	2	0	0%
Kosovo	2	0	0%
Montenegro	2	0	0%
Slovakia	2	1	50%
Slovenia	2	2	100%
Bosnia and Herzegovina	3	0	0%
Cyprus	5	0	0%
Faroe Islands	5	1	20%
Serbia	8	1	13%
Latvia	8	4	50%
Belarus	11	8	73%
Lithuania	17	1	6%
Switzerland	19	10	53%
Bulgaria	21	3	14%
Luxembourg	21	7	33%
Estonia	30	8	27%
Croatia	31	1	3%
Ukraine	36	3	8%
Hungary	44	27	61%
Romania	46	2	4%
Norway	64	8	13%
Czech Republic	86	39	45%
Greece	98	1	1%
Finland	202	52	26%
Austria	225	50	22%
Poland	234	35	15%
Ireland	247	30	12%
Denmark	380	153	40%
Portugal	400	93	23%
Belgium	400	130	33%
Italy	448	29	6%
Netherlands	588	294	50%
Spain	868	53	6%
United Kingdom	1006	351	35%
Sweden	1021	532	52%
France	1727	104	6%
Germany	8374	3913	47%

Table 28: Wind park statistics by country

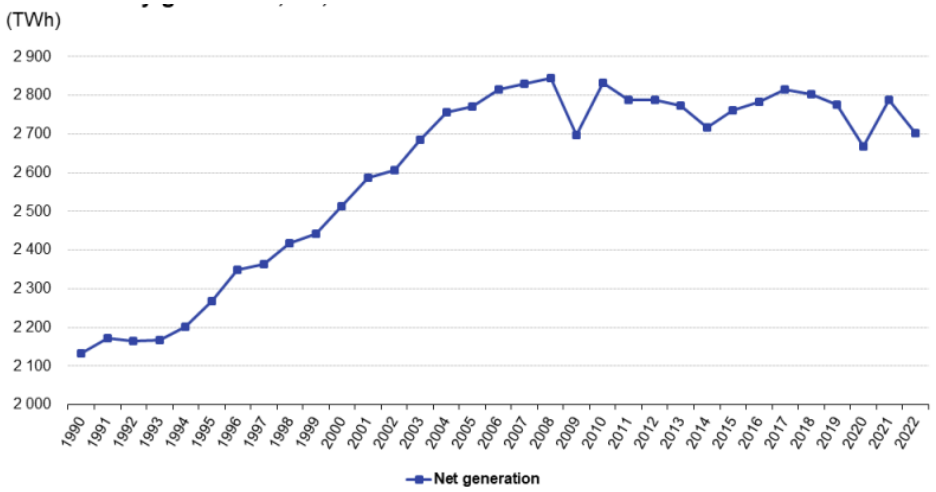

Figure 64: Total electricity consumption in EU (1990-2022)

A.2.4 Land-Use Comparison

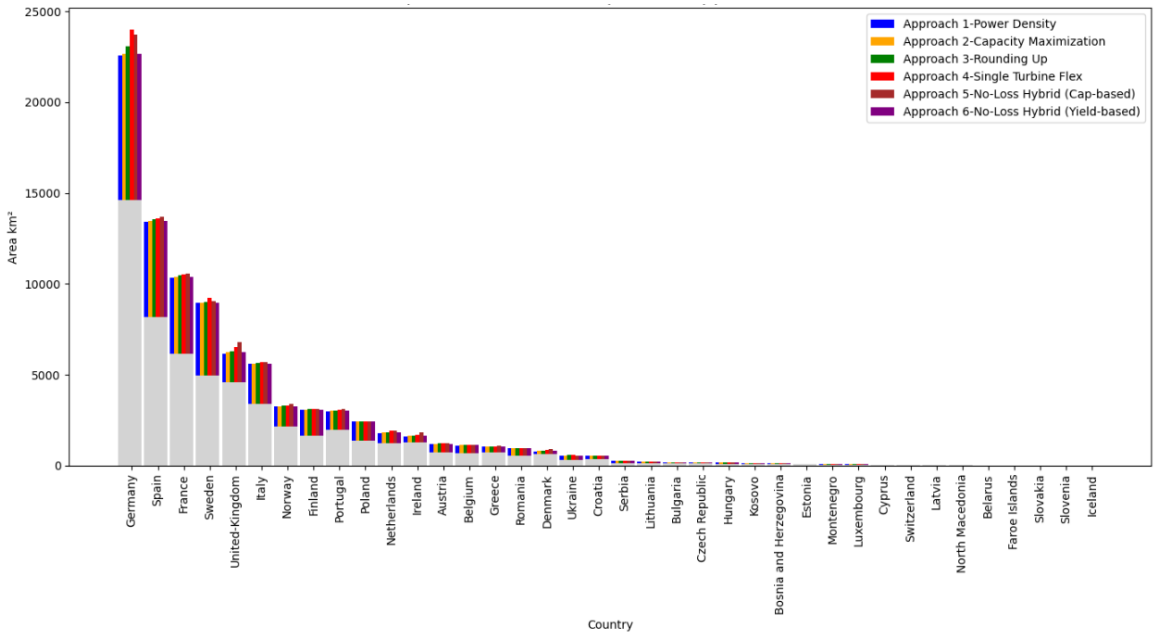

Figure 65: Required land area to reach repowered capacity comparison Baseline vs. Repowered for all approaches

Table 29: Wind park data by country (in km^2)

Country	Total Park Area (km^2)	Land Area (km^2)	WindPark (%)
Germany	6441.883	357 590.000	1.8015
Netherlands	557.973	41 540.000	1.3432
Belgium	303.570	30 530.000	0.9943
Luxembourg	24.892	2590.000	0.9611
Portugal	873.622	92 230.000	0.9472
United-Kingdom	2021.534	243 610.000	0.8298
Ireland	554.812	70 280.000	0.7894
Spain	3604.776	505 970.000	0.7124
Denmark	272.789	42 920.000	0.6356
Italy	1499.923	302 068.000	0.4966
France	2721.663	549 087.000	0.4957
Sweden	2174.631	528 861.000	0.4112
Austria	329.359	83 879.000	0.3927
Kosovo	36.487	10 887.000	0.3351
Greece	323.954	131 960.000	0.2455
Finland	725.835	338 460.000	0.2145
Poland	606.812	312 710.000	0.1940
Montenegro	25.029	13 810.000	0.1812
Croatia	150.130	88 070.000	0.1705
Cyprus	15.038	9250.000	0.1626
Norway	948.959	624 499.000	0.1520
Faroe Islands	1.560	1393.000	0.1120
Romania	241.797	238 400.000	0.1014
Lithuania	54.110	65 290.000	0.0829
Serbia	56.133	84 990.000	0.0660
Bosnia and Herzegovina	33.345	51 210.000	0.0651
Estonia	29.116	45 340.000	0.0642
Czech Republic	48.867	78 871.000	0.0620
Bulgaria	51.044	111 000.000	0.0460
Hungary	41.527	93 030.000	0.0446
Switzerland	14.257	41 290.000	0.0345
North Macedonia	7.473	25 710.000	0.0291
Ukraine	135.422	603 550.000	0.0224
Latvia	11.333	64 590.000	0.0175
Slovenia	0.369	20 480.000	0.0018
Belarus	3.223	207 610.000	0.0016
Slovakia	0.559	49 030.000	0.0011
Iceland	0.322	103 000.000	0.0003